

Aus dem Institut für Klinische Molekularbiologie  
(Direktor: Prof. Dr. Schreiber)  
der Christian-Albrechts-Universität zu Kiel

**Fundamental differences of the hematopoietic growth factors  
Flt3L and GM-CSF on experimental colitis depend on  
type I-IFN mediated antimicrobial effects on  
intestinal immune response.**

Inauguraldissertation  
zur  
Erlangung der Doktorwürde  
der Medizinischen Fakultät  
der Christian-Albrechts-Universität zu Kiel

vorgelegt von

**Konrad Arnold Altfried Aden**

aus **Essen**

Kiel 2011

1. Berichtstatter: Prof. Dr. Philip Rosenstiel

2. Berichtstatter: Prof. Dr. Jobst Sievers

Tag der mündlichen Prüfung: 22.3.2011

Zum Druck genehmigt, Kiel, den 22.3.2011

Gez.: Cascorbi

Ich versichere hiermit an Eides Statt, dass meine Dissertation mit dem Thema:

**Fundamental differences of the hematopoietic growth factors Fms-like tyrosine 3-kinase ligand and GM-CSF on experimental colitis depend on type I-IFN mediated antimicrobial effects on intestinal immune response.**

abgesehen von Ratschlägen meines Doktorvaters und meiner sonstigen akademischen Lehrer, nach Form und Inhalt meine eigene Arbeit ist, dass ich außer den in der Arbeit aufgeführten keine weiteren Hilfsmittel benutzt habe. Teile dieser Ergebnisse wurden als Poster auf der Digestive Disease Week (DDW) 2008, San Diego sowie auf der DDW 2010, New Orleans präsentiert.

Ich widerspreche nicht nach §5, Abs. 2k der Promotionsordnung der Teilnahme von Zuhörern an der mündlichen Doktorprüfung.

Kiel, den 4.3.2010

## **Meinen Eltern**

# Content

<b>Content</b> .....	<b>I</b>
<b>Abbreviations</b> .....	<b>III</b>
<b>Figure Legend</b> .....	<b>V</b>
<b>Table Legend</b> .....	<b>V</b>
<b>I. Introduction</b> .....	<b>1</b>
<b>Crohn's Disease and Ulcerative Colitis</b> .....	<b>1</b>
Introduction: .....	<b>Fehler! Textmarke nicht definiert.</b>
Clinical and pathologic features .....	1
Epidemiology .....	2
Environmental factors .....	3
Genetics .....	3
<b>Intestinal immunity and pathophysiology of Crohn's Disease</b> .....	<b>6</b>
Mucosal Barrier .....	6
Innate Immunity in Crohn's disease .....	7
<b>The implications of hematopoietic growth factors on intestinal inflammation.</b> .....	<b>9</b>
GM-CSF as a therapeutic agent in IBD.....	9
The role of dendritic cells in the intestinal immune response.....	10
Dendritic cell amplification as a therapeutic target in intestinal inflammation.....	11
Fms-like tyrosine kinase 3 Ligand (Flt3L) .....	11
<b>Experimental outline</b> .....	<b>12</b>
<b>II. Materials and methods</b> .....	<b>14</b>
<b>Animals</b> .....	<b>14</b>
<b>Induction and evaluation of experimental colitis using Dextran Sodium Sulfate (DSS)</b> <b>14</b>	<b>14</b>
Clinical scoring of DSS colitis .....	14
Macroscopic and histological assessment of colonic inflammation.....	15
Myeloperoxidase Assay .....	15
<b>Cellculture</b> .....	<b>16</b>
General conditions for working with cellcultures .....	16
Celllines .....	17
Primary cells .....	17
Isolation of splenocytes from mice spleen.....	17
Isolation of CD11c <sup>+</sup> Dendritic Cells using magnetic cell sorting (MACS®) .....	18
Gentamicin protection assay.....	19
<b>Working with Nucleid Acids</b> .....	<b>20</b>
Total RNA Isolation from cell culture and whole tissues.....	20
Isolation of poly A <sup>+</sup> messenger RNA using the Oligotex® mRNA Kit.....	21
Reverse Transcription .....	22
Polymerase chain reaction.....	23
Whole genome expression profiling using Agilent chips.....	25
<b>Immunohistochemical Methods</b> .....	<b>27</b>
Flow Cytometry .....	27
Immunohistochemistry.....	28
Statistical Analysis.....	29
<b>III. Results</b> .....	<b>30</b>
<b>Characterisation of GM-CSF and Flt3L effects on DC growth in mice in vivo</b> .....	<b>30</b>
Immunophenotype of splenic DC.....	30
Growth effects on intestinal DC .....	32
<b>Evaluation of Flt3L effects in mouse models of acute colitis</b> .....	<b>33</b>
DSS-induced acute colitis in balb/c mice.....	33

DSS-induced acute colitis in RAG1 <sup>-/-</sup> mice .....	38
<b>Functional analysis of GM-CSF and Flt3L treatment in mice in vivo.....</b>	<b>41</b>
Priming effects of GM-CSF and Flt3L on TLR-9 stimulation.....	41
Priming effects of GM-CSF and Flt3L on TLR-7 stimulation.....	44
<b>Characterization of IFN-I effects on intestinal immunity.....</b>	<b>47</b>
Whole mouse genome transcription profiling .....	47
Real Time PCR confirmation of IFN-I dependent gene induction.....	50
Evaluation of the gentamicin protection assay .....	52
GM-CSF, but not Flt3L, enhances antimicrobial peptide gene induction in a TLR-9 and IFN-I dependent mechanism. ....	55
<b>IV. Discussion.....</b>	<b>58</b>
<b>Background and experimental outline .....</b>	<b>58</b>
<b>Characteristics and limitations of the DSS model.....</b>	<b>59</b>
<b>Flt3L and GM-CSF mediated dendritic cell growth .....</b>	<b>60</b>
<b>Flt3L dependent DC expansion in the context of intestinal inflammation.....</b>	<b>61</b>
<b>Flt3L and GM-CSF priming effects on TLR-signalling.....</b>	<b>62</b>
<b>IFN-I increases bacterial clearance and induces antimicrobial peptide expression.....</b>	<b>64</b>
<b>Outlook.....</b>	<b>65</b>
<b>V. Summary.....</b>	<b>67</b>
<b>VI. Literature .....</b>	<b>68</b>
<b>Additional information - Materials .....</b>	<b>76</b>
<b>Publications and activities .....</b>	<b>79</b>
<b>Acknowledgements .....</b>	<b>80</b>
<b>Curriculum vitae.....</b>	<b>81</b>

## Abbreviations

A	Adenin
A. bidest	Aqua bidestilled
AB	antibody
ATCC	American type culture collection
bp	base pairs
BSA	Bovine Serum Albumin
C	Cytosin
c	concentration
CARD	Caspase-activating recruitment domain
CD	Cluster of differentiation
CD	Crohn's Disease
cDNA	complementary DNA
cm	centimeter
CpG	Cytosin-phosphatidyl-Guanin
DAI	Disease activity index
DC	Dendritic cell
Defcr	Defensin related cryptidin
DEPC	Diethylpyrocarbonate
DMEM	Dulbecco's modified eagle medium
DNA	desoxyribonucleid acid
dNTP	Desoxyribonucleidtriphosphat
DSS	Dextran Sodium Sulfate
DTT	Dithiothreitol
EDTA	Ethylendiamintetraacetate
et. al.	et alii
FACS	Fluorescence assisted cell sorting
FBS	Fetale bovine serum
Flt3L	Fms-like tyrosin kinase 3 Ligand
g	Gramm
G	Guanin
GM-CSF	Granulocyte/macrophage colony stimulating factor
GVA	Glycerol vinyl alcohol
h	Hour
H <sub>2</sub> O	Water
HIV	Human immunodeficiency virus
IBD	Inflammatory bowel disease
IFN	Interferon
IgG	Immunoglobulin G
IHC	Immunohistochemistry
IL	Interleukin
IRF	Interferon regulatory factor
IDC	Lymphoid Dendritic cell
M	molar (mol/l)
MACS	Magnetic cell sorting
mDC	Myeloid Dendritic cell
mg	milligram (10 <sup>-3</sup> g)

MHC	Major histocompatibility complex
ml	milliliter
MMLV	Mus musculus lentivirus
MPO	Myeloperoxidase
mRNA	messenger Ribonucleic Acid, messenger RNA
ms	Mouse
ng	nanogramm ( $10^{-9}$ g)
nm	Nanometer
NOD	Nucleotide oligomerization domain
oct	Optimal cutting temperature
OD	Optical density
<i>p</i>	Probability
PAMP	Pathogen associated molecular patters
PBS	Phosphate buffered saline
PCR	Polymerase chain reation
pDC	plasmacytoid Dendritic cell
peg.	pegylated, associated with Poly Ethylen Glycol
PFA	Paraformaldehyde
pg	picogramm ( $10^{-12}$ g)
pH	<i>potentia hydrogeni</i>
RNA	Ribonucleid Acid
RNAse	Ribonuclease
rpm	rotations per minute
RPMI	Roswell Park Memorial Institute
rRNA	ribosomal RNA
RT	Room Temperature
RT-PCR	Reverse Transcription PCR
Sa	Streptavidin
sec.	Second
SI	Small intestine
SNP	Single Nucleotide Polymorphism
ssRNA	Single-Stranded Ribonucleid Acid
T	Thymin
Tab.	Table
<i>Taq</i>	<i>Thermophilus aquaticus</i>
TBE	Tris/Borate/EDTA
TLR	Toll like receptor
tRNA	transcriptional RNA
u	Units
U	Uracil
UC	Ulcerative Colitis
μl	microliter
μM	micromolar ( $10^{-6}$ mol/l)



## Figure Legend

Figure 1 Flow cytometrical analysis of DC population in spleen. ....	31
Figure 2 Immunohistochemistry of Dendritic Cells in colon sections. ....	32
Figure 3 Disease activity index (DAI).....	34
Figure 4 Colon length .....	34
Figure 5 Histology of colon sections .....	35
Figure 6 Myeloperoxidase assay in colon homogenates from DSS induced colitis.....	36
Figure 7 Proinflammatory gene expression in colon samples from DSS-induced colitis.....	36
Figure 8 Flow cytometry of splenocytes from DSS and DSS+Flt3L treated mice.....	37
Figure 9 Disease activity index in DSS-induced colitis in RAG1 <sup>-/-</sup> mice.....	39
Figure 10 Colon length in after DSS-induced colitis in RAG1 <sup>-/-</sup> mice.....	39
Figure 11 Histology of colon section in DSS-induced colitis in RAG1 <sup>-/-</sup> mice. ....	41
Figure 12 TNF- $\alpha$ protein levels in colon homogenates. ....	40
Figure 14 Real Time PCR of IFN-I and IFN-I inducible gene expression in small intestine.....	43
Figure 13 Real Time PCR of IFN-I and IFN-I inducible gene expression in spleen.....	44
Figure 15 Real Time PCR of IFN-I and IFN-I inducible gene expression in colon.....	44
Figure 16 Real Time PCR of TLR-7 induced IFN-I and IFN-dependent gene expression.....	46
Figure 17 <i>CARD 15</i> and <i>hBD 3</i> gene expression in HCT 116 epithelial cell line. ....	50
Figure 18 <i>CARD 15</i> and <i>hBD 3</i> gene expression in HT 29 epithelial cell line.....	51
Figure 19 Real Time PCR analysis of AMP gene expression in CD11c <sup>+</sup> DCs. ....	52
Figure 20 Gentamicin protection assay.....	53
Figure 21 Flow cytometry of isolated CD11c <sup>+</sup> DCs.....	54
Figure 22 Gentamicin protection assay in CD11c <sup>+</sup> DCs.....	54
Figure 23 Real Time PCR analysis of IFN-I gene expression in colon samples of mice.....	56
Figure 24 Real Time PCR analysis of AMP gene expression in colon samples of mice.....	57

## Table Legend

Table 1 Disease activity index, .....	15
Table 2 Myeloperoxidase assay, Buffers and reagents.....	15
Table 3 Reverse Transcription, reagents.....	22
Table 4 Polymerase chain reaction, reagents.....	23
Table 5 RNA Preparation and array hybridization design.....	26
Table 6 cDNA Master Mix .....	26
Table 7 Transcription Master Mix .....	27
Table 8 Statistical evaluation of Flt3L and GM-CSF effects on Dendritic cell growth in vivo. ....	30
Table 9 DSS-induced colitis in balb/c mice.....	33
Table 10 DSS-induced colitis in RAG1 <sup>-/-</sup> mice. Treatment groups. ....	38
Table 11 GM-CSF and Flt3L priming of TLR-9 activation in mice.....	41
Table 12 GM-CSF and Flt3L priming of TLR-7 activation in mice.....	45
Table 13 Whole genome array, TLR-9 stimulation .....	48
Table 14 Whole genome array, TLR-7 stimulation .....	49
Table 15 Influence of 440c AB on TLR-9 and IFN-I dependent gene expression.....	55
Table 16 List of Antibodies. ....	76

## I. Introduction

The presented study was designed to gain insight into the pathophysiology of inflammatory bowel disease using a mouse model of intestinal inflammation. This study was a follow up study of previous clinical and experimental research describing the role of GM-CSF as a therapeutic target in patients suffering IBD. The first part of the introduction deals with clinical, epidemiological aspects of IBD as well as with common theories explaining the pathophysiology of IBD. The second part of the introduction ( see: **Innate immunity in Crohn's disease** ) reveals the rationale for the presented study and key findings of the previous studies, the performed experiments are based on.

### **Crohn's Disease and Ulcerative Colitis**

Inflammatory bowel disease is a chronic relapsing inflammation of the digestive tract, which, may either affect the entire digestive tract from mouth to anus (Crohn's disease) or is limited to the colon (ulcerative colitis). Crohn's disease was named after the US physician Burril B. Crohn, who first described the disorder in 1932 [1]. Ulcerative colitis was first described by the British physician Sir Samuel Wilks in 1859 [2, 3]. Although CD and UC are clinically, pathologically and biochemically distinguishable diseases, multiple epidemiologic and genetic features suggest that they may be disease variants of a common underlying etiology. It is generally agreed that inflammatory bowel disease (IBD) is a multifactorial disease, caused by the interplay of genetic susceptibility and misbalanced host-pathogen interactions [4].

### **Clinical and pathologic features**

#### **Crohn's Disease**

Chronic inflammation and ulceration in CD predominantly affect the terminal ileum and colon, but any portion of the digestive tract from the mouth to the anus can be involved. About two-thirds of patients have only involvement of the small intestine. Because various sites can be affected, CD has a variable clinical appearance; patients may present with general discomfort, abdominal pain and/or diarrhoea. Notably, the diarrhoea in CD seldom includes gross macroscopic bleeding, which is a typical feature in UC. Extraintestinal manifestations are seen in about 50% of CD patients. Areas affected include joints (monoarthritis, sacroileitis) and liver (cirrhosis, pericholangitis). Aside from differences in

clinical presentation, CD has macroscopic and microscopic features that make it clearly distinguishable from UC. Intestinal involvement in CD is frequently segmental; that is, lengths of diseased bowel are separated from apparently normal tissue (“skip lesions”). The hallmark of CD on endoscopy is patchy ulcers in the intestinal mucosa that later develop into deep transmural fissures. The classical microscopic feature of CD is the presence of granulomas, which can be distinguished from those of tuberculosis by the absence of caseous necrosis. Historically, when tuberculosis was more prevalent, CD was often confused with intestinal tuberculosis [5, 6].

### **Ulcerative colitis**

In contrast to CD, mucosal involvement in ulcerative colitis (UC) is restricted to the colon and is continuous in its distribution. Some cases are confined to the rectum, others to the rectum and sigmoid, while others may exhibit a total colitis extending into the caecum. Because UC affects the colon, bloody, mucoid diarrhoea in addition to abdominal spasm is the main clinical symptom. Due to extensive diarrhoea (10-20 bloody stools/day) patients may display hypoproteinemia and anemia. Extraintestinal manifestations are similar to CD, however they are less common in UC as compared to CD. In UC the colon usually displays broad superficial ulcerations, which seldom progress into deep ulcers affecting the muscle layer. Finally UC, as well as CD, is recognized as a premalignant condition, as it is associated with a highly increased risk of colorectal carcinoma[5, 6].

### **Epidemiology**

The highest incidence and prevalence rates of UC and CD have been reported from North America, the UK and northern Europe. It is a common observation that high prevalence of immune-related disorders (allergic rhinitis, atopic dermatitis, etc.) correlates with high socioeconomic standards. Rates of these conditions have been noted to rise in countries as socioeconomic standards begin to improve, e.g. southern Europe, China[7]. Among the Northern American population white (43.6 per 100.000) and African-American (29.8 per 100.000) people have higher prevalence rates than asian (5.6 per 100.000) and hispanic (4.1 per 100.000) individuals [8]. The idea of racial influence on disease prevalence and severity is further supported by a study showing racial differences in disease localization and extraintestinal manifestation [9]. Among all ethnic groups Jews have the highest risk for IBD. A population study in Baltimore revealed that the incidence among Jews was 13 per 100.000 compared with a rate of 3.8 per 100.000 in non-Jews [10]. Ethnic differences in population

studies lend further support to the importance of genetic factors in disease development. On the other hand, Ashkenazi Jews from Israel had a markedly decreased risk for UC than those from Northern America or Europe, suggesting that environmental factors play also an important role in the aetiology of IBD [11].

### **Environmental factors**

The highest incidence rates of IBD are found in North America and northern Europe, whereas the lowest incidence rates are reported from South America, southeast Asia and Africa (with the exception of South Africa). Although geographical circumstances could account for the variations in disease frequency, it is more likely related to differences in socioeconomic levels between the civilized western and the developing southern countries. This possibility is supported by the observation of increasing incidence rates among immigrants from low-incidence regions moving to high incidence regions [12]. Moreover, incidence rates are currently increasing in regions facing excessive industrialisation such as China [13]. Socioeconomic factors specifically linked to medical circumstances include sanitation, hygiene and access to medical treatment, as well as nutrition and drug exposure. Lifestyle in the western world indisputably contributes to increasing incidence rates. However, it is difficult to pinpoint the forces that are actually independently responsible for IBD onset. Breastfeeding, for example, confers passive immunity while the child's intestinal immune system is still developing, and it has been reported to provide protection against IBD in offspring [14]. Nutrition seems to play a crucial role in IBD development as nutrition habits in the western world have changed dramatically over the past 100 years with a constant increase in carbohydrate and lipid intake.

An interesting link is observed between increased distribution of refrigerated meat consumption in the past 60 years and Crohn's disease emergence.

Meat refrigeration, according the "cold-chain-hypothesis", favours growth of psychotropic bacteria, such as *Yersinia enterocolica* and *Listeria monocytogenes*, which are found in the intestine of Crohn's disease patients [15, 16].

### **Genetics**

The importance of genetics in the etiology of IBD is underscored by three observations, namely (i) familial aggregation, (ii) twin studies and (iii) gene defects found in IBD patients.

**Familial aggregation**

Having a first-degree relative with CD or UC is still the highest individual risk factor for UC and CD [17]. People with CD have a first-degree relative who also has CD in 2.2 – 16.2% of cases and with any inflammatory bowel disease in 5.2 – 22.5% of cases.

The risk of Crohn's Disease in a sibling of a Crohn's Disease patient is even higher than the average risk for a first-degree relative. In familial studies with affected parent-child pairs, parent and child were concordant for disease type in 75.3%, disease extent in 63.6% and extraintestinal manifestations in 70.1% of cases. Concordance for disease type (81.6%), extent (76%) and extraintestinal manifestation (83.8%) was even higher in affected sibling pairs [18]. Genetic anticipation, i.e. earlier onset in offspring of parents with disease, has been reported for both UC and CD in a Jewish population, though this may not apply to patients with inflammatory bowel disease in general [19, 20].

**Twin Studies**

As monozygotic twins are genetically identical, any disease solely caused by genetic alterations should be present in both. Consequently, the strongest evidence for the contribution of genetic factors to the development of inflammatory bowel disease has come from mono- and dizygotic twin studies. Tysk et al. showed a concordance in monozygotic twins of 58.3% for Crohn's disease and 6.3% for ulcerative colitis, compared to 3.9% (CD) and 0% (UC) in dizygotic twins [21]. Several additional studies have confirmed this data, though with less extreme concordance rates of CD and UC in monozygotic twins [22, 23].

**IBD – Genes**

Due to the feasibility of whole genome sequencing and the access to large sample numbers, a variety of genes have been discovered that putatively confer increased risk for IBD. However, IBD is considered to be a non-Mendelian polygenic disorder, and it is still far from fully elucidated to what extent genetic alterations influence disease risk. Genetic alterations that have been found to be associated with IBD can be stratified according their physiologic function in genes involved in (i) innate immune response, (ii) antigen-presentation, (iii) maintenance of epithelial integrity and (iv) intestinal drug transport. The role of genetic mutations in inflammatory bowel disease will be demonstrated with the *CARD15* gene and its implication as a genetic risk factor for IBD.

***CARD15 (NOD2) gene mutations in inflammatory bowel disease***

The *CARD15* gene on chromosome 16 encodes the intracellular protein nucleotide oligomerization domain (NOD) 2. NOD2 is an intracellular receptor involved in innate immune defence against microbial invasion in the intestinal tract. NOD2 has a tripartite domain structure with a c-terminal leucine rich repeat (LRR) region, which is involved in ligand recognition, a central NOD domain that undergoes self-oligomerization and has ATPase activity and an n-terminal CARD-CARD domain that interacts with downstream adaptor molecules resulting in activation of the transcription factor NF $\kappa$ B and subsequent transcription activation of pro-inflammatory genes. Genetic studies of large cohorts of Crohn's patients revealed homozygous mutations of the *CARD15* gene, which encodes NOD2 in 10-15% of patients with CD [24-26]. Mutations are found in the LRR domain of NOD2 and include single nucleotide polymorphism (SNP) changes in (R702W) or (G908R) or frame shift mutation of NOD2 (L1007fsinsC), leading to a partial truncation of the LRR [27].

The NOD2 LRR region is required for the recognition of muramyl-dipeptide (MDP), a cell wall component of gram-positive and gram-negative bacteria [28]. The Crohn-associated variants occur in the leucine-rich repeat domain and interfere with MDP recognition ability and thereby diminish NF $\kappa$ B activation [29]. Pathogen detection and subsequent NF $\kappa$ B activity seems to play a key role in effective bacterial clearance, and its dysregulation largely contributes to the genesis of mucosal inflammation. As an example, compared to healthy controls, colons from patients with CD exhibited reduced copy numbers of the human beta-defensin 2 (HBD2) gene [30], the transcription of which is tightly regulated in a NOD2-NF $\kappa$ B mediated pathway and nullified in impaired HEK 293 cells that contain the NOD2 3020insC frame-shift mutation [31].

The clinical appearance of excessive NF $\kappa$ B-signalling and pro-inflammatory cytokine secretion in the mucosa of CD patients can be explained by a secondary overreaction of the mucosal immune system in response to primary "immunodeficiency" due to "loss-of-function" mutation of the NOD2.

Another view at the pathophysiology of intestinal inflammation has recently been introduced by a transgenic mouse model, carrying a frameshift mutation equivalent to the L1007fsinsC found in humans. These mice showed a "gain-of-function" mutation in NOD2 leading to excessive NF $\kappa$ B-signalling and IL-1 $\beta$  secretion [32]. These data indicate that the

exact molecular mechanisms in the genesis of chronic inflammation are not fully understood.

## **Intestinal immunity and pathophysiology of Crohn's Disease**

### **Mucosal Barrier**

The first line of protection against enteric microbial infiltration is the physical barrier of the mucosal epithelium, composed largely of enterocytes, M-cells, goblet cells, paneth cells and the surface mucus layer. The epithelial lining acts as a selectively permeable membrane, allowing entry of luminal nutrients, water and ions but preventing entry of pathogens. Mucosal permeability is known to be increased in active CD due to the effects of inflammatory mediators [33], but there is conflicting evidence regarding the relative contribution of predisposing genetic and environmental factors to this defect. It is assumed that loss of epithelial integrity is a very early event in disease progress, as permeability changes have been described in patients up to 8 years before disease onset [34] as well as in healthy first-degree relatives of IBD patients [35].

The importance of the epithelial barrier is highlighted by the multiplicity of experimental colitis models targeting the disturbance of epithelial integrity either due to chemical induction in Dextran sodium sulfate (DSS)-colitis or gene deletion (*MDR1*<sup>-/-</sup> mice) [36]. Beyond the passive barrier function, that prevents pathogens from mucosal entry, mucus secretion from goblet cells actively clears the bacterial load from the epithelium. Maintenance of constant mucus flow is a prerequisite for a healthy microbial-host interaction by preventing too "intimate" contact between mucosa and microbes. This view is supported by recent findings, that deletions in the *Muc2* gene, which encodes Muc2 mucin, a major component of the intestinal mucus barrier, led to spontaneous colitis in *Muc2*<sup>-/-</sup> mice [37].

Notably, the mucosal epithelium may play an important role in innate immunity, initiating the release of proinflammatory cytokines in response to microbial exposure and providing regulation of the ensuing inflammatory response. Circulating components of the innate immune system, such as neutrophils, macrophages, dendritic cells, natural killer (NK) cells and complement proteins, are positioned beneath the basement membrane to respond rapidly to translocating microbes and to stimulate the adaptive immune response (T-cells and B-cells) [38].

**Innate Immunity in Crohn's disease**

In an environment inundated with potentially harmful microbes, survival depends on rapid defence mechanisms. For this purpose, nature endowed multicellular organisms with a variety of archaic protection tools, commonly summarized as innate immunity. These “archaic protection tools” exert their function at the level of recognition, i.e. the sensing of potentially harmful microbes, as well as at the level of execution, i.e. the initiation of the appropriate defence stimulus against pathogens. Unlike receptors of the adaptive immune system, which are equipped with an infinite number of antigen-specific receptors due to rearrangement of the T-cell receptor variable region, the number of ligand-specific receptors in the innate immune system is restricted and commonly referred to as Pattern Recognition Receptors (PRRs). Cells involved in the innate immune response are equipped with a variety of extracellular and intracellular PRRs, each of which sense a specific bacterial pattern or Pathogen associated molecular pattern (PAMP). PAMPs are conserved molecular structures present in pathogens (e.g. lipopolysaccharide, a cell wall component of gram-positive and gram-negative bacteria). PAMPs include viral nucleic acids, bacterial and fungal cell wall components, flagellar proteins and more. The most prominent representatives of PRRs are Toll-like receptors (TLR) and Nod-like receptors (NLR). PRRs are expressed on the mucosal epithelium and sense microbial load on the luminal side of the gut. Moreover, circulating components of the innate immune system, such as neutrophils, natural killer (NK) cells, macrophages and dendritic cells also harbor multiple PRRs. Positioned beneath the epithelial layer, they rapidly sense transmigrated microbes. Upon stimulation, PRRs initiate an individual intracellular signalling cascade leading to the production of immunomodulatory and chemotactic cytokines.

The link between CD and innate immunity is supported by several observations, which shall be briefly introduced:

**I. Genetic alterations in key players of innate immunity impair innate immune function**

Several susceptibility genes for IBD have been identified. In the healthy state, many of these gene products play an important role in innate defence mechanisms, regulatory cytokine signaling and intestinal barrier integrity [26, 27, 39-43]. These observations lead to the assumption, that defective immune response towards microbes is a crucial step in the pathogenesis of IBD. Deleterious immune response towards a certain pathogen is the result of either misled microbe recognition or misled immune effects in response to its recognition.



This idea is further supported by studies showing that colonic sections of patients, carrying one or more polymorphisms of the NOD2 gene exhibit impaired secretion of granulocyte macrophage colony stimulating factor (GM-CSF)[44] and other pro-inflammatory cytokines, such as TNF- $\alpha$  and Interleukin-1 $\beta$  [45] in response to NOD2 stimuli. Moreover, synergism between TLR- and NOD2-signalling is abolished in cells bearing NOD2 polymorphisms [45]. Receptors of the TLR-family are also associated with IBD and altered immune recognition. The Asp299Gly polymorphisms in the lipopolysaccharide (LPS) receptor TLR-4 is associated with impaired LPS signalling and increased susceptibility to gram-negative infection. Franchimont et al. raised evidence for a genetic association of the Asp299Gly polymorphism with CD and UC [46]. These data support the idea that defective signalling of TLR-4 and other PRRs could engender an inappropriate innate and adaptive immune response necessary to eradicate pathogens, thus resulting in more severe inflammation.

Impaired immune mechanisms against microbes also contribute to the genesis of intestinal inflammation. As an example, defensins and defensin-related cryptidins belong to the family of antimicrobial peptides (AMP) that act as the first line of extracellular defense in the intestine. They are expressed in the epithelium and paneth cells throughout the full length of the gut. Polymorphisms in the transcription factor TCF-4 lead to impaired secretion of the antimicrobial peptides and are strongly associated with small intestinal Crohn's disease[43]. Furthermore, mice with constitutively downregulated cryptidin expression are at increased risk for developing intestinal inflammation[47].

Taken together, the association of CD and susceptibility genes important for immune elements supports the role of innate immune dysfunction in the development of IBD.

## **II. Genetic disorders with immunodeficiencies present CD-like symptoms**

A typical histological feature of CD is the presence of granulomas in the affected mucosa. Generally, granulomas are the hallmark of failure of the cellular inflammatory response to remove foreign material due to impaired neutrophil function. Impaired neutrophil function is visible in congenital disorders such as glycogen storage disease (GSD-1b). Interestingly, a high percentage of patients suffering GSD-1b are also affected by gastrointestinal disorders almost indistinguishable from the symptoms of CD. Of patients identified with GSD-1b, 28% had documented inflammatory bowel disease (IBD) and an additional 22% had symptoms highly suggestive of IBD [48]. Therefore, the link between innate immunity and CD is supported by several genetic disorders with innate immune deficiencies that present a CD-

like phenotype. Patients, treated with the hematopoietic growth factor G-CSF had improvement or resolution of gastrointestinal disorders.

Also, impairments in critical functions of neutrophils, including migration, phagocytosis and superoxide production, have been demonstrated repeatedly in patients with active CD [49, 50].

## **The implications of hematopoietic growth factors on intestinal inflammation**

### **GM-CSF as a therapeutic agent in IBD**

Granulocyte macrophage colony stimulating factor (GM-CSF) belongs to a family of colony stimulating factors that regulate the proliferation of hematopoietic cells. Other members of the CSF family include granulocyte CSF (G-CSF), macrophage CSF (M-CSF) and multi CSF (mCSF), also known as IL-3.

GM-CSF, is a growth factor that primarily regulates the growth, differentiation and function of two types of white blood cells, the granulocytes and the monocyte-macrophages. It may thus be assumed that granulocyte and monocyte-macrophage growth is essentially dependent on GM-CSF. However, GM-CSF is difficult to detect in the circulation, being found in one study to be present at low levels in only half of adult human serum samples [51]. Moreover GM-CSF<sup>-/-</sup> mice exhibit normal hematopoietic function, suggesting additional physiological function of GM-CSF apart from cell growth and differentiation [52]. GM-CSF is a pleiotropic cytokine involved in inflammation and the host response. On the one hand, GM-CSF itself is produced by various cells in response to inflammatory stimuli, and, on the other hand, GM-CSF promotes inflammatory response. GM-CSF is produced by epithelial cells, smooth muscle cells and monocytes upon cytokine (IL-1 $\beta$ , TNF- $\alpha$ ) or TLR (LPS) activation [53]. GM-CSF has priming effects on cytokine-producing cells[54] and increases phagocytosis of bacteria by human neutrophils [55]. GM-CSF<sup>-/-</sup> mice show increased susceptibility to infection with *Listeria monocytogenes* [52, 56] and *Mycobacterium tuberculosis* [57].

Animal studies with GM-CSF<sup>-/-</sup> mice indicate a crucial role of GM-CSF-mediated immune function in the pathogenesis of IBD. Following 2.5% DSS administration, GM-CSF<sup>-/-</sup> mice developed more severe colitis than Wild type (WT) littermates. Disease activity was correlated with increased bacterial load in colon sections from the DSS-treated animals [58]. More evidence that GM-CSF essentially orchestrates innate immunity is seen in studies showing that patients with IBD have elevated serum levels of autoantibodies against GM-CSF, which is associated with impaired antimicrobial activity of neutrophils [59]. Exogenous

administration of GM-CSF in patients with Crohn's disease decreases disease severity and increases quality of life [60]. Though there is convincing evidence that GM-CSF effects on intestinal immunity are significantly intertwined with the pathogenesis of IBD, little is known about the molecular mechanisms by which GM-CSF influences intestinal immunity.

There is evidence that GM-CSF induces the expansion of dendritic cells (DCs) [61], a heterogeneous population of antigen presenting cells (APCs) that contribute to innate immunity and orchestrate the adaptive immune response [62].

In a mouse model of experimental colitis, exogenous GM-CSF administration ameliorated disease severity as evidenced by all clinical and biological markers. Interestingly, GM-CSF effects on colitis were associated with GM-CSF-mediated hematopoietic effects on DCs. Following GM-CSF administration, mice displayed increased numbers of plasmacytoid DCs (pDCs), a DC subpopulation specifically involved in the physiologic production of IFN-I. Interestingly, therapeutic GM-CSF effects on experimental colitis could be abolished by functional blocking of Interferon-I secretion in pDCs [63]. These findings are consistent with recent findings, underlining the special role of DCs and IFN-I in the regulation of intestinal colitis [64].

### **The role of dendritic cells in the intestinal immune response**

Dendritic cells play a pivotal role in the orchestration of the innate and adaptive immune response, as they are (i) antigen-presenting cells, (ii) equipped with a variety of PRR's (e.g. TLR) for sensing microbial infection and (iii) produce multiple cytokines in response to TLR activation that either induce or dampen T-cell activation [65].

Dendritic cells were first described by Steinman, when he and his colleagues were looking for accessory cells mediating immune response between antigens and T- and B-lymphocytes [66, 67]. These novel cells were termed dendritic cells from the Greek word "dendron", which means "tree-like". With their long dendrites, DCs reach between the epithelial layer into the intestinal lumen where they survey the microbial composition.

At least six different DC subsets have been described in mouse spleen and lymph nodes, including the conventional DC, also known as myeloid DC (CD11c<sup>+</sup>, CD11b<sup>+</sup>, CD8a<sup>-</sup>), lymphoid DC (CD11c<sup>+</sup>, CD11b<sup>-</sup>, CD8a<sup>+</sup>) and the plasmacytoid DC (CD11c<sup>+</sup>, B220<sup>+</sup>, Ly6c<sup>+</sup>, mPDCA-1<sup>+</sup>) [65], a subset capable of producing large amounts of IFN-I in response to viral infection [68, 69]. DCs survey the intestinal lumen, phagocytose and process antigens and present them to T-cells. The intertwined communication between T-cells and DCs is the key step for the

regulation of “peripheral tolerance”. During ongoing inflammation the immune system has to deal with the infection in a way that, on one hand, (i) secures the entire resolution of infection and, on the other hand, (ii) prevents the body from noxious overreactions potentially harmful for the body itself. This tight regulation is balanced by DCs that either induce a Th-1/2 reaction to produce antibodies against presented antigens or activate regulatory T-cells in an IL-10-dependent manner, which in turn suppress Th-1/-2 cell activity. In the exploration of the role of DCs in the genesis of IBD, the focus has been expanded to the IFN-producing ability of DCs, namely of pDCs, which are the major producer of type I-IFN [70].

### **Dendritic cell amplification as a therapeutic target in intestinal inflammation**

From the following characteristics of DCs it can be deduced, that DCs putatively protect against experimental colitis:

1. DCs are located in the lamina propria of the gut, positioned beneath the basement membrane. IBD is associated with epithelial barrier defects, allowing microbe translocation into the mucosa. Therefore, DCs act as a perfect early sensor of bacterial invasion.
2. DCs are endowed with a multitude of receptors of the innate immune system including TLRs. TLRs specifically recognize bacterial patterns derived from bacteria, fungi and viruses. Upon ligation, TLRs induce a signal cascade leading to the induction of pro-inflammatory cytokines, the ensuing chemotaxis of immune cells and the consequent clearance of bacteria. Among other factors, IFN-I, which is secreted from DCs upon TLR-9 stimulation, plays a decisive role. pDCs are the major source of IFN-I production.
3. IFN-I has a unique immunomodulatory function, which is mainly involved in protective effects in experimental colitis.

To test the hypothesis that amplification of DC numbers in vivo plays a potentially therapeutic role in intestinal inflammation, the previously described effect of GM-CSF was chosen to be tested. For this purpose, the use of the hematopoietic growth factor Fms-like tyrosine kinase 3 ligand was chosen, as it mimics GM-CSF effects on DC growth.

### **Fms-like tyrosine kinase 3 Ligand (Flt3L)**

Flt3L is a hematopoietic growth factor. The ligand binds the tyrosine kinase with homology to c-Kit (the receptor for stem cell factor) and c-fms (the receptor for M-CSF)[71]. Fms-like

tyrosine kinase is expressed in mouse short-term hematopoietic stem cells and multi-potent progenitors, in common lymphoid progenitors, common myeloid progenitors and at lower levels on fractions of granulocyte-macrophage progenitors as well as in mature DC's [72, 73]. Flt3 ligand-deficient mice, mice treated with an inhibitor of Flt3 tyrosine kinase as well as mice deficient for STAT3 (a transcription factor activated in the Flt3 cascade) showed drastically reduced numbers of interferon-producing cells (IPC) and DCs [74, 75] *in vivo*, indicating its essential role in the development of DCs. Flt3L is commonly used for the exploitation of DCs by *in vitro* Flt3L-mediated differentiation of bone marrow cells into bone marrow derived dendritic cells (BMDC). *In vivo* treatment of Flt3L in mice results in the expansion of dendritic cells that express both of the major DC surface markers, MHC-II and CD11c [76]. Fms-like tyrosine 3-kinase ligand (Flt3L) is a hematopoietic growth factor that is necessary for the differentiation of DCs from hematopoietic stem cells [77]. *In vivo* treatment with Flt3L expands DCs, including IFN-I producing pDCs, in the intestinal lamina propria [78] and increases IFN-I production in response to immunostimulation [79].

### **Experimental outline**

The aim of the present study was to prove the hypothesis that the amplification of DCs in mice using the hematopoietic growth factor Fms-like tyrosine 3-kinase ligand leads to augmented mucosal tolerance and a therapeutic response in IBD mouse models through effects on tolerogenic dendritic cells.

Support for this hypothesis is found in the following observations:

- (i) GM-CSF and Flt3L are both hematopoietic growth factors that can be exogenously administered to mice to induce the growth of CD11c<sup>+</sup> DCs, including the plasmacytoid DCs, which are the major producer of IFN-I.
- (ii) Exogenous treatment with Flt3L increases the production of IFN-I in response to TLR stimulation *in vivo*.
- (iii) IFN-I is a cytokine that positively modulates the intestinal immune response. The therapeutic effects of GM-CSF administration are linked with the IFN-I production ability of pDCs, as functional blocking of IFN-I secretion reverses the therapeutic outcome of GM-CSF treatment in experimental colitis.

This hypothesis will be addressed through three objectives:

- (i) To compare the influence of exogenously administered GM-CSF and Flt3L on DC

and DC subset growth in mice, using flow cytometry and immunohistochemistry.

- (ii) To prove the efficacy of exogenous Flt3L treatment in the DSS model of experimental colitis, defined by the outcome of clinical (disease activity index) and biological markers (pro-inflammatory gene expression).
- (iii) To define the influence of the hematopoietic growth factors GM-CSF and Flt3L on Toll-like receptor-mediated type I-IFN production of dendritic cells in mice.

## II. Materials and methods

### Animals

Specific pathogen-free, female, 6-8 week-old Balb/c mice and 6-8 week-old RAG1<sup>-/-</sup> mice were purchased from the Frederick Cancer Research and Development Center (Frederick, MD). Animals were housed in the Washington University School of Medicine barrier facility, maintained on light/dark cycles of 12 hours and fed a standard rodent chow diet. Procedures involving animal care were conducted in conformity to national and international laws and policies. The Washington University Animal Studies Committee approved all experimental procedures.

### Induction and evaluation of experimental colitis using Dextran Sodium Sulfate (DSS)

For DSS-induction, Balb/c mice were treated with 5 % Dextran Sodium Sulfate (USB, Ohio) for 7 days in sterile drinking water. Disease Activity Index (DAI) was daily recorded. After 7 days exposure to DSS, mice were sacrificed following halothane (Halocarbene Laboratories, River Esge, NJ) inhalation. Their colons were immediately excised from the cecum to the pelvic brim and their length was measured in centimetres. Colons were equally divided into pieces for RNA Isolation and Histology, respectively. The acute colitis induced by a single cycle of DSS administration is a T-Cell independent inflammation. It is typically characterized by colonic epithelial-cell death, mucosal oedema and the subsequent accumulation of neutrophils. Neutrophils are necessary to limit bacterial translocation to the adjacent tissues. As a consequence phagocytic monocytes and macrophages invade the inflamed tissue to remove dead cells and tissue debris and help to restore the physiologic function of the inflamed mucosa.

### Clinical scoring of DSS colitis

Clinical scoring of disease severity comprised the parameters weight loss, stool consistency and fecal blood, equally weighed in a disease activity index (DAI) as previously published [80]. Feces were subjected to occult blood testing using the seracult test (Propper Manufacturing, Long Island, NY). Stool consistency was assessed by manual exploration. Scores are defined as follows:

**Table 1 Disease activity index,**

Comprising body weight change, stool consistency and fecal blood. Total score is defined by the average of all individual scores in each category.

Score	Weight loss (%)	Stool Consistency	Fecal Blood
4	>20%	Watery	Gross macroscopic bleeding
3	11-20%	Loose	Blood trace on stool
2	6-10%	pasty to soft	Positive hemocult
1	1-5%	pasty but formed	negative
0	0%	well-formed	negative

### Macroscopic and histological assessment of colonic inflammation

Due to extensive inflammation in colon, DSS-treated mice typically display colonic shortening. At necropsy colon length was measured and the average value of each treatment group compared to another.

After colon excision, a portion of distal colon was fixed in 10 % neutral formalin buffer (Sigma, St. Louis, MO). Five-micrometer paraffin sections were cut transversely and stained with hematoxylin and eosin (H&E) for histological evaluation.

### Myeloperoxidase Assay

Neutrophil invasion plays an important role in the perseverance of ongoing inflammation and can be quantitatively assessed by detection of a myeloperoxidase substrate, an oxygen radical produced by neutrophil granulocytes. All buffers and reagents were manually prepared and listed below. On the day of the experiment snap frozen colons were thawed on ice and the weight was taken on a scale. All steps were performed on ice.

**Table 2 Myeloperoxidase assay, Buffers and reagents**

Buffer	Ingredients
Homogenate Buffer	0.5% HTAB, 10mM MOPS Solution, pH 7.0 adjusted
Sodium Acetate Buffer	Sodium Acetat, pH 6.0 adjusted
Assay Solution A	Tetramethylbenzidine, HCL, DMSAO
Assay Solution B	Sodium Acetate Buffer, Assay Solution A
Assay Solution C	Sodium Acetate Buffer, Hydrogen Peroxide
Assay Solution D	Sodium Acetate Buffer, Assay Solution C



Colons were placed back in 2 ml cryotubes (Sarstedt, Newton, NC), 750  $\mu$ l of homogenate buffer was added and colons were homogenized at least 30 seconds with a PowerGen 125 homogenizer (Fischer Scientific, Rockford/ IL).

Colon homogenates were transferred in fresh 1.7 ml microtubes and sonicated for 15 seconds with a Misonix Sonicator (Fisher Scientific, Rockford/IL). Sonication was followed by centrifugation at a table centrifuge for 15 min at 4 °C and 13.000 rpm.

After centrifugation the clear supernatant was transferred into a new 1.7 ml microtube, whereas the pellet, containing tissue debris, was discarded. The sonication-centrifugation cycles were repeated until the supernatant became clear and no remaining debris pellet after centrifugation was visible.

The clear supernatant was transferred into a fresh 1.7 ml tube and 10  $\mu$ l from that supernatant were transferred into a 96-well flat bottom plate (Nunc, Rochester, NY). The remaining supernatant was stored in -80 °C as stock solution for further experiments. 490  $\mu$ l of homogenate buffer were added to each well containing the 10  $\mu$ l sample to produce a 1:50 dilution. From the 1:50 dilution 40  $\mu$ l of sample were added to each well of a new 96 well plate and 200  $\mu$ l of Assay Solution B were added. Samples always run in quadruplicate. 25  $\mu$ l of Assay Solution D were added to each well and carefully stirred with the pipette to start the reaction. The plate was left uncovered for 30 minutes at RT. After 30 minutes a color change became visible and the reaction was stopped by adding 45  $\mu$ l of 1N Sulfuric Acid to each well.

The absorbance was measured at 450 nm with a Lightphotometer. Raw data were first subtracted with absorbance of negative control (homogenate buffer) and then adjusted to colon weight of each sample (MPO Units/mg colon).

## **Cell culture**

### **General conditions for working with cell cultures**

Work with cell culture was performed under sterile conditions, namely all materials and buffers and media used were sterile and every step was performed under a cell culture bench with laminar airflow. The human colon carcinoma cell lines HT-29 and HCT-116 were purchased from the American Type Culture Collection (ATCC, Manassas, VA). Both cell lines were supplemented with DMEM-Medium (Biowhittaker, Walkersville, MD) , enriched with 10 % FBS and 1% Streptomycin/Penicillin (Cellgro, Manassas, VA) and cultured at 37 °C and 5%

CO<sub>2</sub>. Cell medium was exchanged every second day and at 75% confluency cells were passaged into new cell culture flask. For this purpose cells were washed twice with PBS and incubated with 1x Trypsin/EDTA solution (Cellgro, Manassas, VA) for 5 min. at 37 °C and 5% CO<sub>2</sub>. Enzymatic digestion was stopped by adding FBS-containing cell medium and cells were vigorously resuspended by pipetting the cell solution up and down in a sterile 50 ml pipette tube and thereafter transferred in a new sterile 150 cm<sup>2</sup> flask. For stimulation purpose cells were transferred in 6-well dishes (Nunc, Rochester, NY) and allowed to grow until they reached 75% confluency.

### **Cell lines**

*HT-29*: This human epithelial cell lines derives from the adenocarcinoma of the colon, isolated from a 44 year old male in 1964. HT-29 cells have an epithelial-like appearance, grow as a monolayer and adhere to the cell bottom.

The division rate is every 40-60 hours. HT-29 were fed with standard cell culture medium every 2-3 days. After reaching 75 % confluency cells were trypsinized and transferred into new 150 cm<sup>2</sup> flask filled with 25 ml cell medium or subjected to cell stimulation respectively.

*HCT-116*: Human epithelial cell line with epithelial morphology derived from a colorectal carcinoma of a white male.

Adherent HCT-116 cells were fed with standard cell culture medium every 2-3 days.

### **Primary cells**

#### **Isolation of splenocytes from mice spleen**

On the day of tissue acquisition cutting board, forceps, tweezers were cleaned with ethanol and flamed over a gas flame. Mice were anaesthetized with halothane inhalation and sacrificed by cervical dislocation. The abdomen was opened with a small cut at the pelvic region and the opened abdominal wall was pulled to the cervical direction. Next, the peritoneum was carefully opened with a tweezers and the spleen bluntly removed with a forceps. The spleen was placed in a 5 cm<sup>2</sup> petri dish (BD Bioscience/CA) filled with 5 ml digestion solution (RPMI 1640, 10% FCS, 1% Penicillin/Streptomycin, 30 U/ml Collagenase VIII (Sigma/MO)). The spleen was injected with 1 ml of digestion solution using a 1 ml syringe and 26g needle until spleen turned pale. Then, the spleen was cut into small pieces using a razor blade, transferred into a 15 ml conic tube (Falcon) and incubated for 30 minutes at 37

°C in a shaker at 80 rpm. Next, the digested spleen was plunged through a 40 µm cell strainer (BD), placed on a 50 ml conical tube (Falcon) with the backside of a 2ml syringe. Cell strainer was filled with ice cold PBS to recover any remaining cell from the cell strainer and whole cell solution was centrifuged at 4 °C and 1200 rpm for 7 minutes. For hemolysis 5 ml/spleen of ACK lysis buffer was added and incubated for 5 minutes at room temperature. After hemolysis 20 ml of ice cold PBS was added and cells were spun again under same conditions. After centrifugation supernatant was removed and cells resuspended in 15 ml PBS.

### **Isolation of CD11c<sup>+</sup> Dendritic Cells using magnetic cell sorting (MACS®)**

The principle of magnetic cell sorting is the use of antibodies conjugated to 50 nm sized magnetic particles. In a first step, the antibody is added to a cell suspension and allowed to react with cells, bearing the specific antigen on its cell surface (e.g. CD11c-Antigen). In the second step, the entire cell solution is loaded onto a column, which is placed into the magnetic field of a separator. While the magnetically labelled cells are retained on the column, unlabelled cells flow through and this fraction is thereby depleted from the magnetically labelled. In a last step the column is replaced from the magnetic field and the positive, magnetically labelled, fraction can be eluted. [81]. All reagents and materials necessary for magnetic bead separation were purchased from Miltenyi Biotech (Auburn, CA). CD11c<sup>+</sup> Dendritic cells were isolated from mouse spleens. After preparing a single-cell solution by enzymatic disaggregation with Collagenase D (for details see above), cells were collected in a 15 ml tube, washed with 14 ml Automacs Running Buffer® (further mentioned as "Buffer") and centrifuged for 7 min. at 1200 rpm and +4 °C (Centrifuge conditions didn't alter, if not mentioned elsewhere). Supernatant was removed and cells resuspended in 400 µl buffer / 10<sup>8</sup> total cells. In order to prevent unspecific Fc-receptor mediated magnetic labelling, 1 µg/ 1 mio. cells anti-mouse CD16/CD32 receptor block was added. Next 100 µl MicroBeads CD11c / 10<sup>8</sup> total cells were added and allowed to incubate for 15 min at +4°C. Then the entire cell solution was washed with 2 ml buffer and centrifuged. Again, the supernatant was taken off and cells were resuspended in 500 µl buffer / 10<sup>8</sup> total cells. The cell solution was now loaded onto a pre-wetted column, placed in magnetic separator and allowed to run through in a 5 ml tube, placed below the separator. The column was thereafter washed three times with 500 µl buffer. In a last step, the column was removed from the separator, placed into a new 5 ml tube and 1 ml buffer was added onto the column.

The column, containing the positive magnetically labelled fraction, was eluted by firmly plunging the volume into the new 5 ml tube. The positive fraction was loaded onto a new column and the entire procedure was repeated in order to obtain higher purity. Cell viability and cell number were checked by mixing equal volumes of cell solution and 0.4% trypan blue stain and injecting 10  $\mu$ l of mixed solution in a Neubauer counting chamber. Under a microscope cell number of the central 25 blocks were counted and total cell number estimated by the following calculation: Final count  $\times$  2 (Trypan dilution)  $\times$   $10^4$  = cells/ml (e.g. 100 cell count =  $2 \times 10^6$  cells/ml). After cell count, total splenocyte isolation was accomplished and cells were subjected to flow cytometry, in-vitro stimulation or magnetic bead cell isolation respectively. For stimulation purpose, cells were resuspended in Dendritic Cell-Medium (RPMI-1640 + 10% FCS + 2mM L-Glutamine + 1% non essential AS, 1% sodium pyruvate + 1% Penicillin/Streptomycin) at a density of 5 mio. cells/ml and seeded in 6-well plates

#### **Gentamicin protection assay**

Treated HT-29, HCT-116 cells were 7-10 days post-confluent. One day before experiment, the regular cell medium was exchanged with cell medium, containing 1% FBS. Serum starvation was performed overnight. In a different set of experiment freshly isolated CD11c<sup>+</sup> DC were used instead of epithelial cells lines. On the same day bacterial colonies were prepared. For that purpose a loop of fresh *S. typhimurium* stock were streaked on McConkey-Agar plates. Primary, secondary and tertiary streaking was performed and at least two bacterial plates were streaked to ensure sufficient number of bacterial colonies for experiment. The day after, colonies from bacterial culture were dissolved in PBS and diluted 100 times (990  $\mu$ l PBS + 10  $\mu$ l of bacterial culture dissolved in PBS). In order to determine the number of bacteria, the optical density (OD) from the 1:100 dilution was measured using a photometer at 600 nm wavelength. Observed OD of diluted bacterial culture was multiplied by 100 dilution factor to obtain final OD of culture OD (1 OD =  $1 \times 10^8$  bacteria per ml of PBS solution). On the next morning, cells were treated according stimulation protocol and vehicle control in 1% FBS containing media for 24 hours. The day after, cell number of one individual well was counted by scrapping the cells in PBS. *S.typhimurium* was added apically to treated cells at a concentration of 10 bacteria/cell in serum free media and incubated for 1 hour at 37 °C. After 1 hour incubation cells were washed with hank's balanced salt solution (HBSS) and complete cell medium containing Gentamicin (100 mg/ml)

was added to cells and incubated for 90 minutes. Cells were then washed with PBS and 1% Triton-X buffer (500 ml/well of 6-well plate) for 15 minutes at room temperature. Triton-X buffer is required for efficient cell lysis thereby releasing the intracellular salmonella bacteria. Cell lysates were then diluted with 1 ml LB media and 50  $\mu$ l of the stock was spread on McConkey-Agar plates using plastic streaker (Nunc, Rochester, NY). Bacteria were allowed to grow overnight at 37 °C. On the following morning agar plates were withdrawn from incubator and bacterial colony forming units were counted.

## **Working with Nucleid Acids**

### **Total RNA Isolation from cell culture and whole tissues**

Total RNA from mouse tissue or epithelial cell lines respectively was performed using Trizol<sup>®</sup> Reagent (Invitrogen, Carlsbad, CA). The Trizol one step isolation is based on the RNA isolation method, first described by Chomczynsky and Sacchi [82]. In short, the phenol and guanidine-isothiocyanate solution is used to denature containing proteins and to solve denaturated proteins in the hydrophobic phenol solution. At the day of sacrifice, tissues were chopped in small pieces and transferred into 2 ml cryotubes, filled with 1 ml of Trizol reagent, and snapped frozen in liquid nitrogen. Tissues were subsequently homogenized with a homogenizer (PowerGen 125, Fischer Scientific) at full speed until tissues were fully dissolved. The tissues homogenates were transferred into autoclaved 1.7 ml tubes and incubated for 5 min at room temperature (RT). 200  $\mu$ l Chloroform per 1 ml Trizol were added to the tissue homogenates, vortexed vigorously and spun in a table centrifuge (Centrifuge 5415R, Eppendorf) at full speed and 4 °C for 15 min. The centrifugation step separates the solution into an aqueous and an organic phase. The organic phase contains proteins and DNA, whereas the RNA is dissolved in the aqueous phase. After centrifugation the upper aqueous phase is carefully removed and transferred into a new 1.7 ml tube, containing 500  $\mu$ l ice cold isopropanol. RNA and isopropanol are again vortexed and incubated for 10 min at RT, followed by an additional centrifugation at 4 °C and full speed for 15 min. During this centrifugation step the RNA precipitates and becomes visible as a gel-like pellet on the bottom of the tube. The RNA pellet is washed with 1 ml ice cold 75% Ethanol, diluted in DEPC-treated Water, and again spun for 10 minutes at full speed and 4 °C.

The supernatant is then removed and the clearly visible RNA pellet is dried by turning the 1.7 ml tubes upside down on a paper towel. According to a rough eye estimation of the pellet

size, between 10 and 50  $\mu$ l of DEPC-treated water is added to the dried RNA pellet. RNA is allowed to redissolve on ice for 4 cycles of 15 min, interrupted by vigorous vortexing.

Purity and concentration of RNA is controlled by 260/280-ratio in the photometric analysis. RNA was considered pure at a ratio higher than 1.85. RNA integrity is confirmed by electrophoretic separation of 1  $\mu$ g RNA on a 1% agarose gel, containing ethidium-bromide, in TBE-buffer at 90mV voltage and 90 min. running time. Optical affirmation of RNA integrity is performed under a UV-lamp in a gel-documentation chamber. Intact RNA typically presents a 18S- and 28S-band of the ribosomal RNA (rRNA) whereas multiple or smeared bands indicate rRNA degradation. DNA contamination is excluded by test PCR with RNA samples, using the PCR protocol in Tab. 4. Only RNA samples that had no amplification of  $\beta$ -actin were used for reverse transcription.

### **Isolation of poly A<sup>+</sup> messenger RNA using the Oligotex<sup>®</sup> mRNA Kit**

Dextran Sodium Sulfate, which was used for induction of experimental colitis in mouse, interferes with the RNA and inhibits appropriate reverse transcription. Therefore isolation of pure poly A<sup>+</sup> mRNA is a prerequisite for reliable gene expression analysis in DSS treated mice. For this purpose the Oligotex mRNA Kit (Quiagen, Valencia/CA) was used to separate the poly A<sup>+</sup> mRNA from any remaining RNA fragments, as ribosomal (rRNA) or transcriptional RNA (tRNA). The core of the Oligotex technique are polystyrene latex particles that covalently bind polyadenylic acid sequences. Any buffers used in this procedure were provided by the manufacturer. The chemical ingredients of these buffers were not listed in the instructor's manual. Total RNA was isolated from the tissue of interest using Trizol, as described above. 0.25 mg of total RNA were transferred in a 1.5 ml tube and RNase-free water was added until a final volume of 250  $\mu$ l, as well as the equal volume of OBB Buffer (Quiagen, Valencia/CA) and 15  $\mu$ l Oligotex solution. For accurate homogenization the tube was flicked several times and then incubated at 70 °C for 3 minutes in a heating block to disrupt secondary structure of RNA.

After incubation time the tube was removed from the heating block (VWR Scientific) and placed into a pre-warmed (25 °C) water bath to allow hybridization between the Oligotex particles and poly-A tail of the mRNA. After 10 minutes hybridization the Oligotex-mRNA complex was spun down in a table centrifuge for 2 minutes at maximum speed. Due to centrifugation the Oligotex-mRNA complex was clearly visible as a white pellet on the bottom of the 1,5 ml tube. The above supernatant was carefully removed, the pellet

resuspended in 400  $\mu\text{l}$  OW2 buffer by pipetting and finally transferred onto a small spin column, placed in a fresh 1,5 ml tube. The tube, including the containing spin column with the resuspended Oligotex-mRNA solution was spun down for 1 minute at highest speed. During this step, the Oligotex-mRNA complex binds to the column membrane. The column membrane was washed, by repeating the washing-centrifuging cycle with 400  $\mu\text{l}$  OW2 Buffer. Finally, the spin column was transferred in a new 1,5 ml microcentrifuge tube. 25  $\mu\text{l}$  OEB Buffer (Quiagen), preheated in a 70 °C heated heating block, was transferred onto the column and pipetted up and down, in order to moisturize the entire resin with the mRNA containing membrane. The microcentrifuge with the containing spin column were again spun at highest speed for 1 minute. To obtain highest yield of mRNA, this procedure was repeated, again with 25  $\mu\text{l}$  of OEB Buffer. At the last step, for concentration purpose, the 50  $\mu\text{l}$  mRNA solution was spun in a vacuum centrifuge for 15 min at full speed and constant vacuum.

### Reverse Transcription

One step reverse transcription was performed using Super Script Reverse Transcriptase II and random hexamer primer (Invitrogen, Carlsbad, CA). The technique of random primers was first mentioned by Feinberg and Vogelstein. In this approach small nucleotide fragments are designed, containing all 4 nucleotides mixed together on a random basis. At a primer length of 8 nucleotide there are  $4^8 = 65.563$  combinations in the mixture, and leads to a high possibility that a primer can bind to any mRNA sequence. RNA purity was confirmed by photometric analysis of the 260/280 ratio.

**Table 3 Reverse Transcription, reagents**

Material	Volume ( $\mu\text{l}$ )
random hexonucleotide primers (3000ng/ $\mu\text{l}$ )	0,08
dNTPs (stock: 100 mM)	0,10
5X first strand buffer	4,00
0.1 M DTT	2,00
DEPC treated water	9,52
Ribonuclease inhibitor (40 U/ $\mu\text{l}$ )	1,00
Reverse Transcriptase (200 U/ $\mu\text{l}$ )	1,00

RNA was defined pure at a ratio above 1.85. For a single 20  $\mu\text{l}$  sample of reverse transcription the following reagents were added: To the final volume of 18  $\mu\text{l}$  reaction solution 2  $\mu\text{l}$  of RNA (equals 1-5 $\mu\text{g}$ ) was added, mixed carefully by pipetting up and down and incubated at RT for 10 min to allow primer association to target RNA. This procedure was followed by 50 min at 42 °C and 15 min at 72 °C in a gradient cycler (PTC-200/MJ Research). After the last step the total reaction volume was cooled down by transferring the reaction tubes on ice and 180  $\mu\text{l}$  DEPC-Water was added to a final volume of 200  $\mu\text{l}$  . Efficiency of reverse transcription was tested by Real Time RT-PCR using the housekeeping gene  $\beta$ -actin.

### Polymerase chain reaction

The polymerase chain reaction (PCR) is a technique, used for the amplification of a specific sequence of the DNA [83]. The name derives from one of its key components of the reaction, the DNA polymerase. DNA polymerase amplifies a piece of DNA by in-vitro enzymatic replication. The duplicated DNA itself is used as a template for further DNA copying thus initiating a *chain reaction* in which the DNA is exponentially amplified. Sequence specific DNA amplification is granted by using primers, binding at the complementary 3' end of the target sequence, while presenting the 5' end of the new synthesized DNA matrix.

The PCR reagents for a single PCR are listed in Tab. 4.

**Table 4 Polymerase chain reaction, reagents**

Material	Volume ( $\mu\text{l}$ )
Primer-forward (100 $\mu\text{m}$ )	0.08
Primer-reverse (100 $\mu\text{m}$ )	0.08
SYBR-Green I (10.000x)	0.05
dNTP-Mix (100 $\mu\text{m}$ )	0.05
miliQ dH <sub>2</sub> O	18.96
Taq DNA Polymerase (5 U/ $\mu\text{l}$ )	0.14

The Desoxynucleotid-Triphosphate (dNTP) mixture contains the Nucleotides Adenin, Thymin, Guanin, Cytosin, essential for the synthesis of the complementary DNA sequence. PCR Buffer contains magnesium, a co-factor of the DNA Polymerase. Binding of magnesium ions to the



holoenzyme DNA Polymerase is a prerequisite for proper function. The PCR reaction mixture is heated in a Thermocycler (BioRad) to 95 °C for 5 minutes to ensure complete disaggregation of the cDNA (“Denaturation”). That followed the reaction is cooled down to 55-65 °C and the single stranded primer “anneal” to the specific complementary sequence on the target strand by establishing hydrogen bonds between the purines and pyrimidines respectively (“Annealing”). In the “elongation” step the reaction volume is reheated to 72 °C. The optimum temperature in this step depends on the DNA polymerase used. Common *Taq*-Polymerase has its optimum activity at 72-75 °C. At this step the DNA polymerase binds to the primer and synthesizes a new complementary DNA strand by adding dNTP’s in 5’ to 3’ direction. The *Taq*-Polymerase synthesizes approximately 1000 bp per minute and the elongation time is consequently adjusted to length of the expected DNA strand. The “denaturation-annealing-elongation” cycle is repeated and with every repeat the quantity of target DNA, that is the DNA within the primer region, duplicates. With 20 cycles the DNA has a 10<sup>6</sup>-fold amplification. The number of cycles performed in each PCR depends on various aspects, e.g. the starting quantity of target DNA in the PCR probe.

**a) Semi quantitative PCR with Ethidium bromide agarose gel detection**

The PCR run can be broken up into three phases, namely (i) exponential-, (ii) linear- and (iii) plateau phase.

In the initial exponential phase the number of DNA is exactly doubling with every cycle, assuming a 100 % efficiency. With rising accumulation of target DNA substrates for PCR reaction, e.g. dNTP’s, primer, exhaust and by-product that hamper PCR efficiency, e.g. Pyrophosphate, originate. The reaction rate decreases from exponential to a linear growth rate and finally reaches the plateau phase. In the plateau phase all reagents are entirely exhausted, DNA accumulation stops and PCR products can degrade.

Semi quantitative PCR evaluates the quantity of sample DNA from the plateau phase and gives a rough estimation of DNA quantity (“semi”).

Semi quantitative PCR was performed e.g. for testing binding accuracy and efficiency of newly designed primers. 1% agarose is solubilised in TBE-Buffer by boiling for 1 min. in a microwave. The mixture is carefully cooled down and 5 µl Ethidium Bromide (Sigma, St. Louis) is added. Ethidium bromide intercalates with double-stranded DNA and can be detected under a UV-lamp. The viscous liquid is loaded in a gel chamber and 5-10 dentate comb to perform the sample pockets. The hardened agarose gel is fully covered with TBE-Buffer, 5 µl

100 bp DNA-Ladder (Promega, Madison, WI) and the PCR samples are loaded on the gel. DNA fragments are electrophoretically separated (90-120 mV) according to their base pair length. Densitometric evaluation of DNA bands is performed under a UV-light.

#### **b) Real Time PCR**

Real Time PCR is the state of the art technology for quantitative assessment of multiple DNA probes. This technique was used for messenger RNA gene expression profiling in various samples, e.g. control vs. stimulated samples. In contrast to common thermal cycler, Real Time PCR cycler are equipped with a UV-lamp and a Charge-Coupled Device (CCD)-Camera enabling fluorescence signal detection after every cycle in every single probe. SYBR-Green I (Molecular Probes, CA) is used as a fluorescence dye that intercalates with double stranded DNA. As DNA quantity accumulates after every cycle so does the fluorescence intensity of the DNA probe. In contrast to detecting absolute quantities of DNA in semi-quantitative PCR, Real Time PCR measures the kinetic of DNA amplification. Quantification threshold is the number of cycles, when the fluorescence signal emerges clearly distinguishable from the background signal of the DNA probe ( $C_t$ -Value). The  $C_t$ -Value originates during the exponential phase of DNA amplification and facilitates a more accurate estimation of starting DNA quantity, than the semi-quantitative PCR. For the analysis of cytokine and defensin gene expression, gene specific mRNA sequence were obtained from the genome data base of the National center of biotechnological information (NCBI) (Bethesda, Maryland). Gene-specific primers were designed using the software *Primer express* (Applied Biosystems, CA). As far as possible primers were designed with the desired characteristics of 200-400 bp length and an annealing temperature of 60°C. Designed nucleotides were synthesized by IDT (Coralville, IA).

#### **Whole genome expression profiling using Agilent chips**

Table 5 shows the standard workflow of RNA preparation and array hybridization design. For sample cDNA synthesis 1  $\mu$ l total RNA (~ 200ng) was mixed with 1,2  $\mu$ l T7 promoter and nuclease-water was added to a final volume of 5,8  $\mu$ l. Nucleotides were denatured by incubating the reaction for 10 min. at 65 °C followed by a 5 min. incubation step on ice. For a single volume the following cDNA Master Mix was prepared, as seen in Table 6. 4,4  $\mu$ l cDNA Master Mix were added to a each sample tube and incubated at 40 °C for 2 hours, followed

by a 15 min. incubation at 65 °C and 5 min. on ice. In the meantime the Transcription Master Mix was prepared (Table 7).

**Table 5 RNA Preparation and array hybridization design**

Steps	
1	cDNA synthesis of total RNA
2	cRNA synthesis and amplification
3	cRNA purification
4	Preparation of hybridization sample
5	17-hour hybridization
6	Wash
7	Scan

Next, 0,5 µl either Cy3-CTP or Cy5-CTP was added to each tube and carefully mixed.

To each sample 14.5 µl Transcription Master Mix was added and the reaction was again incubated for 2 hours at 40 °C.

**Table 6 cDNA Master Mix**

Material	Volume (µl)
5x First strand buffer	2
0.1 M DTT	1
10mM dNTP	0.5
MMLV RT	0.6
RNase Out	0.3

Obtained cRNA was purified using RNeasy Mini spin columns (Qiagen®). 80 µl nuclease-free water was added to each tube to a final volume of 100 µl. Next, 350 µl RLT Buffer was added and mixed, followed by addition of 250 µl Ethanol. 700 µl of cRNA Mix was loaded on a RNeasy mini spin column, placed in a 2ml tube and centrifuged for 30 sec. at 13.000 rpm. The flowthrough was discarded and the RNeasy mini spin column transferred on a new 2ml tube, 500 µl RPE Buffer were added to the column and again centrifuged for 30 sec. at 13.000 rpm. The flowthrough was discarded. Again, 500 µl RPE were added to the columns and centrifuged for 60 sec. at 13.000 rpm.

For RNA elution the RNeasy mini spin column was placed in a new 1.5 ml tube, 30  $\mu$ l nuclease-free water was added to the column, incubated for 2 min. and centrifuged for 60 sec. at 13000 rpm.

**Table 7 Transcription Master Mix**

Material	Volume ( $\mu$ l)
Nuclease-free water	3,83
4x Transcription Buffer	5
0.1 M DTT	1.5
NTP Mix	2
50% PEG	1.6
RNase Out	0.12
Inorganic Pyrophosphatase	0.15
T7 RNA Polymerase	0.3

The elution step was repeated. RNA quantity was evaluated using spectrophotometric analysis. For the hybridization step equivalent volumes of 1  $\mu$ g Cy3 and 1  $\mu$ g Cy5 labelled RNA was mixed with 11  $\mu$ l 10x blocking reagent and filled with nuclease-free water to a final volume of 52.8  $\mu$ l. 2.2  $\mu$ l fragmentation buffer was added to a final volume of 55 $\mu$ l, gently vortexed and incubated at 60 °C for 30 min. in a dark chamber.

To each tube 55 $\mu$ l hybridization buffer was added, mixed well by pipetting and the entire hybridization solution was loaded onto an array and incubated for 18 hours at 65 °C. After the hybridization step the array was washed with washing buffer ( 1min with Washing Buffer 1, 2 min with Washing Buffer 2) , provided by the manufacturer, and finally rinsed with Washing Buffer 3. At the end of the procedure the glass array was inserted into an Agilent microarray scanner and analysed using Agilent feature extraction software.

## **Immunohistochemical Methods**

### **Flow Cytometry**

Flow cytometry was used for immunophenotypic screening of whole splenocytes. Cell surface protein detection was performed with either primary antibodies (antibody with specific affinity to cell surface protein, directly conjugated to a fluorescent dye) or

biotinylated antibodies (antibody with specific affinity to cell surface protein, conjugated to biotin) that were incubated in a second step with streptavidin, conjugated to a fluorescent dye. After whole splenocyte acquisition (Details see: Cell isolation) cells were blocked with blocking buffer (50  $\mu$ l/1mio cells), transferred into v-bottom 96-well plates (Nunc, NY) at a density of 1mio. cells/well and were incubated for 20 min. at +4 °C.

In the meantime antibody dilution were prepared on ice. If not explicitly mentioned, a 1:50 dilution in blocking buffer was used. Next, biotinylated antibodies were added to 96-well, according to flow cytometry protocol (50  $\mu$ l/well) and incubated on ice. After another 20 min. 100  $\mu$ l washing buffer was added to every well and the 96-well plate was placed in a centrifuge and spun for 5 min. at 1200 rpm and +4 °C. The supernatant was carefully removed using a multichannel pipette. Next 50  $\mu$ l of primary or streptavidin antibody were added to each well and again incubated for 20 min. at +4 °C. In a final step cells were again centrifuged, supernatant removed and cells were fixed in a paraformaldehyd containing solution. Flow cytometry was performed on an analyzer modified to 2 lasers and 5 fluorescent detectors (BD-Bioscience/CA), according to manufacturers protocol. Dead cells were excluded based on forward and side light scatter. Statistical evaluation was performed with FlowJo® software (Tree Star, Or).

### **Immunohistochemistry**

After tissue removal from sacrificed mice, colons were rinsed with cold PBS and afterward rinsed with OCT® liquid. Approximately 5 cm long colon sections were embedded in plastic molds, filled with OCT® and snap frozen in liquid nitrogen. From each tissue 3 different 5  $\mu$ m thick sections were cut using a cryostat, sections were stored onto slides and kept at -20 °C. For immunohistochemical staining, tissues were fixed in 4% paraformaldehyde (PFA) for 10 min. After fixing, tissues were washed three times in PBS for at least 5 min. Next, tissues sections were circumscribed on the slide with a hydrophobic ImmEdge pen. Then, tissues were blocked, using a ready to use blocking solution (Pierce) for 10 min, by carefully pipetting 100  $\mu$ l of blocking solution on the tissues area, which was circumscribed prior with the hydrophobic pen. Slides were placed in a humid chamber, filled with water. In the meantime 1  $\mu$ l of AB was added to 99  $\mu$ l Blocking solution (Pierce, Rockford, IL) and kept on ice and protected from light. After 10 minutes incubation, the blocking buffer was aspirated from slide and 100  $\mu$ l of antibody solution/well was added. Slides were placed back in the humid chamber, lid was closed to protect dye conjugated antibodies from light and kept at

RT for 1 hour. After 1 hour incubation slides were washed 3 times with PBS for each 5 minutes. After the third wash, PBS was fully aspirated and slides were allowed to dry for 10 minutes. Tissue sections were covered with one drop of glycerol-vinyl-alcohol (GVA) mount (Zymed, San Francisco, CA) and a coverglass was gently placed on the top of each section to prevent any bubbles between coverglass and tissue. Again, the slides were allowed to dry for 10 minutes. Four-color fluorescence microscopy of cryosections was performed with an Olympus BX51 equipped with 100W mercury lamp (Olympus) and a SPOT RT CCD camera (Diagnostic Instruments). Monochrome images (1200 pix 31600 pix = 885 3 1180 mm with 103 objective; 440 3 586 mm with 203 objective, 12-bit depth) were acquired through fluorescence filters optimized for DAPI, FITC, TRITC, and Cy5 (Chroma). Images were acquired, processed to reduce background, pseudo-colored, and merged with SPOT RT camera software.

### **Statistical Analysis**

Statistical analysis of significance was determined by Student's *t*-test for unpaired data with Welch correction using GraphPad InStat (GraphPad Software, San Diego, CA). A  $P < 0.05$  was considered significant.

### III. Results

#### Characterisation of GM-CSF and Flt3L effects on DC growth in mice in vivo

Sainathan et al. have previously shown that daily treatment with 5  $\mu\text{g}$  of the hematopoietic growth factor GM-CSF ameliorates DSS-induced colitis [63]. This effect was mainly mediated by GM-CSF induced expansion of IFN-I producing pDCs. In order to define the role of Flt3L mediated DC expansion on the clinical outcome of experimental colitis, the first aim was to define the appropriate concentration of Flt3L, necessary to achieve effects on DC growth *in vivo*, similar to the therapeutic GM-CSF dose of 5  $\mu\text{g}/\text{mouse}$ . In detail Flt3L concentration was defined to be appropriate, that equals GM-CSF in its capacity to expand splenic (i)  $\text{CD11c}^+, \text{MHC-II}^+$  DCs and (ii)  $\text{CD11c}^+, \text{B220}^+, \text{Ly6c}^+, \text{mPDCA-1}^+$  plasmacytoid DCs. For this purpose, mice were treated with either 5  $\mu\text{g}$  pegGM-CSF (n=3) or 20 $\mu\text{g}$  Flt3L (n=3) or left untreated (n=3) for 4 consecutive days. After 4 days of treatment, mice were sacrificed, spleens removed and pooled according to treatment group. Splenocytes were stained with AB and subjected to FACS analysis. The presented data are representative of 3 individual experiments.

#### Immunophenotype of splenic DC

Total splenocytes obtained from mice were subjected to FCS and SSC gating to exclude dead cells and further gated for total dendritic cells ( $\text{CD11c}^+, \text{MHC-II}^+$ ).

Compared to untreated animals (4.1% of total splenocytes,  $1.2 \times 10^6$  cells/spleen), GM-CSF (12.6% of total splenocytes,  $8.4 \times 10^6$  cells / spleen) and Flt3L (10.5% of total splenocytes,  $6 \times 10^6$  cells/spleen) both increase the absolute number of DC in spleens (Table 8).

**Table 8 Statistical evaluation of Flt3L and GM-CSF effects on Dendritic cell growth in vivo.**

	$\text{CD11c}^+ / \text{MHC-II}^+$	$\text{B220}^+, \text{Ly6c}^+, \text{CD11c}^+, \text{mPDCA-1}^+$	$\text{CD11c}^+, \text{CD11b}^+$	$\text{CD11c}^+, \text{CD8a}^+$
Control	4.1 +/- 0.3 %	0.7 +/- 0.1 %	1.6 +/- 0.1 %	0.8 +/- 0.3 %
GM-CSF	12.6 +/- 3.5 %	2.1 +/- 0.1 %	11 +/- 2.6 %	1.9 +/- 0.4 %
Flt3L	10.5 +/- 1.5 %	2.2 +/- 0.1 %	3.2 +/- 1.3 %	1.7 +/- 0.2 %

In order to identify the number of pDCs ( $\text{B220}^+, \text{Ly6c}^+, \text{CD11c}^+, \text{mPDCA-1}^+$ ), total splenocytes were gated for  $\text{B220}^+$  and  $\text{Ly6c}^+$  expression. Double positive cells ( $\text{B220}^+, \text{Ly6c}^+$ ) were subsequently gated for their expression of  $\text{CD11c}^+$  and  $\text{mPDCA-1}$ . Cells, with positive signal for all 4 markers ( $\text{B220}^+, \text{Ly6c}^+, \text{CD11c}^+, \text{mPDCA-1}^+$ ), were defined as plasmacytoid dendritic cells. As shown in Figure 3D, control mice have a very low number of pDCs (0.7% of total

splenocytes,  $0.2 \times 10^6$  cells/spleen). The number of pDCs in splenocytes is expanded upon GM-CSF and Flt3L treatment.

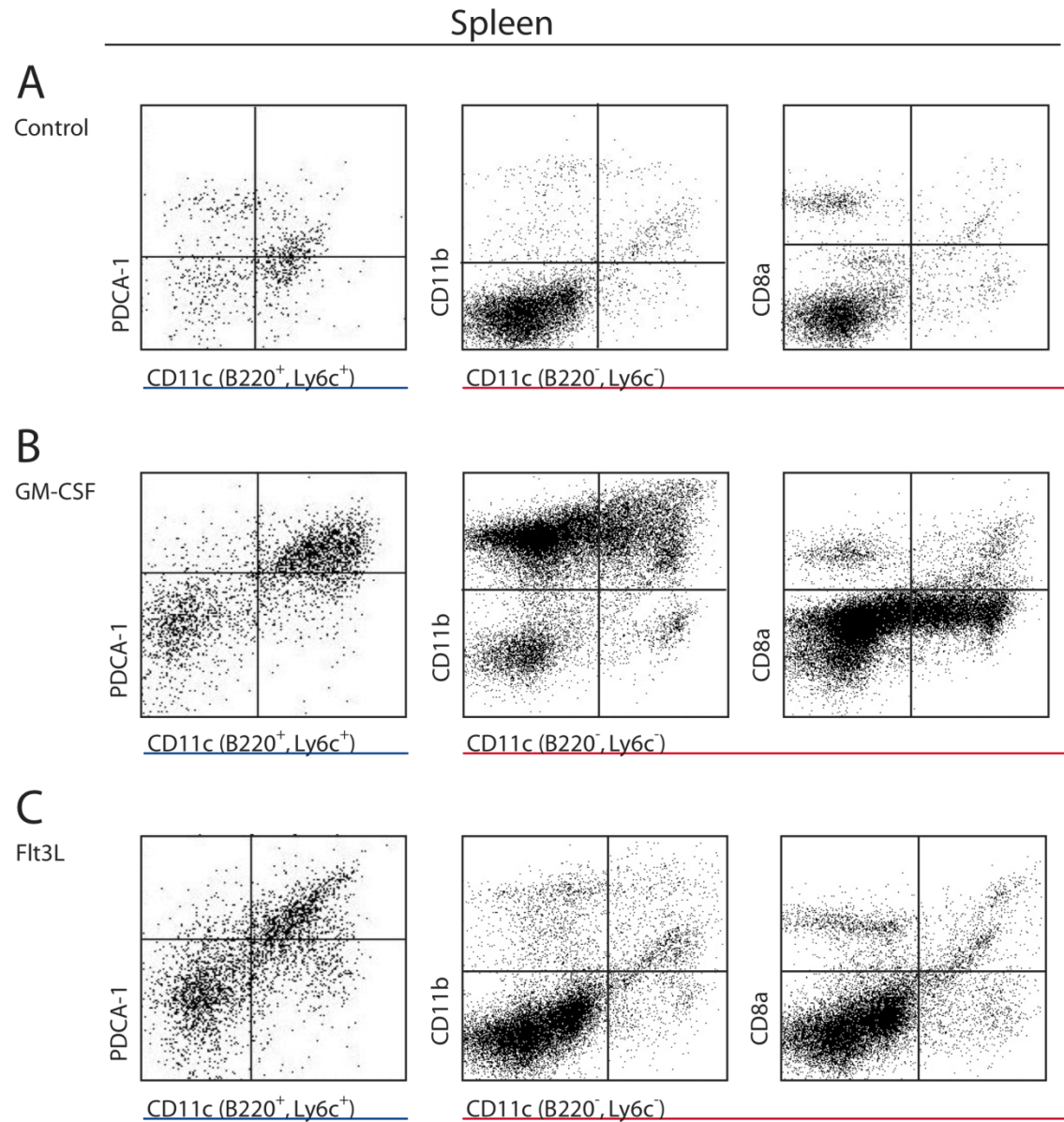


**Figure 1** Flow cytometrical analysis of DC population in spleen.

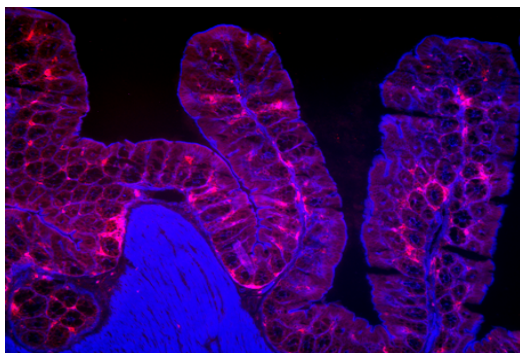
DC subsets were detected by CD11c<sup>+</sup> gating and subsequent analysis of pDC (CD11c<sup>+</sup>, B220<sup>+</sup>, Ly6c<sup>+</sup>, mPDCA-1<sup>+</sup>), mDC (CD11c<sup>+</sup>, B220<sup>-</sup>, CD11b<sup>+</sup>, CD8a<sup>-</sup>) or IDC (CD11c<sup>+</sup>, B220<sup>-</sup>, CD8a<sup>+</sup>) surface marker expression.

Daily administration of Flt3L and GM-CSF over the time course of 4 days showed a comparable capability of expanding pDC population in spleen (GM-CSF: 2.2% of total splenocytes,  $1.4 \times 10^6$  cells/spleen; Flt3L: 2.3% of total splenocytes,  $1.1 \times 10^6$  cells/spleen). B220<sup>-</sup>, Ly6c<sup>-</sup> - double negative cells were consecutively investigated for their expression of CD11c, CD11b (myeloid DC) or CD11c, CD8a (lymphoid DC). Again, GM-CSF and Flt3L similarly expanded CD11c<sup>+</sup>, CD8a<sup>+</sup> IDC (GM-CSF: 1.8% of total splenocytes,  $1.3 \times 10^6$  cells/spleen; Flt3L:



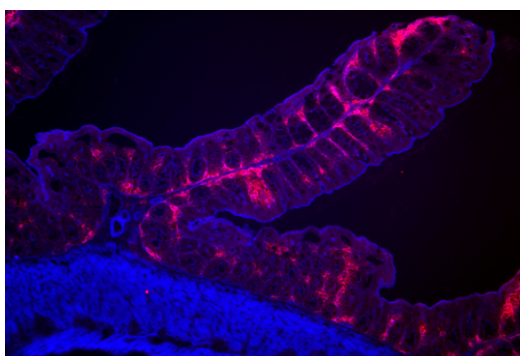
1.7 % of total splenocytes,  $0.85 \times 10^6$  cells/spleen) compared to untreated mice (0.8 % of total splenocytes,  $0.24 \times 10^6$  cells/spleen). Interestingly, GM-CSF is more capable of mDC expansion (11% of total splenocytes,  $7.7 \times 10^6$  cells/spleen) than Flt3L treatment (3% of total splenocytes,  $1.5 \times 10^6$  cells/spleen). These data indicate, that Flt3L treatment has an equivalent potency to expand the number of total CD11c<sup>+</sup>, MHC-II<sup>+</sup> DCs as well as B220<sup>+</sup>, Ly6c<sup>+</sup>, CD11c<sup>+</sup>, mPDCA-1<sup>+</sup> pDCs in mice.

A



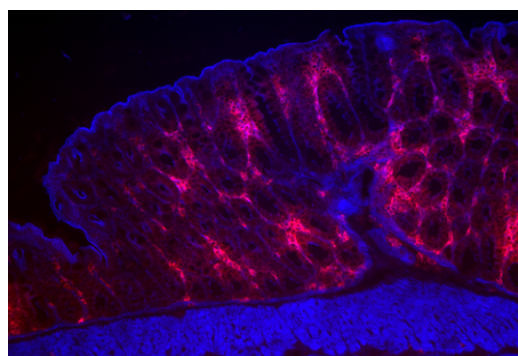
Control

B



GM-CSF

C



Flt3L

### Figure 2 Immunohistochemistry of Dendritic Cells in colon sections.

Functional comparison of the hematopoietic effects of exogenous GM-CSF and Flt3L on DC growth *in-vivo*. Balb/c mice were treated with 5 $\mu$ g GM-CSF (n=3), 20 $\mu$ g Flt3L (n=3) or PBS (n=3) for 4 consecutive days. DCs are present in the lamina propria of colon in (A) normal mice and their number is expanded after treatment of mice with (B) GM-CSF or (C) Flt3L. Fluorescence microscopy images of colon stained with Phalloidin to demonstrate actin filaments and anti-CD11c (Phycoerythrin) to detect DC are shown (20x magnification).

### Growth effects on intestinal DC

Colons from mice were subjected to immunohistochemical staining with anti-CD11c AB. Untreated animals show a uniform distribution of CD11c<sup>+</sup> DCs in the large intestine, mainly localized in the lamina propria of the colonic tissue (Figure 2a). Daily treatment with GM-CSF and Flt3L equally expands CD11c<sup>+</sup> DCs. (Figure 2b,c). These data indicate, that the effects of

GM-CSF and Flt3L treatment on DC expansion is not restricted to the splenic tissue, but is also found in the intestine.

## Evaluation of Flt3L effects in mouse models of acute colitis

### DSS-induced acute colitis in balb/c mice.

#### Experimental outline

In order to study the impact of Flt3L treatment on acute intestinal inflammation, acute colitis by adding 5 % DSS to the drinking water for 7 days and treated Balb/c mice with (DSS+Flt3L, n=5) or without (DSS, n=5) daily injections of 20µg Flt3L. Control mice received sterile drinking water with (Flt3L, n=5) or without (Control, n=5) daily Flt3L injections. This experiment was repeated 3 times.

**Table 9 DSS-induced colitis in balb/c mice.**

Treatment Group	Control	DSS	Flt3L	DSS+Flt3L
Number of mice treated/experiment	5	5	5	5
Total number	15	15	15	15

### Phenotype

#### Disease activity index

Disease activity index (DAI) was measured, comprising weight loss, rectal bleeding and stool consistency. DAI increased in DSS and DSS+Flt3L treated animals and became significant on day 4 (Figure 3). DAI reached maximum on day 7. As expected, animals treated with DSS exhibited an increase of DAI compared to untreated animals (DSS: 2.6, \*\*P< 0.005 vs. Control). Surprisingly, Flt3L co-treatment in DSS group elicited higher DAI, compared to DSS animals alone, which however reached no statistical significance (DSS+Flt3L: 3.2, ##P < 0.005 vs. Control). Flt3L-alone treated mice as well as control mice showed no increase of DAI over the time course of 7 days.

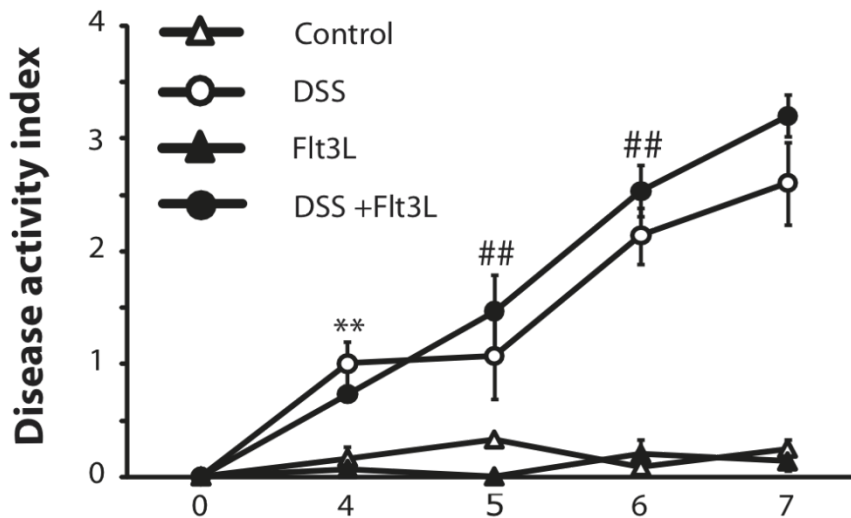


**Figure 3 Disease activity index (DAI)**

Flt3L treatment has no protective effect in DSS-induced colitis. DAI increased in DSS (\*\* $P < 0.005$  vs. Control) and DSS+Flt3L (### $P < 0.005$  vs. Control) treated mice over the time course of treatment.

### Colon length

In addition to clinical markers, colon length was measured at necropsy. As a consequence of intestinal inflammation, oedema evolves in the colon and leads to colonic shortening. Thus, the evaluation of colon length in the DSS colitis is therefore another clinical marker for severity of inflammation.

Colon length in DSS (7.3 cm, \* $P < 0.05$ ) exhibited significant shortening compared to untreated controls (9.7cm). Comparing colon length of DSS and DSS +Flt3L cohorts, Flt3L-treatment significantly increased colonic shortening (6.4cm vs 7.3, ### $P < 0.05$ )(Figure 4).

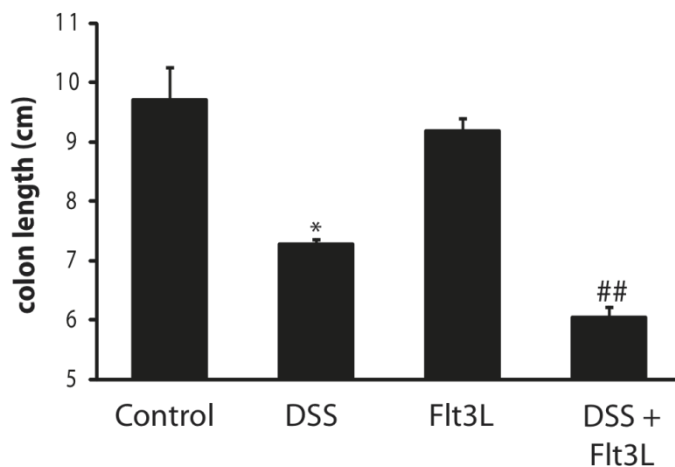


**Figure 4 Colon length**

Flt3L+DSS treated mice show significantly reduced colon length compared to DSS treatment alone, indicating severer inflammation (\* $P < 0.05$  DSS vs. Control, ### $P < 0.05$  DSS+Flt3L vs. DSS). Data are expressed as the mean +/- SEM.

### Histology

Histological examination of H&E stained colon sections displayed a loss of crypt architecture, ulcerations and increased neutrophil invasion in both DSS and DSS+Flt3L groups ( Figure 5), whereas colons from control and Flt3L-alone treated mice resembled healthy mucosa (data not shown).

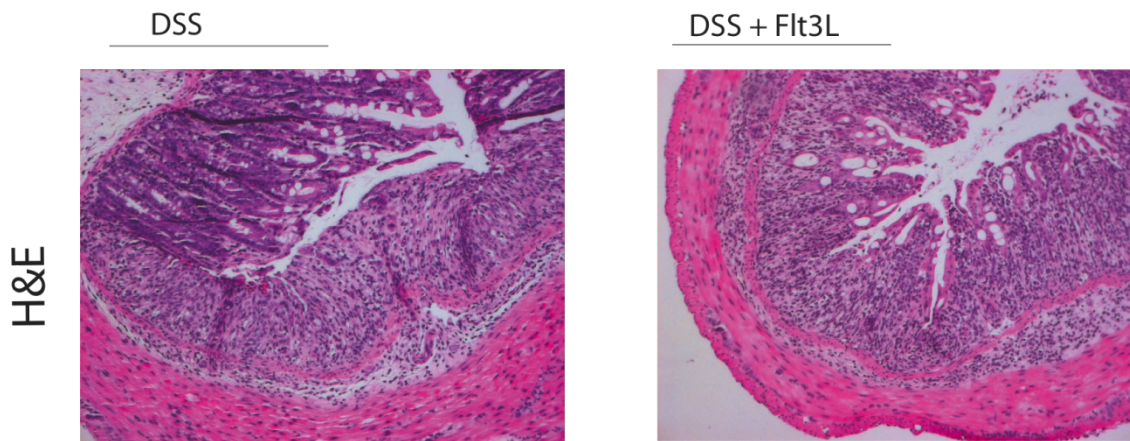


**Figure 5 Histology of colon sections**

Inflammatory infiltrates and loss of crypt architecture in histological sections of DSS and DSS+Flt3L treated animals. H&E Staining, 20x magnification.

### Biological marker of intestinal inflammation

#### Myeloperoxidase Assay

Neutrophil granulocyte invasion plays an important role in the perseverance of ongoing inflammation and can be quantitatively assessed by detection of myeloperoxidase, an enzyme produced by neutrophil granulocytes. Colons of sacrificed mice were subjected to myeloperoxidase assay. Compared to baseline units in control mice, myeloperoxidase units (Figure 6) were consistently increased in colons of DSS treated animals (3.8 U/g colon) vs. control colons (0.8 U/g colon, \*P < 0.05 vs. Control).

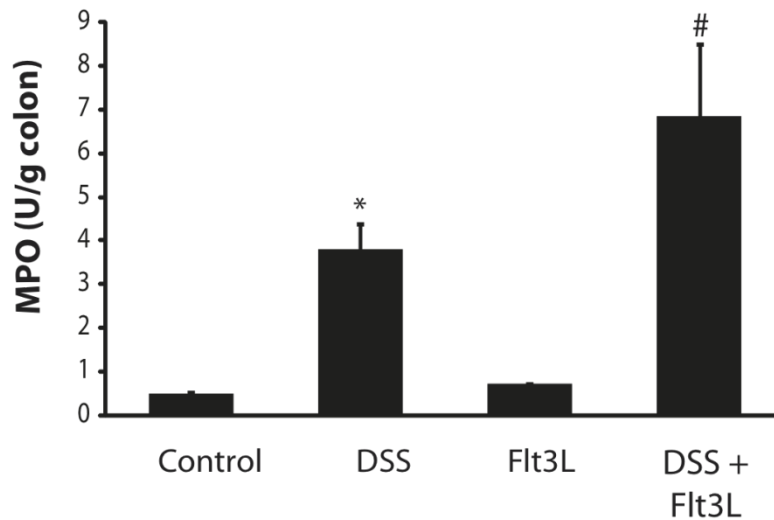


**Figure 6 Myeloperoxidase assay in colon homogenates from DSS induced colitis.**

MPO activity is increased in DSS groups, but is surmounted in DSS+Flt3L treatment groups ( $P^* < 0.05$ , vs. Co;  $P^{\#} < 0.05$  vs. DSS). Data are expressed as the mean +/- SEM.

Colons from mice, co-treated with Flt3L (DSS+Flt3L) treatment, displayed increased myeloperoxidase activity (6.8 U/g,  $^{\#}P < 0.05$  vs. DSS). The myeloperoxidase activity in colon sections from Flt3L-treated animals was at the same level as in the control-treatment group (0.6 U/g colon).

### Proinflammatory gene expression

Proinflammatory gene expression was assessed by Real Time PCR (Figure 7) of colon homogenates.

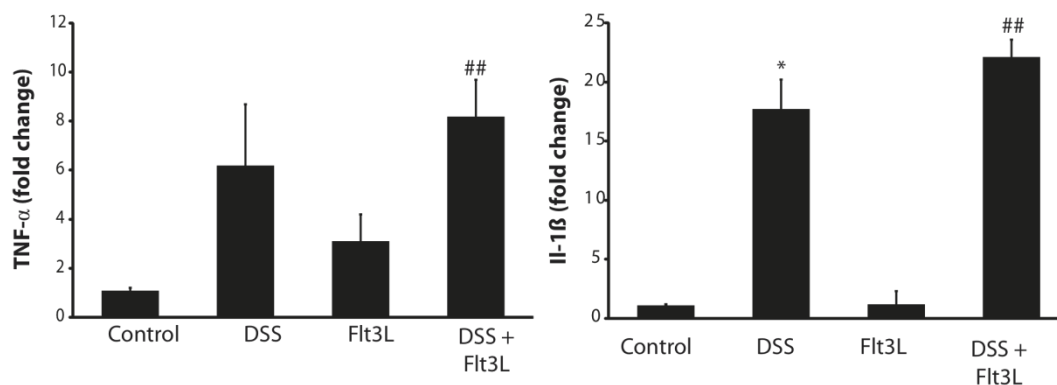


**Figure 7 Proinflammatory gene expression in colon samples from DSS-induced colitis.**

Gene expression of TNF- $\alpha$  and IL-1 $\beta$  is increased in colon samples from DSS ( $*P < 0.05$  vs. Co) and DSS+Flt3L treated animals ( $^{\#}P < 0.01$  vs. Co). Data are expressed as the mean +/- SEM.

The gene expression level of the proinflammatory cytokine TNF- $\alpha$  (DSS+Flt3L: 8.2-fold,  $^{##}P < 0.005$  vs. Control) and Interleukin-1 $\beta$  (DSS: 17.7-fold,  $^*P < 0.05$  vs. Control; DSS+Flt3L: 22.2-fold,  $^{##}P < 0.005$  vs. Control) were increased in both, the DSS and the DSS+Flt3L treatment group, when compared to untreated animals. Treatment with Flt3L alone did not show any alteration in pro-inflammatory gene expression compared to untreated animals.

### Flow Cytometry

In order to describe the hematopoietic effects of Flt3L treatment on the DC growth, excluding the possibility of a lack of therapeutic effect due to a lack of hematopoietic effect, mice were sacrificed, spleens removed and pooled according to treatment group. Splenocytes were stained with AB and subjected to FACS analysis. After dead cell exclusion by FSC and SSC gating, splenocytes were analysed for their antibody signal of CD11c-PE and MHC-II FITC. Double positive cells, were defined as DCs. As seen in figure 8, DSS-treated splenocytes display a number of 2.92 % CD11c $^+$ ,MHC-II $^+$  DCs of total analysed splenocytes. Mice, treated with the hematopoietic growth factor Flt3L showed more than a 2-fold increase of CD11c $^+$ ,MHC-II $^+$  DCs (7.47 %), compared to DSS-mice. These data indicate, that Flt3L has a hematopoietic effect in DSS-treated mice and thereby excludes the possibility, that a lack of therapeutic effect evolves from a lack of function of Flt3L in general.

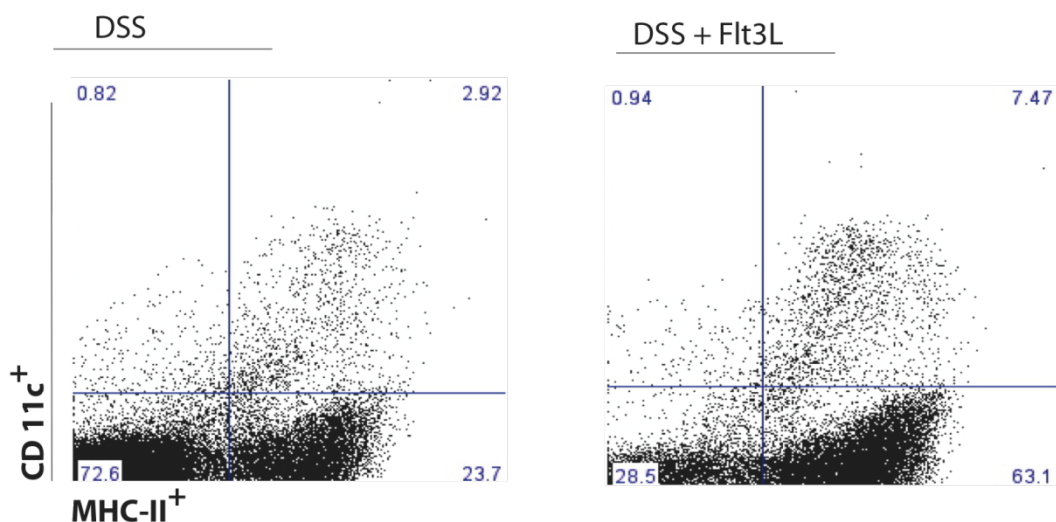


**Figure 8 Flow cytometry of splenocytes from DSS and DSS+Flt3L treated mice.**

Hematopoietic effects of daily Flt3L injection on DC growth were determined by flow cytometry on day 7. Splenocytes (n=5/group) were stained with antibodies against CD11c and MHC-II antigens and CD11c $^+$ , MHC-II $^+$  cells were defined as DC's.

Taken together, the phenotypical data, comprising weight loss and colon length, as well as the biological marker, myeloperoxidase assay and proinflammatory gene expression, indicate, that daily administration Flt3L has no protective effect in the DSS-induced acute colitis in balb/c mice.

### DSS-induced acute colitis in RAG1<sup>-/-</sup> mice

#### Experimental outline

The initial hypothesis claimed a protective role of Flt3L in the acute colitis model. The results described above however failed to approve a protective role of Flt3L treatment.

As Flt3L treatment in mice increased the number of pDCs in a similar manner as GM-CSF it was assumed, that Flt3L, similar to GM-CSF, protects from experimental colitis in a pDC-IFN-I dependent manner. The protective IFN-I effects were individually described to independent of the adaptive limb of the immune system, indicating a role in the modulation of innate immunity.

**Table 10 DSS-induced colitis in RAG1<sup>-/-</sup> mice. Treatment groups.**

Treatment Group	Control	DSS (4%)	DSS (4%)+Flt3L (20µg/mice)
Number of mice treated	3	5	5

To explore whether Flt3L effects are independent of the adaptive arm of the immune system, the DSS model was examined in T- and B-cell deficient mice. Therefore, DSS-induced acute colitis was induced in T- and B-cell deficient mice. Mice homozygous for a deletion in the recombinant activating gene (RAG1<sup>-/-</sup>) lack mature B and T cells. Acute colitis was induced by adding 4% DSS to the drinking water for 7 days and RAG1<sup>-/-</sup> mice were treated with (DSS+Flt3L, n=5) or without (DSS, n=5) daily i.p. injections of 20 µg Flt3L. Control RAG1<sup>-/-</sup> (Control, n=3) received sterile water.

#### Phenotype

Disease activity index (DAI) was measured, comprising weight loss, rectal bleeding and stool consistency. Animals treated with DSS and DSS+Flt3L exhibited an increase of DAI compared to untreated animals (DSS: 4, \*P < 0.005, DSS+Flt3L: 4,3, \*P < 0.005).

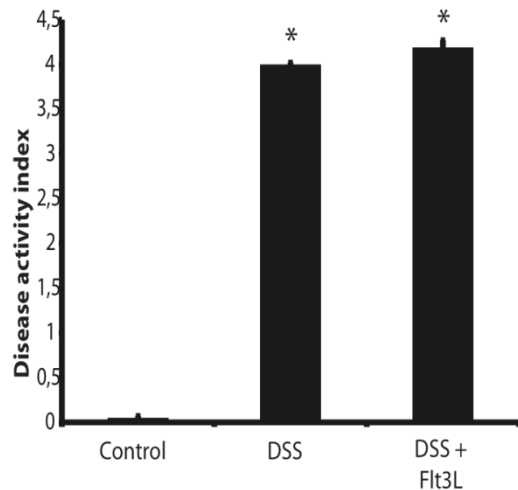


**Figure 9 Disease activity index in DSS-induced colitis in RAG1<sup>-/-</sup> mice.**

Flt3L+DSS treatment does not reduce disease activity according to DAI, compared to DSS treatment alone (\*P<0.05 vs. Co). Data are expressed as the mean +/- SEM.

In addition to clinical markers, colon length was measured at necropsy. As seen in figure 10, colon length in DSS (6 cm) and DSS+Flt3L (5,4 cm \*P < 0.05 vs. DSS) exhibited significant shortening compared to untreated controls (9,4cm).

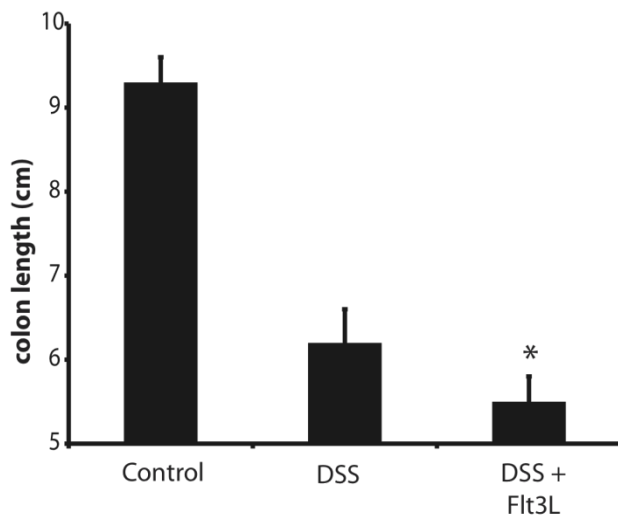


**Figure 10 Colon length in after DSS-induced colitis in RAG1<sup>-/-</sup> mice.**

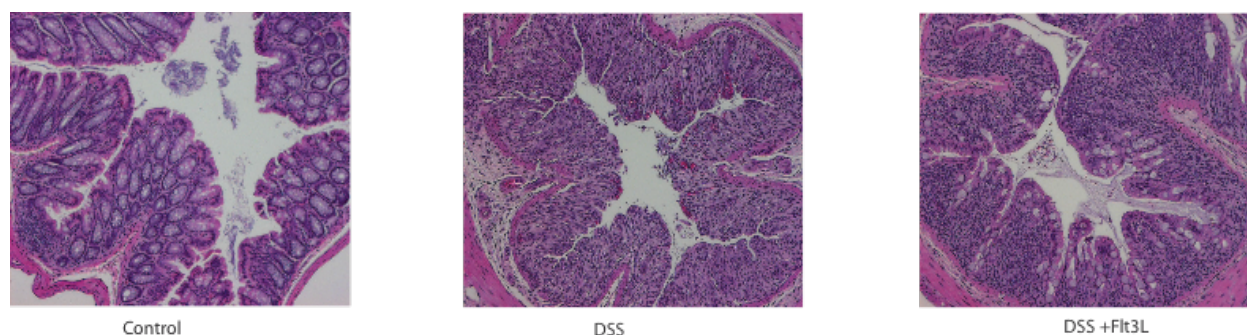
Colonic shortening is visible in DSS mice, but DSS+Flt3L co treatment significantly reduces colon length (\*P<0.05 vs. DSS). Data are expressed as the mean +/- SEM.

### Histology

H&E staining in DSS treatment group shows mucosal ulceration and crypt damage, compared to healthy control (Figure 11), similar to that observed in wildtype mice.

Flt3L treatment in DSS colitis showed no amelioration in mucosal damage.





#### Histology of colon section in DSS-induced colitis in RAG1<sup>-/-</sup> mice.

Inflammatory infiltrates and loss of crypt architecture in histological sections of DSS and DSS+Flt3L, but not in untreated animals (Magnification 20x).

#### Biological marker of intestinal inflammation

Colon homogenates were subjected to TNF- $\alpha$  detection using an ELISA detection kit (Biossource). Production of the proinflammatory cytokine TNF- $\alpha$  in colon tissues was significantly increased in DSS+Flt3L treated animals, compared to DSS treatment group alone (\*P<0.05 vs. DSS). Taken together, these clinical and biological data indicate, that daily administration Flt3L has no ameliorative effect on the severity of clinical and biological markers of inflammation in DSS-induced acute colitis in RAG1<sup>-/-</sup> mice.

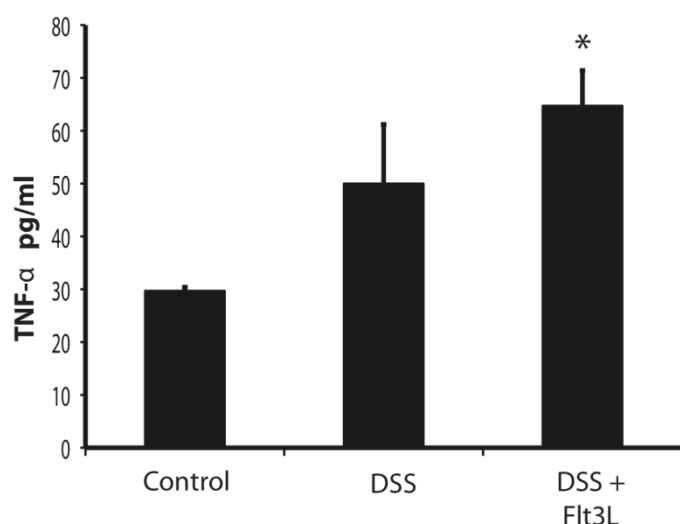


**Figure 11 TNF- $\alpha$  protein levels in colon homogenates.**

Colon homogenate samples from DSS treated animals show increased concentration of TNF- $\alpha$  protein. DSS+Flt3L co-treatment significantly increases TNF- $\alpha$  load (\*P<0.05 vs. DSS). Data were obtained by ELISA and are expressed as the mean  $\pm$  SEM.

### Functional analysis of GM-CSF and Flt3L treatment in mice *in vivo*.

CpG motifs exert protective effects in mouse models of intestinal inflammation and multiple studies create persuasive evidence that these effects at least partly depend on a TLR-9-dependent IFN-I secretion. [64, 84, 85] Sainathan et al. recently reported that the beneficial effects of GM-CSF treatment in mouse models of IBD are also mediated by IFN-I dependent mechanism, as functional blocking of the IFN-I secretion in pDCs reversed the outcome in acute colitis. Flt3L, similar to GM-CSF, expands the *in vivo* number of pDCs, but fails to protect mice from severe colitis. The question was posed, whether the opposite clinical outcome between Flt3L and GM-CSF mediated DC expansion is associated with opposite effects on TLR-9 mediated IFN-I secretion, induced by *in vivo* stimulation with CpG motifs?

### Priming effects of GM-CSF and Flt3L on TLR-9 stimulation

In order to assess the influence of GM-CSF and Flt3L mediated DC expansion on the *in vivo* production of IFN-I in response to TLR-9 stimulation, Balb/c mice were administered with GM-CSF (5µg/mice), Flt3L (20µg/mice) or PBS for 4 consecutive days. On day 5 mice received intraperitoneal injections of 200µg of ODN1018, a synthetical ligand of the TLR-9 receptor. After 18 hours of stimulation, mice were sacrificed and tissues (spleen, colon, small intestine) were obtained, subjected to RNA isolation and further prepared for Real Time RT-PCR analysis.

**Table 11 GM-CSF and Flt3L priming of TLR-9 activation in mice.**

Experiment was performed 3 times with equal treatment groups size.

Treatment Group (n=number of animals)					
Control (n=3)	PBS	PBS	PBS	PBS	PBS
Control + CpG (n=3)	PBS	PBS	PBS	PBS	CpG-ODN (200µg)
GM-CSF + CpG (n=4)	GM-CSF (5µg)	GM-CSF (5µg)	GM-CSF (5µg)	GM-CSF (5µg)	CpG-ODN (200µg)
Flt3L + CpG (n=4)	Flt3L (20µg)	Flt3L (20µg)	Flt3L (20µg)	Flt3L (20µg)	CpG-ODN (200µg)
Time	24h	24h	24h	24h	18h

Using Real Time RT-PCR, IFN-I genes as well as multiple IFN-I dependent and regulatory genes upregulated upon IFN-I stimulation were measured.

The detection of type I-IFN on mouse serum protein level is limited by the absence of reliable detection kits. Real Time PCR was used to detect mRNA Expression of IFN-I genes (IFNa2, IFNa9), as well as the type I-IFN inducible/regulatory genes (Ifit3, IRF7) in spleen, small intestine and colon tissues. Irf7, is a rate limiting transcription factor located in the

center of a self-amplifying positive feedback loop of massive IFN- $\alpha$  production [86]. The inducibility of IFN- $\alpha$  production in various tissues/cells and their steady state level of IRF7 proteins are known to be closely correlated [87]. Therefore, the detection of IFN-I inducible gene expression, is a much more reliable approximation of IFN-I expression on the protein level, as the single gene expression detection of IFN-I genes.

In spleen samples, (Figure 13) CpG treatment alone led to an increase in mRNA production of IFN- $\alpha$ 2 (8.2-fold), IFN- $\alpha$ 9 (4.7-fold), Ifit3 (2.9-fold) and IRF-7 (2.8-fold), compared to control samples. Splens from mice, pretreated with GM-CSF before CpG administration, displayed an increase in the fold induction of IFN-I and IFN-I inducible genes, compared to CpG-alone treated animals: IFN $\alpha$ 2 (50.2-fold, \*P < 0.05 vs. Co+CpG), IFN $\alpha$ 9 (52.7-fold, \*P < 0.05 vs. Co + CpG ), Ifit3 (15.8-fold, \*P < 0.05 vs. Co + CpG), IRF-7 (22.7-fold, \*P < 0.05 vs. Co + CpG).

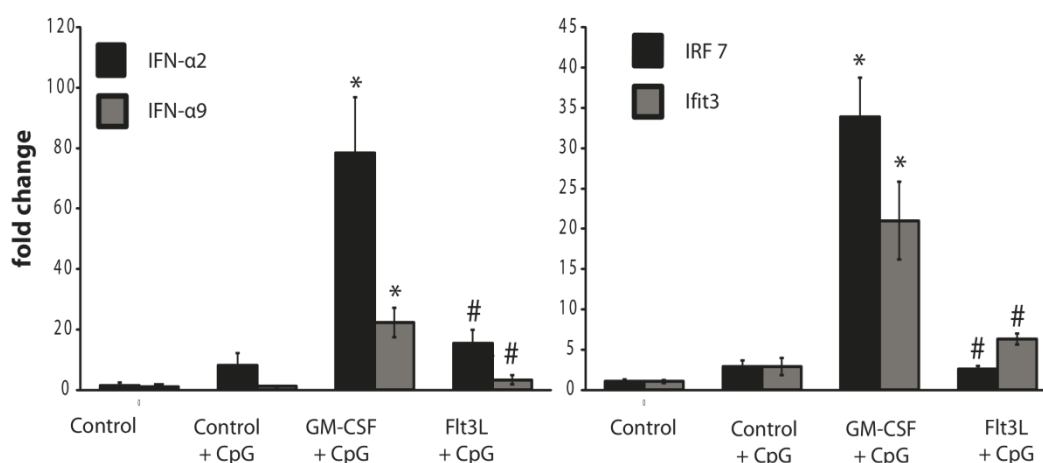


**Figure 12 Real Time PCR of IFN-I and IFN-I inducible gene expression in spleen.**

GM-CSF, but not Flt3L potentiates CpG induced IFN-I gene expression(\*P<0.05 vs Co+CpG; #P<0.05 vs. GM-CSF+CpG). Data are expressed as the mean +/- SEM.

Figure 13 exhibits, that Flt3L treated animals showed a markedly decreased augmentation in IFN $\alpha$ 2 (15.3-fold, #P < 0.05 vs. GM-CSF + CpG ), IFN $\alpha$ 9 (3.3-fold, #P < 0.05 vs. GM-CSF + CpG ), Ifit3 (6.3-fold, #P < 0.05 vs. GM-CSF + CpG ), IRF-7 (2.6-fold, #P < 0.05 vs. GM-CSF + CpG), compared to GM-CSF+CpG treatment group.

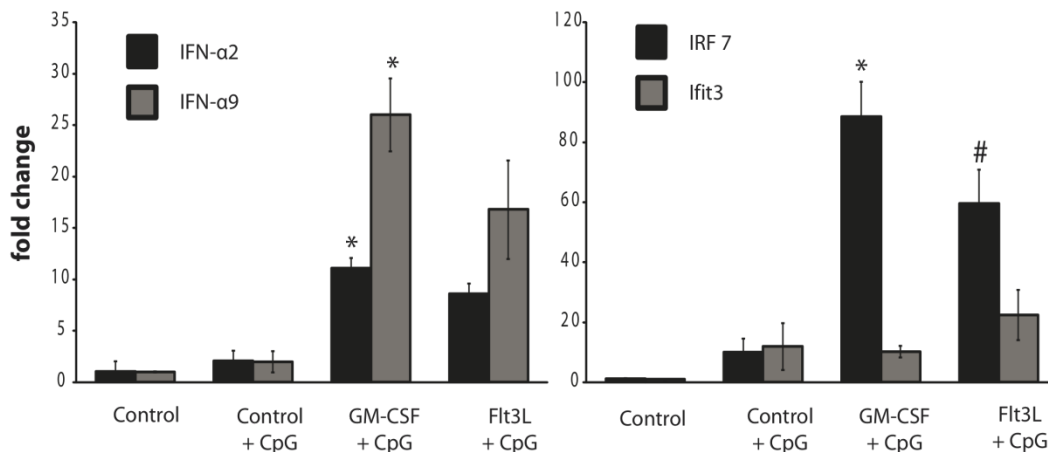


**Figure 13 Real Time PCR of IFN-I and IFN-I inducible gene expression in small intestine.**

GM-CSF, but not Flt3L potentiates CpG induced IFN-I gene expression (\* $P < 0.05$  vs Co+CpG; # $P < 0.05$  vs. GM-CSF+CpG). Data are expressed as the mean +/- SEM.

According to the findings in splenic tissues, CpG treatment induced a moderate mRNA production of IFN $\alpha$ 2 (2.1 fold), IFN $\alpha$ 9 (2-fold), Ifit3 (11.9-fold), IRF-7 (9.9-fold) in small intestine (Figure 14). GM-CSF pretreated animals displayed an upregulation of IFN $\alpha$ 2 (11.2-fold, \* $P < 0.05$  vs. Co+CpG), IFN $\alpha$ 9 (25.9-fold, \* $P < 0.05$  vs. Co+CpG), Ifit3 (10.2-fold, no statistical significance), IRF-7 (88-fold, \* $P < 0.05$  vs. Co+CpG). These findings were contrasted with findings in FLT3L pretreated animals, which displayed diminished upregulation to subsequent CpG-treatment: IFN $\alpha$ 2 (8.6-fold), IFN $\alpha$ 9 (16.7-fold), Ifit3 (22.4-fold), IRF-7 (59.5-fold, # $P < 0.05$  vs. GM-CSF+CpG). Again, in colon tissues (Figure 15), GM-CSF treatment more effectively potentiates CpG mediated type I-IFN production than Flt3L treatment. Real Time PCR analysis of gene expression in colon tissues revealed, that CpG treatment led to a moderate increase in IFN $\alpha$ 2 (13.8-fold), IFN $\alpha$ 9 (3.4-fold), Ifit3 (6.8-fold), IRF-7 (2.5-fold) messenger RNA. GM-CSF more effectively than Flt3L potentiated CpG mediated IFN $\alpha$ 2 (61-fold vers. 13,3 fold), IFN $\alpha$ 9 (24.8-fold vers. 3.4 fold), Ifit3 (33.2-fold vers. 16,4 fold), IRF-7 (8.3-fold vers. 3.7-fold).

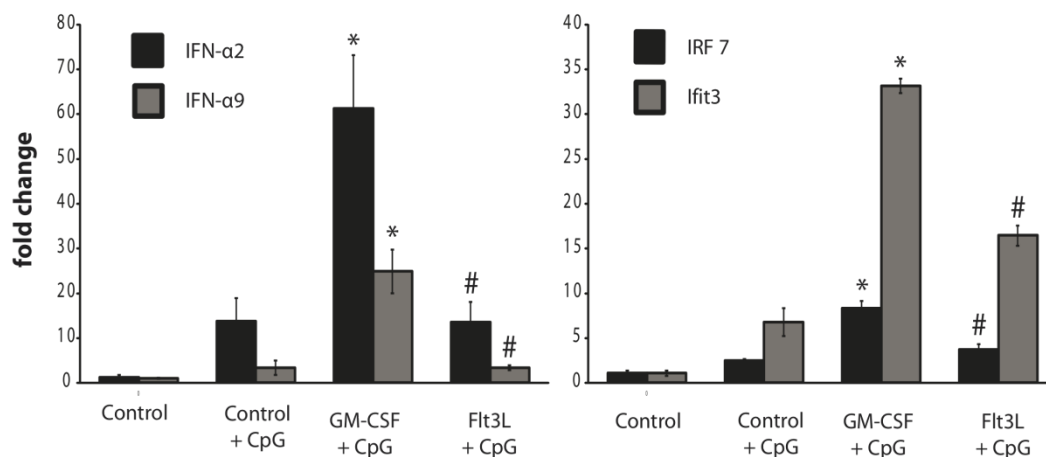


**Figure 14 Real Time PCR of IFN-I and IFN-I inducible gene expression in colon.**

GM-CSF, but not Flt3L potentiates CpG induced IFN-I gene expression (\* $P < 0.05$  vs Co+CpG; # $P < 0.05$  vs. GM-CSF+CpG). Data are expressed as the mean  $\pm$  SEM.

These results indicate, that GM-CSF, but not Flt3L, potentiates the TLR-9 mediated type I-IFN production *in vivo*, as seen in spleen, small intestine and colon. Flt3L treated animals show a level of type I-IFN production that is slightly increased, compared to baseline gene expression after CpG stimulation in control animals.

### Priming effects of GM-CSF and Flt3L on TLR-7 stimulation

In order to define, whether differential priming effects of GM-CSF and Flt3L on TLR mediated IFN-I induction are restricted to the TLR-9 signalling cascade or can be observed in other TLR-dependent pathways, the above described experiment was implemented in the TLR-7 system. Apart from the TLR-9 agonist CpG, Imiquimod is a very potent inducer of type I-IFN production [88]. Imiquimod, also known as R-837, binds to the intracellular TLR-7 receptor and initiates a signal transduction cascade similar to the TLR-9 activation cascade, as described above. Mice were treated for 4 consecutive days with GM-CSF and Flt3L. On day 5 100 $\mu$ g Imiquimod was i.p. administered and mice were sacrificed after 18 h stimulation. RNA was isolated and transcribed to cDNA from spleen, small intestine, colon and subjected to real time RT-PCR. Treatment with imiquimod (Figure 16 A and B) alone increased splenic IFN $\alpha$ 2 (53.8-fold), IFN $\alpha$ 9 (26.3-fold), Ifit3 (14.7-fold) and IRF-7(1.1-fold) gene expression. This response was augmented in mice, pretreated with GM-CSF before TLR-7 stimulation [IFN $\alpha$ 2 (511.9-fold), IFN $\alpha$ 9 (348.7-fold), Ifit3 (44.6-fold), IRF-7(4.5-fold)], but not in mice pretreated with Flt3L [ IFN $\alpha$ 2(31.8-fold), IFN $\alpha$ 9(16.8-fold), Ifit3(25.6-fold), IRF-7(1.2-fold)]. The same gene expression pattern were observable in small intestinal gene expression analysis: Co+Imiquimod (IFN $\alpha$ 2: 7.5-fold; IFN $\alpha$ 9: 6-fold; Ifit3: 4-fold; IRF-7: 12.5-fold), GM-

CSF+Imiquimod (IFN $\alpha$ 2: 11.5-fold; IFN $\alpha$ 9: 8.2-fold; Ifit3: 3.9-fold; IRF-7: 45.4-fold), Flt3L+Imiquimod (IFN $\alpha$ 2: 9.3-fold; IFN $\alpha$ 9: 5.8-fold; Ifit3: 4.4-fold; IRF-7: 33.7-fold) (Figure 16C and D), as well as in gene expression analysis from colon samples: Co+Imiquimod (IFN $\alpha$ 2: 3.1-fold; IFN $\alpha$ 9: 2.9- fold; Ifit3: 4.8-fold; IRF-7: 3.3-fold), GM-CSF+Imiquimod (IFN $\alpha$ 2: 16.3-fold; IFN $\alpha$ 9: 6.7-fold; Ifit3: 6.5-fold; IRF-7: 6.6-fold), Flt3L+Imiquimod (IFN $\alpha$ 2: 15.7-fold; IFN $\alpha$ 9: 6.8-fold; Ifit3: 10.9-fold; IRF-7: 5.8-fold) (Figure 16 E and F).

**Table 12 GM-CSF and Flt3L priming of TLR-7 activation in mice.**

Experiment was performed 2 times with equal treatment group size.

Treatment Group (n=number of animals)					
Control (n=3)	PBS	PBS	PBS	PBS	PBS
Control + Imiquimod (n=3)	PBS	PBS	PBS	PBS	Imiquimod (100 $\mu$ g)
GM-CSF + Imiquimod (n=4)	GM-CSF (5 $\mu$ g)	GM-CSF (5 $\mu$ g)	GM-CSF (5 $\mu$ g)	GM-CSF (5 $\mu$ g)	Imiquimod (100 $\mu$ g)
Flt3L + Imiquimod (n=4)	Flt3L (20 $\mu$ g)	Flt3L (20 $\mu$ g)	Flt3L (20 $\mu$ g)	Flt3L (20 $\mu$ g)	Imiquimod (100 $\mu$ g)
Time	24h	24h	24h	24h	18h

These data show that GM-CSF more effectively than Flt3L potentiates the imiquimod dependent type I- IFN production in spleen, small intestine and colon.

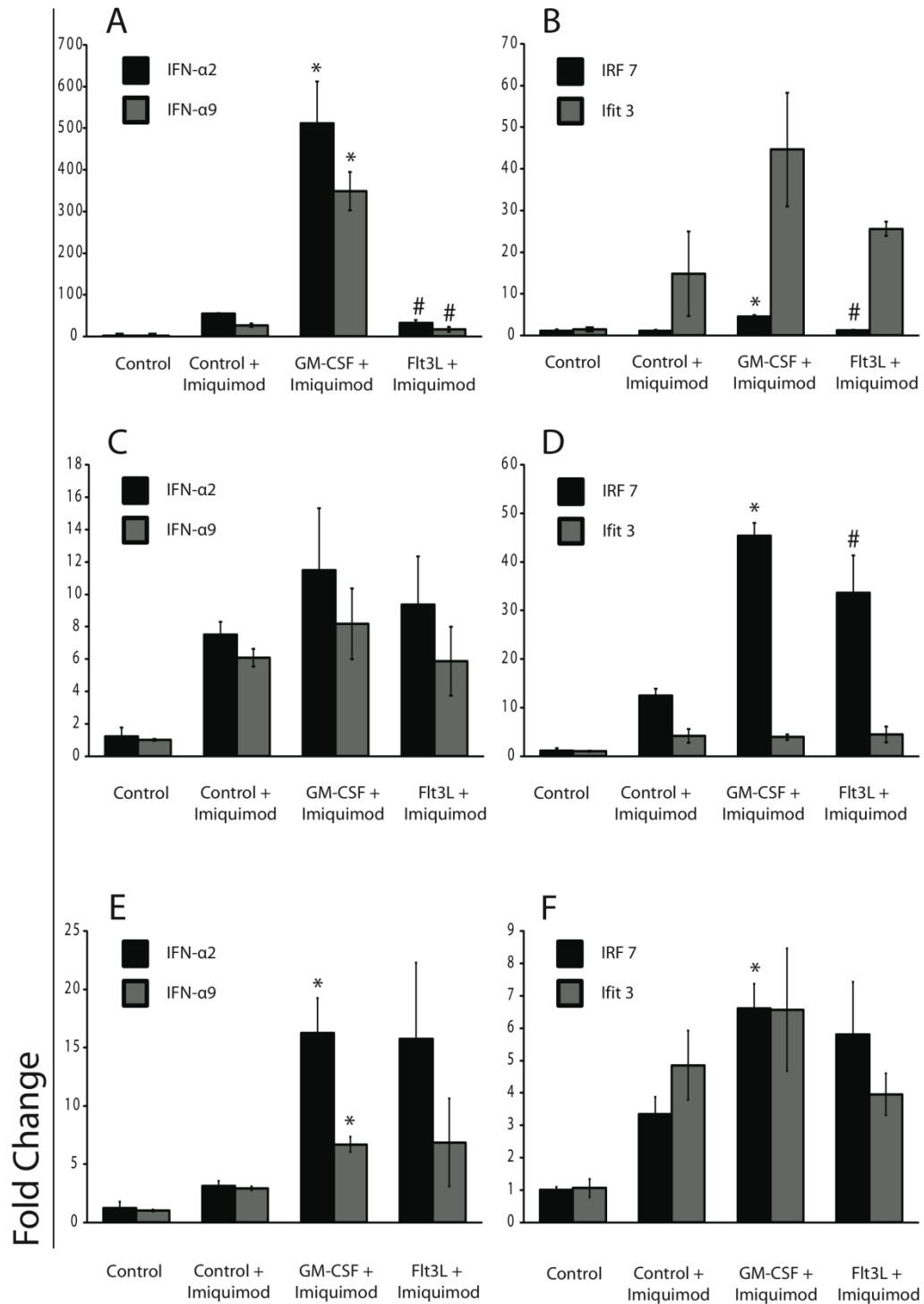


**Figure 15 Real Time PCR of TLR-7 induced IFN-I and IFN-dependent gene expression.**

GM-CSF, but not Flt3L potentiates Imiquimod induced IFN-I gene expression (\* $P < 0.05$  vs Co+CpG; # $P < 0.05$  vs. GM-CSF+CpG). Data are expressed as the mean  $\pm$  SEM.

### **Characterization of IFN-I effects on intestinal immunity**

Mice, treated with either GM-CSF or Flt3L show dramatic differences in their IFN-I gene expression in response to TLR-9 and TLR-7 stimuli. These findings highly correlated with opposite therapeutic effects of GM-CSF and Flt3L in DSS-induced colitis.

It was therefore assumed, that IFN-I is a key cytokine that modulates intestinal immunity and thereby protects from intestinal inflammation. In an attempt to define the molecular effects of IFN-I on intestinal mucosa whole genome gene expression profiling of mouse tissues was performed.

### **Whole mouse genome transcription profiling**

RNA, isolated from colonic samples from mice treated with CpG-ODN or Imiquimod (see Table 11,12 and Figures 13-16), were subjected to whole genome expression profiling using Agilent<sup>TM</sup> chips. In detail, the RNA from 3 individual tissues from 3 individual mice of one treatment group (Control, Control+CpG/Imiquimod) was mixed together and loaded on a gene chip. Gene expression profiling was performed 2 times for each treatment group (Control vs. Control + CpG, Control vs. Control + Imiquimod). As seen in table 13, CpG-ODN treatment in mice leads to a strong signal of interferon-inducible genes. Moreover CpG treatment groups exhibits a cluster of antimicrobial peptides, which has highly upregulated compared to non-treated animals. Array data from Imiquimod treated animals show a cluster of interferon-dependent genes that are upregulated in colons from mice treated with Imiquimod. Interestingly there was a large cluster of upregulated genes encoding for AMPs that were also increased in the Imiquimod treatment group (Table 14). This result allows the assumption, that AMPs expression is dependent on either TLR stimulation, IFN-I stimulation or both.



**Table 13 Whole genome array, TLR-9 stimulation**

Gene array showing upregulated gene clusters in mice spleen in response to 18h TLR-9 (CpG-ODN) stimulation. Data are expressed as the ratio of the signal of CpG treated vs. control treated mice. SEM in brackets.

Gene Accession	Gene Name	Gene Description	CpG vs. Control
		<u>IFN-I-inducible genes / -regulatory genes</u>	<u>AVG</u>
NM_145227	Oas2	Mus musculus 2'-5' oligoadenylate synthetase 2	9,6 (0,1)
NM_011940	Ifi202b	Mus musculus interferon activated gene 202B	4,0 (0,5)
NM_001033632	Ifitm6	Mus musculus interferon induced transmembrane protein 6	2,3 (0,1)
NM_016850	Irf7	Mus musculus interferon regulatory factor 7	4,5 (0,4)
NM_133871	Ifi44	Mus musculus interferon-induced protein 44	9,8 (0,4)
NM_008331	Ifit1	Mus musculus interferon-induced protein with tetratricopeptide repeats 1	8,6 (2,3)
NM_008332	Ifit2	Mus musculus interferon-induced protein with tetratricopeptide repeats 2	5,7 (1,8)
NM_010501	Ifit3	Mus musculus interferon-induced protein with tetratricopeptide repeats 3	5,1 (0,1)
NM_029803	Ifi27	Mus musculus interferon, alpha-inducible protein 27	4,6 (0,3)
		<u>Antimicrobial Peptides</u>	
NM_007847	Defcr20	Mus musculus defensin related cryptdin 20	4,6 (1,1)
NM_007845	Defcr3	Mus musculus defensin related cryptdin 3	4,4 (0,5)
NM_007850	Defcr4	Mus musculus defensin related cryptdin 4	3,6 (0,1)
NM_010031	Defcr-rs10	Mus musculus defensin related cryptdin, related sequence 10	5,4 (0,5)
NM_183268	Defcr-rs12	Mus musculus defensin related cryptdin, related sequence 12	2,3 (0,3)
NM_007847	Defcr-rs2	Mus musculus defensin related cryptdin, related sequence 2	6,7 (1,2)
NM_007852	Defcr-rs7	Mus musculus defensin related cryptdin, related sequence 7	4,1 (0,8)

**Table 14 Whole genome array, TLR-7 stimulation**

Gene array showing upregulated gene clusters in mice colons in response to 18h TLR-7 (Imiquimod) stimulation. Data are expressed as the ratio of the signal of Imiquimod treated vs. control treated mice. SEM in brackets.

Gene Accession	Gene Name	Gene Description	Imiquimod vs. Control
		<u>IFN-I-inducible genes / -regulatory genes</u>	<u>AVG</u>
NM_133871	Ifi44	interferon-induced protein 44	16,4 (1,6)
NM_145227	Oas2	2'-5' oligoadenylate synthetase 2	12,8 (0,6)
NM_008331	Ifit1	interferon-induced protein with tetratricopeptide repeats 1	12,4 (1,2)
NM_011854	Oasl2	2'-5' oligoadenylate synthetase-like 2	12,3 (0,2)
NM_016850	Irf7	interferon regulatory factor 7	5,0 (0,8)
NM_145211	Oas1a	2'-5' oligoadenylate synthetase 1A	4,7 (0,3)
NM_145209	Oasl1	2'-5' oligoadenylate synthetase-like 1	4,2 (0,2)
NM_145153	Oas1f	2'-5' oligoadenylate synthetase 1F	3,8 (0,1)
NM_010501	Ifit3	interferon-induced protein with tetratricopeptide repeats 3	3,5 (0,4)
NM_145226	Oas3	2'-5' oligoadenylate synthetase 3	3,4 (0,1)
NM_008332	Ifit2	interferon-induced protein with tetratricopeptide repeats 2	3,2 (0,2)
NM_028968	Ifitm7	interferon induced transmembrane protein 7	2,8 (0,1)
NM_025378	Ifitm3	interferon induced transmembrane protein 3	2,6 (0,2)
NM_011853	Oas1b	2'-5' oligoadenylate synthetase 1B	2,4 (0,2)
		<u>Antimicrobial peptides</u>	
NM_007847	Defcr-rs2	defensin related cryptdin, related sequence 2	7,2 (5,1)
NM_007847	Defcr-rs2	defensin related cryptdin, related sequence 2	6,6 (4,5)
NM_007845	Defcr-rs10	defensin related cryptdin, related sequence 10	6,3 (4,4)
NM_007848	Defcr-rs7	defensin related cryptdin, related sequence 7	4,4 (2,4)
NM_007846	Defcr-rs12	defensin related cryptdin, related sequence 12	4,3 (2,6)
NM_010039	Defcr4	defensin related cryptdin 4	3,9 (2,6)
NM_001012307	Defcr23	defensin-related cryptdin 23	3,7 (2,5)
NM_007850	Defcr3	defensin related cryptdin 3	3,7 (2,3)
NM_010031	Defa1	defensin, alpha 1	3,4 (2,2)
NM_183268	Defcr20	defensin related cryptdin 20	3,4 (2,2)
NM_007852	Defcr6	defensin related cryptdin 6	3,1 (3,0)
NM_207658	Defcr22	defensin-related cryptdin 22	2,3 (1,3)
NM_007844	Defcr-rs1	defensin related sequence cryptdin peptide	2,2 (1,1)

### Real Time PCR confirmation of IFN-I dependent gene induction

Antimicrobial peptides (AMPs) comprise a large family of AMPs (e.g. Defensins and Defensin-related cryptidins), that act as a first line extracellular defense in the intestine. They are found to be expressed in the full length of the gut in the epithelium and Paneth cells. As gene array data from mice treated with CpG-ODN or Imiquimod indicated that upregulation of Interferon-inducible genes is associated with the upregulation of antimicrobial peptides, it was the further aim to show, whether IFN-I directly induces the expression of AMPs. This experiment was performed in human epithelial cell lines.

### IFN-I effects in human epithelial cell lines

7-10 day post-confluent HCT-116 and HT-29 epithelial cell lines were starved overnight in serum free media and consequently stimulated with 1000 U/ml IFN- $\beta$  for 24 hours or left untreated for the equivalent time range. Following cell harvest, RNA was isolated and subjected to reverse transcription, followed by Real Time RT-PCR evaluation of the human  $\beta$ -defensin 3 (hBD3) and *CARD15* genes.

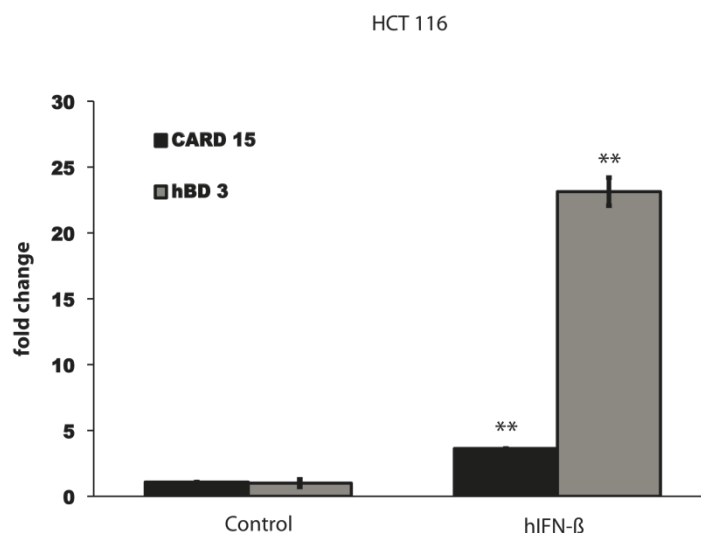


**Figure 16** *CARD 15* and hBD 3 gene expression in HCT 116 epithelial cell line.

Real Time PCR analysis of *CARD 15* and hBD 3 gene expression in HCT 116 epithelial cell line. IFN- $\beta$  induces significant upregulation *CARD 15* and hBD 3 genes expression (\*\* $P < 0.005$  vs. Control). Data are expressed as the mean  $\pm$  SEM.

As seen in figure 20, 24 hour treatment of HCT 116 cells with hIFN- $\beta$  (1000U/ml) resulted in a 3.6-fold induction of *CARD15* (\*\* $P < 0.005$  vs. Control). Gene expression of hBD 3 was 23.3-

fold increased in IFN-I treated cell, compared to non-stimulated HCT 116 cells. Again in HT-29 cells (Figure 21), hIFN- $\beta$  induced 12.4-fold upregulation of *CARD15* (\*\* $P < 0.005$  vs. Control) and 2.6-fold upregulation of hBD 3, compared to non-treated cells. Results are shown as representative of 3 individual experiments. Data are expressed as the mean  $\pm$  SEM.

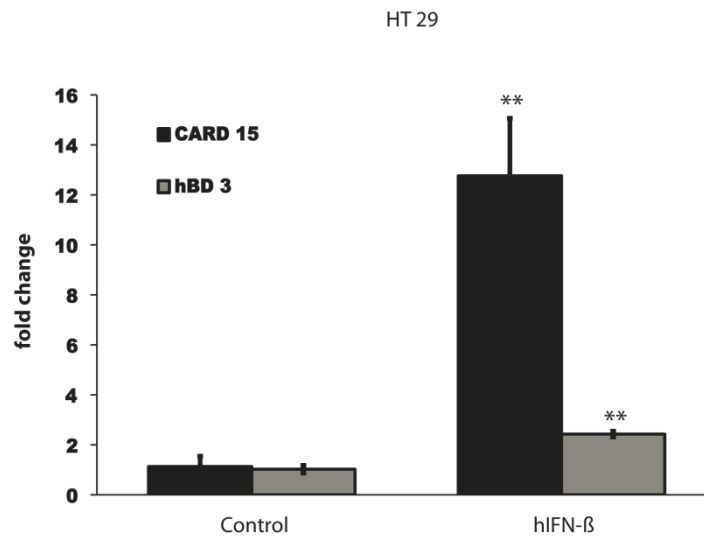


**Figure 17 *CARD 15* and hBD 3 gene expression in HT 29 epithelial cell line**

Real Time PCR analysis of *CARD 15* and hBD 3 gene expression in HCT 116 epithelial cell line. IFN- $\beta$  induces significant upregulation *CARD 15* and hBD 3 genes expression (\*\* $P < 0.005$  vs. Control). Data are expressed as the mean  $\pm$  SEM.

#### **IFN-I effects in mouse Dendritic cells.**

In order to dissect the molecular function of IFN-I on AMP expression, isolated DCs were treated with IFN-I, CpG-ODN with or without the monoclonal AB (mAB) 440c<sup>+</sup>. 440c recognizes a previously uncharacterized member (Siglec-H) of the sialic acid binding immunoglobulin (Ig)-like lectin (Siglec) family; Siglec-H is selectively expressed on pDCs. Siglec-H associates with the adaptor DAP12 for signaling and blocks IFN-I expression following TLR stimulation [89, 90]. As pDCs are the major source of IFN-I production, functional IFN-I blocking is an eloquent way to study the role of IFN-I on gene expression in DCs. As seen in figure 19, stimulation of DCs with 5 $\mu$ g CpG-ODN significantly induces the gene expression of the AMPs Defensin  $\alpha$ 1 (3,8-fold), Defensin-related cryptdin (Defcr) 4 (2,2-fold) and Defcr 6 (3,3-fold), compared to non treated-animals. The inducible effect of CpG-ODN was nullified in DCs, co-treated with CpG-ODN and the antibody 440c. Treatment with IFN- $\alpha$  alone reestablished induction of Defensin  $\alpha$ 1 (10,1-fold, no statistical significance), Defcr 4 (2,1-fold, no statistical significance) and Defcr 6 (4,1-fold). These data indicate, that

CpG-dependent induction of AMPs Defensin  $\alpha$ 1, Defcr 4 and Defcr 6 is mediated by CpG dependent secretion of IFN-I in pDCs, as addition of 440c AB reversed the CpG effects. IFN-I alone induces AMPs gene expression in DCs.

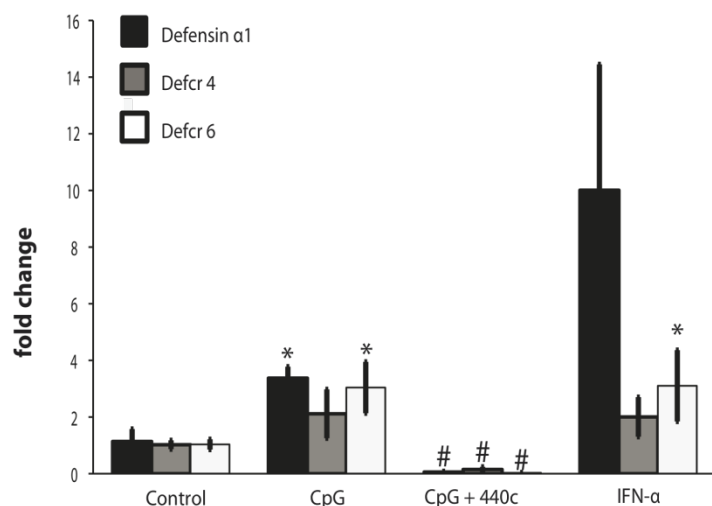


**Figure 18 Real Time PCR analysis of AMP gene expression in CD11c<sup>+</sup> DCs.**

CpG significantly induces the gene expression of AMP (\* $P < 0.05$  vs. Co). CpG effects are blocked by addition of the AB 440c ( $\#P < 0.05$  vs. CpG). IFN- $\alpha$  alone induces AMP expression. Data are expressed as the mean  $\pm$  SEM.

### Evaluation of the gentamicin protection assay

The gentamicin protection assay functions as a simulation of the interaction between intestinal mucosa and pathogens. It assess the number of vital intracellular bacteria and gives a rough approximation of antibacterial effects of reagents, either directly added to the bacteria or secreted from cells into the bacteria containing medium. Due to the close proximity of DCs to intestinal epithelium it was the further aim to describe, whether type I-IFN, secreted from DCs in the lamina propria, has an augmenting effect on the bacterial clearance of the epithelium. For this purpose the gentamicin protections assay model was chosen as a read out of bactericidal effects of IFN-I-initiated cellular programs.

### Human epithelial cell lines

Intestinal epithelial cell lines HCT-116 and HT-29 were chosen as an *in vitro* model to demonstrate antimicrobial I-IFN effects in the epithelium. HCT-116 and HT-29 epithelial cell lines, which are 7-10 day post-confluent, were starved overnight and consequently stimulated with 1000 U/ml IFN- $\beta$  for 24 hours or left untreated for the equivalent time range. Live *Salmonella typhimurium* were added to the epithelial cells and incubated for

1h. The cell monolayers were then treated with gentamicin to kill extracellular organisms and were then washed and lysed under conditions to release viable intracellular organisms. Lysates were streaked into LB agar plates for incubation and colony enumeration. As presented in Figure 16, cells pretreated with hIFN- $\beta$  show a reduction in bacterial colony count in HT-29 (Control: 307 CFU, IFN- $\beta$ : 41 CFU) as well as in HCT 116 (Control: 1614 CFU, IFN- $\beta$ : 344 CFU). Thus demonstrating greater resistance to intracellular organisms following treatment with IFN-I. Data shown are representative of 3 individual experiments.

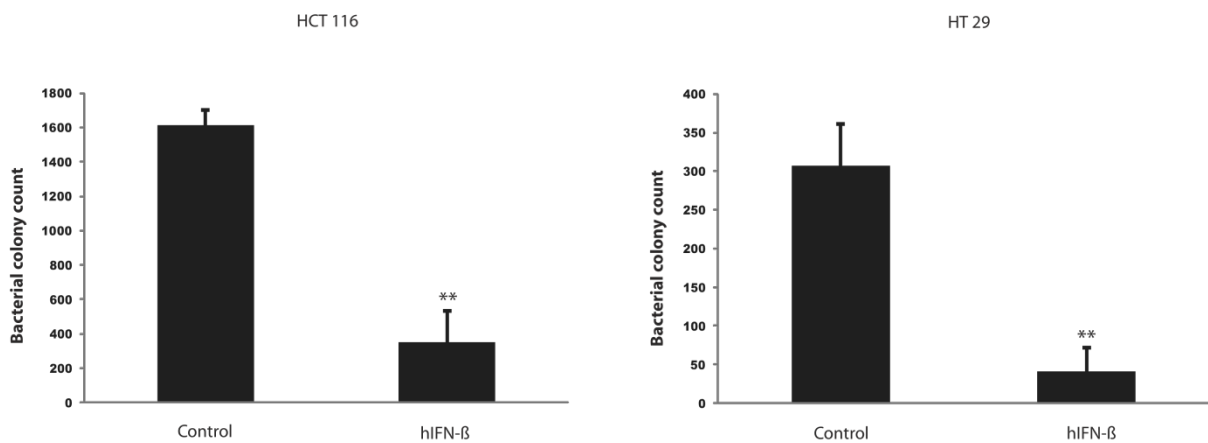


**Figure 19 Gentamicin protection assay**

Type-I IFN increases bacterial killing in human epithelial cell lines. hIFN- $\beta$  treated groups showed significantly diminished bacterial colonies in HCT-116 (\*\* $P < 0.005$  vs. Control) and HT-29 cells (\*\* $P < 0.005$  vs. Control). Data are expressed as the mean  $\pm$  SEM.

### Mouse Dendritic cells

In order to reapprove the previous IFN-I effects on bacterial clearance in primary cells, the gentamicin protection assay was repeated in CD11c<sup>+</sup> cells, isolated from mice.

### Isolation of CD11c<sup>+</sup> and confirmation of DC purity by FACS

CD11c<sup>+</sup> DCs were isolated using MACS cell sorting, as described (Materials and Methods). The confirmation of CD11c<sup>+</sup> DC purity is seen in figure 17. Non-purified total splenocytes and CD11c<sup>+</sup> purified splenocytes, were subjected to FACS analysis. After dead cell exclusion by FSC and SSC gating, splenocytes were analysed for their antibody signal of CD11c-PE and MHC-II FITC. Double positive cells, were defined as DCs. As seen in figure 17a, non-purified splenocytes display a number of 2.48 % CD11c<sup>+</sup>,MHC-II<sup>+</sup> DCs of total analysed splenocytes. After DC isolation, the number of CD11c<sup>+</sup>,MHC-II<sup>+</sup> DCs raised to 93,8 %. For the following experiments mouse DC cell solution were used with a >90% purity of CD11c<sup>+</sup> DCs.

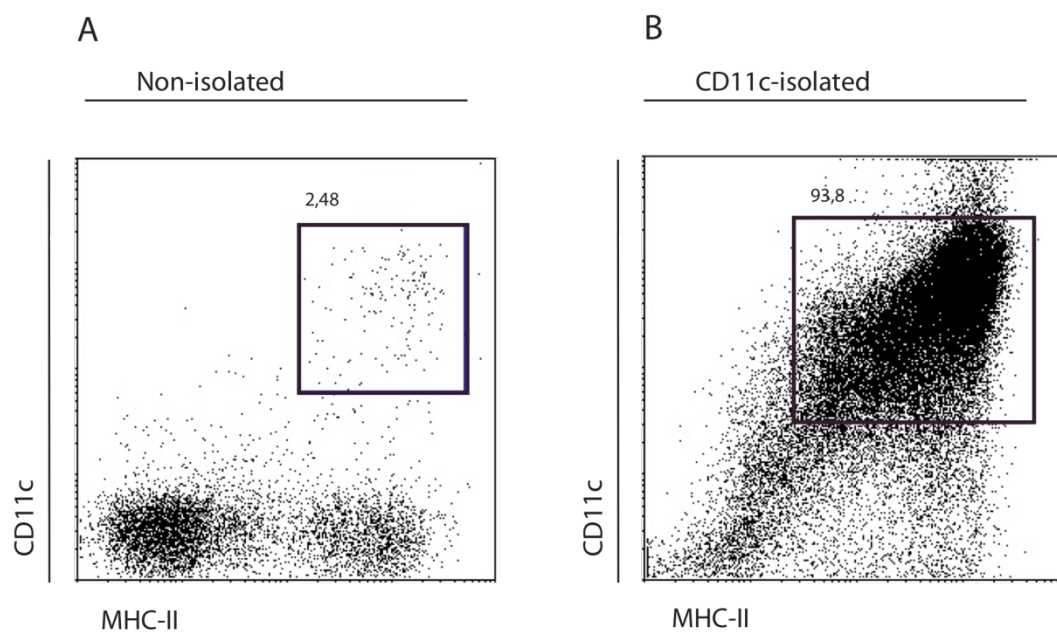


**Figure 20** Flow cytometry of isolated CD11c<sup>+</sup> DCs

Verification of DC purity after isolation of CD11c<sup>+</sup> DCs. Non-isolated and CD11c-isolated DC were subjected to FACS analysis. DC purity risen from 2.48% (non-isolated) to 93.8% (CD11c-isolated) of total splenocytes.

### Gentamicin protection assay

In order to define the antimicrobial effects of IFN-I and two major inducers of IFN-I production, CpG-ODN (TLR-9) and Imiquimod (TLR-7) on DCs, their potential to prevent salmonella invasion into DCs was assessed by performing gentamicin protection assay.

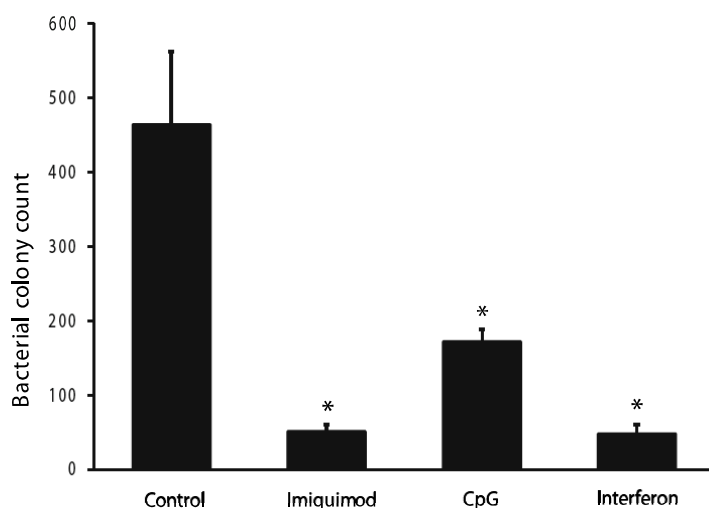


**Figure 21** Gentamicin protection assay in CD11c<sup>+</sup> DCs.

Pretreatment of DCs with Imiquimod, CpG and Interferon significantly reduces bacterial colony count (\*P<0.05 vs.Co). Data are expressed as the mean +/- SEM.

After DC isolation, DCs were allowed to grow in cell media ( $5 \times 10^6$ /ml) overnight and were subsequently treated with mIFN- $\alpha$  (500U/ml), CpG-ODN (5 $\mu$ g/ml) or Imiquimod (10 $\mu$ g/ml) prior to bacterial infection. The following procedure equals the gentamicin procedure performed in epithelial cells lines, as mentioned above. Figure 18 shows the mean value of the bacterial colony count from 1 agar plate. As presented, cells pretreated with Imiquimod (51 CFU) CpG-ODN (187 CFU), Interferon-I (48 CFU) showed a significant reduction of colony forming bacteria, compared to non-treated DCs. Data shown are representative of 3 individual experimen

### **GM-CSF, but not Flt3L, enhances antimicrobial peptide gene induction in a TLR-9 and IFN-I dependent mechanism.**

The previous results indicate that (i) GM-CSF pretreatment in mice enhances in vivo production of IFN-I in response to TLR-9 stimulation and (ii) IFN-I induces the gene expression of AMPs in DCs as well as in epithelial cells. It was therefore a obvious question, whether GM-CSF mediated potentiation of IFN-I secretion in mouse tissues leads to enhanced production of AMPs.

**Table 15 Influence of 440c AB on TLR-9 and IFN-I dependent gene expression.**

Treatment groups. Experiment was performed 2 times with equal treatment group size.

Treatment Group (n=number of animals)					
Control (n=3)	PBS	PBS	PBS	PBS	PBS
Control + CpG(n=3)	PBS	PBS	PBS	PBS	CpG-ODN (200 $\mu$ g)
GM-CSF + CpG (n=4)	GM-CSF (5 $\mu$ g)	GM-CSF (5 $\mu$ g)	GM-CSF (5 $\mu$ g)	GM-CSF (5 $\mu$ g)	CpG-ODN (200 $\mu$ g)
GM-CSF + CpG + 440c(n=4)	GM-CSF (5 $\mu$ g)	GM-CSF (5 $\mu$ g)	GM-CSF (5 $\mu$ g)	GM-CSF (5 $\mu$ g)	CpG-ODN (200 $\mu$ g) + 440c (200 $\mu$ g)
Flt3L + CpG (n=4)	Flt3L (20 $\mu$ g)	Flt3L (20 $\mu$ g)	Flt3L (20 $\mu$ g)	Flt3L (20 $\mu$ g)	CpG-ODN (200 $\mu$ g)
Flt3L + CpG + 440c (n=4)	Flt3L (20 $\mu$ g)	Flt3L (20 $\mu$ g)	Flt3L (20 $\mu$ g)	Flt3L (20 $\mu$ g)	CpG-ODN (200 $\mu$ g) + 440c (200 $\mu$ g)
Time	24h	24h	24h	24h	18h

Again, Balb/c mice were administered with GM-CSF (5 $\mu$ g/mice), Flt3L (20 $\mu$ g/mice) or PBS for 4 consecutive days. On day 5 mice received intraperitoneal injections of 200 $\mu$ g of ODN1018 with or without simultaneous injection of 200 $\mu$ g mAB 440c. After 18 hours of stimulation, mice were sacrificed and tissues (spleen, colon, small intestine) were obtained, subjected to RNA isolation and further prepared for Real Time RT-PCR analysis. Figure 23 exhibits, that GM-CSF treatment, as previously reported, significantly primes in vivo production of IFN-I in



response to CpG administration in colon tissues (\* $P < 0.05$  vs. Control + CpG). Co-treatment with the monoclonal AB 440c significantly reduces gene expression of IFN- $\alpha 2$  (17-fold), IFN- $\alpha 9$  (6.5-fold) and Ifit3 (11-fold) compared to GM-CSF+CpG treatment alone ( $^{\#}P < 0.05$  vs. GM-CSF+CpG). Comparing the effects of 440c in the Flt3L treatment group, no effects were observable between Flt3L+CpG stimulated animals and animals additionally treated with the mAB 440c. However, IFN-I gene induction in colon tissues from Flt3L+CpG treated animals had significantly reduced gene expression levels, when compared to GM-CSF+CpG levels. These data exhibit, that treatment with the mAB 440c significantly diminishes CpG-ODN induced IFN-I production in colon tissues.

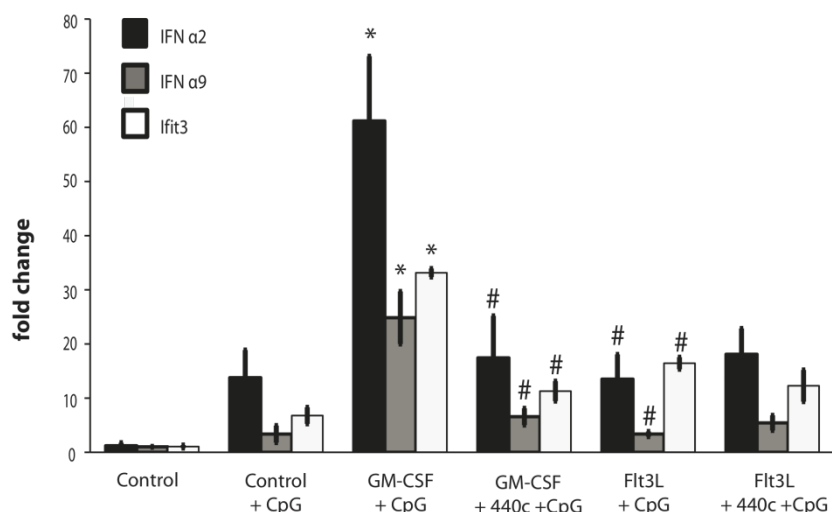


**Figure 22 Real Time PCR analysis of IFN-I gene expression in colon samples of mice.**

GM-CSF pretreatment in mice significantly potentiates subsequent CpG stimuli (\* $P < 0.05$  vs. Control+CpG). IFN-I gene expression is significantly abolished in mice CpG treated mice, when IFN-I secretion in pDCs in blocked with the AB 440c ( $^{\#}P < 0.05$  vs. GM-CSF+CpG). Flt3L pretreatment has significantly diminished priming effects on CpG stimulation. Data are expressed as the mean  $\pm$  SEM.

It was now the further task, to evaluate, whether gene induction of AMPs is induced in a IFN-I dependent mechanism. In another set of Real Time RT-PCR experiments, the gene induction of the AMPs Defensin  $\alpha 1$ , Defcr 4 and Defcr 6 in colon tissues was evaluated (Figure 24). Following CpG treatment in control mice in colon tissues was found an upregulation of Defensin  $\alpha 1$  (2,5-fold), Defcr 6 (3-fold), compared to non-treated animals. Colons from mice, pre-treated with GM-CSF before subsequent CpG stimulation, showed an increase of Defensin  $\alpha 1$  (3,9-fold), Defcr 4 (4,8-fold) and Defcr 6 (8,4-fold), which became significant when compared with animals treated with CpG alone (\* $P < 0.05$  vs. Control+CpG).

Interestingly, CpG-induced expression of AMPs in GM-CSF pre-treated mice was abolished, when mice became mAB440 administration in addition to CpG bolus (GM-CSF+CpG+440c). Gene expression of Defensin  $\alpha$ 1 (2,1-fold), Defcr 4 (1,3-fold) and Defcr 6 (2,6-fold) was significantly diminished compared to GM-CSF + CpG treated mice ( $^{\#}P < 0.05$  vs. GM-CSF+CpG). According to findings in Flt3L+CpG response in IFN-I gene expression, gene induction of Defensin  $\alpha$ 1 (1,9-fold), Defcr 4 (1,1-fold) and Defcr 6 (2,5-fold) in colon tissues was significantly lower, when compared to GM-CSF+CpG treated animals.

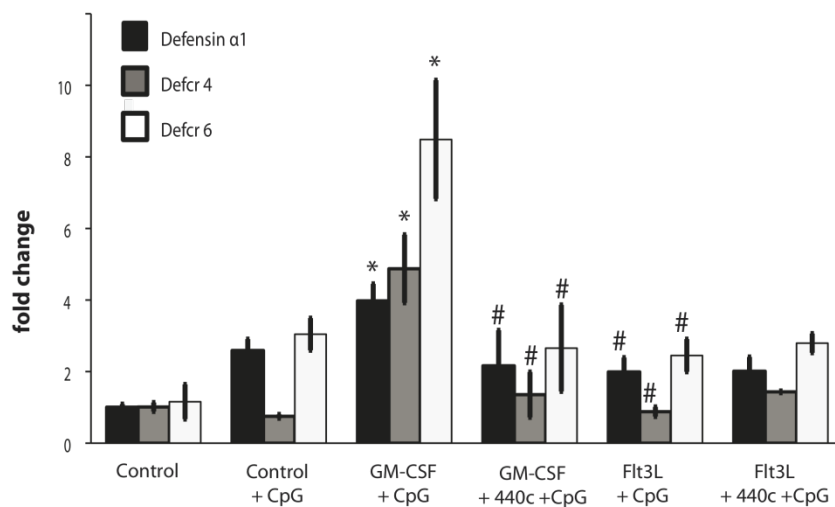


**Figure 23 Real Time PCR analysis of AMP gene expression in colon samples of mice.**

GM-CSF pretreatment in mice significantly potentiates subsequent CpG stimuli ( $*P < 0.05$  vs. Control+CpG). IFN-I gene expression is significantly abolished in mice CpG treated mice, when IFN-I secretion in pDCs in blocked with the AB 440c ( $^{\#}P < 0.05$  vs. GM-CSF+CpG). Flt3L pretreatment has significantly diminished priming effects on CpG stimulation. Data are expressed as the mean  $\pm$  SEM.

These data indicate, that (i) CpG mediated IFN-I induction in colon tissues can be abolished by functionally blocking the IFN-I secretion in pDCs using the mAB 440c and (ii) the behaviour of the CpG mediated IFN-I gene expression pattern strongly correlates with CpG mediated AMP gene expression pattern. The following finding might evolve from the data: IFN-I induces the expression of AMP in mice, an effect which can be enhanced by GM-CSF pretreatment.

## IV. Discussion

### Background and experimental outline

Crohn's disease (CD) and ulcerative colitis (UC) are chronic inflammatory disorders of the gastrointestinal tract. Their pathogenesis remains poorly understood. Current treatments utilize immunosuppressive medications and are often complicated by serious infections. In the previous work, on which this study is founded, disease was approached from a different perspective based on observations made in patients with genetic syndromes involving impaired innate immunity that also develop Crohn's disease. These patients showed clinical responses to granulocyte-macrophage colony stimulating factor (GM-CSF), an agent that stimulates innate immunity [38, 60]. Phase I and II trials of GM-CSF in patients with idiopathic CD confirmed these observations. Therapy led to improvements in Crohn's disease activity scores, endoscopic disease, draining fistulas, and quality of life. The therapeutic benefit of GM-CSF was dependent on DC accumulation and their interferon producing capacity, as functional blocking of Interferon-I secretion in pDC's abolished GM-CSF mediated protection [63]. Previous reports have indicated that GM-CSF and Flt3L expand DC population [91]. This includes expansion of plasmacytoid dendritic cells, which are the major cellular source of IFN-I induced by TLR signaling. IFN-I plays a protective role in the orchestration of immune function in experimental colitis and other immune-related diseases [64, 92]. The aim of the present study was to prove the hypothesis, that amplification of DCs in mice using the hematopoietic growth factor Fms-like tyrosine 3-kinase ligand leads to augmented mucosal tolerance and a therapeutic response in IBD mouse models through effects on tolerogenic dendritic cells.

This hypothesis has three components:

- (i) IBD is associated with epithelial barrier defects that allow microbe translocation into the mucosa. DCs contribute to mucosal tolerance; they are located in the lamina propria of the gut, positioned beneath the basement membrane, and prevent bacterial invasion into the mucosa.
- (ii) Exogenous administration of hematopoietic growth factors, such as GM-CSF and Flt3L, significantly enhances growth of CD11c<sup>+</sup> DCs
- (iii) DCs are endowed with a multitude of receptors of the innate immune system including TLRs. Upon TLR-7/9 ligation, DCs induce a signal cascade leading to the

induction of immunomodulating cytokines, including IFN-I. IFN-I effects on intestinal immunity are associated with protective effects in mouse models of IBD.

### **Characteristics and limitations of the DSS model**

The clinical appearance of IBD is heterogenous in humans as well as in mouse models simulating IBD-like alterations. As the pathogenesis is still not fully understood, mouse models of intestinal inflammation tend to involve a single cause of inflammation instead of reflecting the complex interplay of factors that induce IBD in humans. The DSS-model is based on the assumption that compromised epithelial integrity plays a critical role in the pathogenesis of IBD. Breakdown of “epithelial integrity” includes disruption of the physical barrier, as well as compromised innate immune function of the epithelial lining in the gut. Dysregulated immunity is a crucial step in the development of intestinal inflammation, as the functional characterization of IBD genes indicate (*see Chapter: Mucosal Barrier*). Feeding mice with DSS induces breakdown of epithelial integrity, presumably due to direct toxic effects on epithelial cells of the gut. Mice display IBD-like symptoms, including bloody diarrhoea, weight loss and mucosal ulcerations. The DSS-effects are independent of the adaptive immune system, as IBD-like intestinal alterations are reproducible in RAG1<sup>-/-</sup> mice, which are deficient for T- and B-cells [93]. Together with studies showing that TLR signalling protects against bacterial translocation in DSS inflamed mucosa, these observations indicate, that the DSS-model is useful for describing the importance of the innate immune system in the pathogenesis of IBD.

Therefore, the DSS-model was chosen for the evaluation of the therapeutic potential of Flt3L treatment in IBD, as pharmacological DC amplification was hypothesized to improve intestinal inflammation, in a manner involving the innate immune system. More over, using the DSS model made it possible to compare Flt3L effects with already gained GM-CSF effects in the DSS model. Although the DSS colitis is a well established and widely recognized model of intestinal inflammation, several limitations need to be recognized:

CD and UC are chronic diseases. States of remission are interrupted by states of disease exacerbation. The pathogenesis of IBD is not linked to states of acute inflammation, as many dysfunctions characterizing IBD can be observed before disease onset. In contrast, DSS-induced colitis is an acute colitis, where clinical, biological and morphological inflammation

develops over the time course of 7 days. Therefore DSS-colitis solely reflects the exacerbation stage of IBD and not the chronic state of remission.

This limitation is further highlighted when considering that the DSS model is used to describe the role of the innate immune system in the development of IBD. Innate immune dysfunction itself is not a trigger for developing IBD but rather a state of increased vulnerability to secondary triggers. This idea is supported by observations that knockout mice for IBD risk genes (e.g.  $NOD2^{-/-}$ ) do not develop spontaneous colitis [94]. This observation highlights the central dogma that IBD is the result of an intertwined interplay of risk factors (lifestyle, genetic, environment). Therefore, the DSS model describes the implication of innate immunity in the acute inflammation, but the model cannot be used to draw conclusions about the contribution of innate immune dysfunction in initial disease onset. Finally, it should be recognized that DSS-induced inflammation is mediated by direct toxic deletion of gut epithelial cells in the basal crypts due to dextran sodium sulfate. However, direct toxic effects due to chemical reagents on epithelial cells do not reflect the pathophysiology of chronic intestinal inflammation. Taken together, the DSS model, like any other disease model, is an artificial model that approaches the complexity of disease pathogenesis from one specific point of view.

### **Flt3L and GM-CSF mediated dendritic cell growth**

It was found that GM-CSF and Flt3L significantly increased total  $CD11c^{+}$ ,  $MHC-II^{+}$  DCs in the spleen as compared to control mice. In addition, GM-CSF and Flt3L increased DC abundance in the lamina propria of the colon. Furthermore, GM-CSF and Flt3L expanded pDCs ( $B220^{+}$ ,  $Ly6c^{+}$ ,  $CD11c^{+}$ ,  $mPDCA-1^{+}$ ), the major source of IFN-I producing DCs [95] as well as IDCs and mDCs, as compared to the control. Of note, GM-CSF had more potent stimulatory effects on lymphoid and myeloid DCs populations than Flt3L, a finding which has also been described by others. Daro et al. report in a GM-CSF, Flt3L side by side study, that GM-CSF and Flt3L both increase the total number of  $CD11c^{+}$  DCs. While Flt3L alone increases the number of both  $CD11c^{high}$  and  $CD11c^{low}$ , treatment with GM-CSF alone preferentially induces  $CD11c^{high}$  and not  $CD11c^{low}$  growth [96]. DCs from both GM-CSF and Flt3L treated mice express similarly high levels of surface MHC class II and low levels of costimulatory molecules, like CD40, CD80 and CD86 [61]. In-vitro studies with bone marrow cells indicate that Flt3L-treatment seems to favour differentiation into  $CD11c^{+}$ ,  $B220^{+}$ ,  $CD11b^{-}$ , and  $Gr-1^{+}$  Interferon producing cells, a mechanism that could be reversed by GM-CSF co-

administration [97]. In addition to these findings Xu et al. report, that bone marrow cells cultured in Flt3L-containing medium could be differentiated into three subgroups (B220<sup>+</sup> pDCs, CD8<sup>+</sup>,CD11c<sup>+</sup> DCs and CD8<sup>-</sup>, CD11c<sup>+</sup> DCs), whereas GM-CSF/IL-4 cultured cells lacked the B220<sup>+</sup> pDCs [78, 91].

### **Flt3L dependent DC expansion in the context of intestinal inflammation**

As GM-CSF and Flt3L share the ability to expand the number of pDCs, it was hypothesized, that Flt3L treatment, by expanding dendritic cells, would also protect mice from experimental colitis in an IFN-I dependent manner. Surprisingly, it was found, that Flt3L treated mice responded to DSS-induced colitis with increased disease activity index, increased MPO activity and increased expression of pro-inflammatory genes in balb/c mice. GM-CSF effects in DSS-induced colitis were found to be dependent on IFN-I secretion but independent of the adaptive immune system, as GM-CSF ameliorated DSS colitis in RAG1<sup>-/-</sup> mice. In order to further describe Flt3L effects on innate immunity in the context of DSS-induced colitis, the DSS model was transferred into mice deficient for T- and B-cells. Again it was found that Flt3L-treated mice responded to DSS induced colitis with increased disease activity index, increased MPO activity and increased expression of pro-inflammatory genes in RAG1<sup>-/-</sup> mice. These data are striking as they contradict the hypothesis that expansion of tolerogenic DC strengthens innate immunity and protects from experimental colitis. Unfortunately, no comparable data are available describing the effect of growth factors in models of experimental colitis. In mouse models of lung inflammation, the effect of Flt3L-dependent amplification of lung dendritic cells was tested in the context of *Klebsiella pneumoniae* and *Streptococcus pneumoniae* inhalation. Flt3L treatment in mice amplified pro-inflammatory cytokine production and increased mortality compared to non-treated animals [98, 99]. Together with own observations these studies share the common feature, that expansion of dendritic cells in the affected tissue leads to increased inflammation, which is associated with increased mortality or disease activity respectively.

It is essential to clarify why, in contrast to GM-CSF, Flt3L fails to protect from experimental colitis. The hypothesis that Flt3L and GM-CSF have similar effects on experimental colitis is based on the observation that GM-CSF and Flt3L have similar growth effects on Dendritic cells, mainly plasmacytoid DCs. It is however necessary to mention, that IFN-I production is not entirely restricted to pDCs, but can be exerted by other immune cells, e.g. myeloid DCs (mDCs) and monocytes [100]. GM-CSF induced significant higher cell growth of mDCs than

Flt3L treatment in mice. It is therefore important to consider, whether the number of IFN producing pDCs or the absolute number of IFN producing DCs, including pDCs, mDCs and IDCs, accounts for protective effects in intestinal inflammation models? More over the physiologic role GM-CSF and Flt3L beyond DC growth effects in vivo should be considered. GM-CSF is a physiologic hormone/cytokine with bivalent function. GM-CSF necessarily influences hematopoiesis, more over it is considered as a pro-inflammatory cytokine, which is released upon e.g. TLR stimulation and has priming effects itself on signal transduction necessarily involved in innate immune response [101]. Whereas GM-CSF has a physiological origin, Flt3L is a synthetically designed ligand, which binds to the intracellular Fms-like tyrosine kinase 3. Flt3 is involved in the differentiation of lymphoid and myeloid progenitor cells in e.g. DCs [102]. Little is known about functional Flt3L effects apart from cell differentiation. Studies with GM-CSF<sup>-/-</sup> show increased susceptibility to bacterial infection. However GM-CSF<sup>-/-</sup> do not show deficient hematopoiesis, indicating that GM-CSF has effects on immunity independent of GM-CSF mediated growth effects in DCs [103]. These data indicate that GM-CSF mediated expansion of IFN producing DCs does not exclusively account for disease amelioration in intestinal inflammation.

### **Flt3L and GM-CSF priming effects on TLR-signalling**

The contradictory effects of Flt3L and GM-CSF on experimental colitis appear to be closely connected to the type I-IFN production properties in response to TLR activation. GM-CSF mice displayed a significant higher upregulation of messenger RNA of type I-IFN genes as well as Interferon regulatory genes in response to TLR-7 and TLR-9 activation, compared to Flt3L treated mice. These data are striking, considering the importance of the TLR-IFN mechanism in the regulation of intestinal immunity:

Several years ago the importance of bacterial DNA as an immunostimulatory agent of the vertebrate immune system was described. Subsequently, CpG sequence motifs composed of unmethylated CpG dinucleotides were identified as the immunostimulatory component of bacterial DNA [104, 105]. CpG-containing bacterial DNA can be effectively distinguished from vertebrate DNA as (i) CpG motifs occur randomly in bacterial DNA (1/6) and are rare (“CpG suppression”) in vertebrate DNA (1/60) [106], (ii) cytosines in vertebrates are mostly methylated in contrast to bacterial DNA and (iii) in vertebrates there are significant amounts of motifs that can suppress the stimulatory effects of CpG motifs [107]. CpG-containing oligonucleotide (ODN) motifs directly activate dendritic cells, murine macrophages, B-

lymphocytes, natural killer cells and T- lymphocytes and are dependent on TLR-9-dependent recognition [108, 109]. CpG-containing oligonucleotides that effectively induce IFN-I in pDCs are termed A-type and have a palindromic central CpG motif, which can form a double-stranded region and strings of G residues at both the 3' and 5' end [110]. A-type and conventional single-stranded B-type CpG-containing oligonucleotides traffic differentially in pDC; A-type oligonucleotides are retained in early endosome-like structures and initiate signaling leading to IFN-I production, whereas B-type oligonucleotides traffic to a late endosome/lysosome compartment and more strongly induce inflammatory cytokines, such as TNF $\alpha$  [111]. The effects of CpG-ODN on intestinal immune modulation are not fully understood, though current research indicates local effects on the epithelium, as well as systemic effects in T-cell-dependent and T-cell-independent models. CpG-ODN induces TLR-9-dependent NF $\kappa$ B activation and IL-8 secretion in epithelial cell lines [112]. Moreover, it has been shown, that NF $\kappa$ B activation in the epithelium depends on the polarization of the TLR-9 receptor. Whereas in polarized epithelium basolateral TLR-9 stimulation induces IL-8 secretion, NF $\kappa$ B activation is blunted via apical stimulation, thereby inducing tolerance to subsequent TLR activation [113]. Apical TLR-9<sup>-/-</sup> confers risk to DSS colitis. The effects of CpG-ODN on the outcome of experimental colitis are contradictory. While administration of CpG-ODN prior to DSS exposure confers protection to colitis [84, 114], CpG-ODN addition during ongoing colitis leads to exacerbation [115]. The protective effects of CpG-ODN are at least partly mediated by a TLR-9-dependent IFN-I production, as mice lacking the IFN- $\alpha/\beta$  receptor were resistant to the CpG-ODN effects. Interestingly, the CpG-ODN effects were sustainable even in mice deficient for T- and B-cells, suggesting a protective pathway independent of the adaptive limb of the immune system [84]. Abe et al. suggest a regulatory role of conventional DCs in the outcome of colitis, which is CpG-ODN- and IFN-I-dependent but T-cell independent [64]. On the other hand, Obermeier et al. report that CD4<sup>+</sup>, CD62<sup>+</sup> T-cells from CpG-ODN-treated mice induce less severe colitis than T-cells from control mice, when transferred into severe combined immuno-deficient (SCID) mice devoid of B- and T-cells. The CpG-ODN effect was blunted in TLR-9<sup>-/-</sup>, but it has not been shown whether suppression in TLR-9<sup>-/-</sup> led to aberrant IFN-I, IL-10 or IL-12 secretion [116]. CpG-dependent T-cell tolerance is at least partly mediated by IFN- $\alpha/\beta$  and TGF- $\beta$ , as CD4<sup>+</sup>, CD62<sup>+</sup> T-cells from germ-free donor mice simultaneously treated with CpG-motifs and Anti-IFN- $\alpha/\beta$  or Anti-TGF-



$\beta$  respectively, induced severe colitis in SCID mice, compared to the improvement with CD4<sup>+</sup>, CD62<sup>+</sup> T-cells treated with CpG-ODN alone [85].

### **IFN-I increases bacterial clearance and induces antimicrobial peptide expression**

As the different effects of the hematopoietic growth factors GM-CSF and Flt3L on the TLR-7- and TLR-9-mediated IFN-I secretion *in vivo* were demonstrated, the effect of IFN-I on epithelial resistance to intracellular infection was then investigated. Due to the close proximity of DCs and the epithelial layer in the intestine and the DC's established role as sentinels of bacterial invasion, it was hypothesized that IFN-I would have a direct effect on bacterial clearance by the epithelium. As shown in cell culture experiments, IFN-I stimulation effectively enhanced killing of invading intracellular salmonella. These findings are striking, as they promote the idea that chronic intestinal inflammation could follow as a consequence of impaired mucosal defence on the one hand and an overwhelming bacterial burden on the other. Localised production of IFN-I may also be critical for intracellular killing by other cells, as well. Type I-IFN stimulation of DCs enhanced intracellular bacterial killing in DCs, which illustrates another important defensive strategy used by DCs. Of note direct TLR-7 and TLR-9 stimulation of DCs promoted bacterial clearance to the same extent as type I-IFN. Although it is obvious that IFN-I promotes bacterial killing in epithelial and dendritic cells, the underlying mechanisms are not fully understood. The data showing that IFN-I upregulates epithelial expression of *CARD15/NOD2* suggest that IFN-I may regulate pathways important for intracellular killing, as hypothesized by others [117]. Interestingly, consistent upregulation of a number of AMPs in response to TLR-7 and TLR-9 stimuli was also found. Whole genome expression profiling showed consistent expression of interferon-inducible genes, as well as AMPs, in spleens from mice stimulated with imiquimod (TLR-7) or CpG-ODN (TLR-9). Gene expression of cryptdin 4,6 and defensin  $\alpha$ 1 was visible in freshly isolated DCs, as well as in tissue sections from mice colons. TLR-induced AMP expression seems to be dependent on IFN-I signalling, as (i) AMP gene expression is highly correlated with IFN-I inducible gene expression, (ii) AMP gene expression is nullified when IFN-I secretion in pDCs is blocked in TLR-stimulated cells and (iii) IFN- $\beta$  itself induces AMP gene expression in epithelial cells lines. These findings describe a previously unknown role of IFN-I in the modulation of innate immunity.

Defensins and defensin-related cryptdins belong to the family of AMPs that act as the first line of extracellular defense in the intestine [118]. They are expressed in the full length of the gut in the epithelium and paneth cells. Their importance on intestinal immune function was recently highlighted, as functional variants in the transcription factor involved in AMP expression is associated with CD in humans [43] and mice with constitutive downregulated cryptdin expression have increased risk to intestinal inflammation[47]. These data indicate, that IFN-I mediated upregulation of AMPs is an essential and so far undescribed contribution to a balanced interaction between healthy mucosa and intraluminal pathogens.

In summary, treatment with the hematopoietic growth factor Fms-like tyrosine kinase 3 Ligand (Flt3L) expands immune cells but functionally has no therapeutic effect on experimental acute DSS colitis. Clinical outcome in acute colitis is closely related to the intestinal IFN-I producing capacity in response to TLR stimuli and thereby indicates a crucial role of type I-IFN in the intestinal immune response.

## **Outlook**

This study was designed to gain insight in the role of Interferon-producing DCs in intestinal immunity and the feasibility of therapeutic DCs amplification using Flt3L. Interestingly, the study raised many unexpected questions. Surprisingly, treatment with Flt3L in the DSS model of intestinal inflammation did not improve disease severity but rather increased it. It is therefore an essential question, why Flt3L mediated DC amplification worsened the clinical outcome, whereas GM-CSF mediated DC amplification improved clinical outcome in DSS colitis? This study provides a possible explanation for the contradictory effects: GM-CSF and Flt3L treated mice produce different high amount of IFN-I in response to TLR-9 stimulation. IFN-I has protective effects on intestinal immunity, and as Flt3L treated mice produce far less amounts of IFN-I, they are more susceptible to intestinal inflammation.

It was shown, that IFN-I has stimulating effects on intestinal immunity by increasing intracellular bacterial killing and inducing the gen expression of antimicrobial peptides. It can be therefore assumed, that IFN-I plays a crucial role in the manipulation of innate immune response and may be a therapeutic attempt for patients suffering IBD. Therefore future research should focus on the molecular mechanisms involved in IFN-I effects on intestinal immunity. IFN-I treatment diminishes bacterial load in the gentamicin protection assay. This observation leads to the assumption that IFN-I enhances bactericidal activity, which has a critical impact on the development of colitis. It should be further clarified, whether IFN-I

would have a similar effect in models, in which excessive inflammation response rather than breakdown of barrier function is the causative event ? For instance, can GM-CSF, as the essential promoter of IFN-dependent proliferation, or IFN-I treatment ameliorate disease in the T-cell adoptive transfer model or in colitis that develops spontaneously in IL-10 deficient mice? As IFN-I is alleged to have antimicrobial effects it would be of great interest to describe whether IFN induces changes in the intestinal microbiome, meaning the microbial composition in the intestine? This would be of especial interest, as the presence of microbiota is instrumental in eliciting pathologic inflammation. Studies in germ-free mice models showed that colonization with *E.coli* and *Enterococcus faecalis*, but not with *Bacteroides vulgatus*, triggered chronic experimental inflammation in IL-10  $-/-$  mice. These studies suggest specific “pro-/anti-inflammatory” effects of bacterial strains on intestinal mucosa, which is supported by e.g. promising studies with probiotics in ongoing IBD in mice and human [119-121]. Various studies report marked alterations of gut microbiota in IBD compared to feces from healthy controls and Frank et al. report significant association between clinical severity in IBD and an IBD-specific type of microbiota in gut of patients with IBD, characterized by depletion of commensal bacteria, namely *Firmicutes* and *Bacteroidetes*[122].

## V. Summary

**Background & Aims:** Type I-IFN producing dendritic Cells (DCs) play a crucial role in the regulation of intestinal immune response. GM-CSF and Flt3L are hematopoietic growth factors mediating DC growth. GM-CSF induced expansion of IFN-I producing DCs ameliorates Dextran Sodium Sulfate (DSS) induced colitis. We tested the hypothesis, whether Flt3L mediated DC growth protects mice from experimental colitis.

**Methods:** Therapeutic effect of Flt3L in DSS colitis was examined in Balb/c and RAG1<sup>-/-</sup> mice, evaluating clinical and biological disease signs. The molecular role of GM-CSF and Flt3L on DC growth and TLR-mediated IFN-I production was examined using flow cytometry, immunohistochemistry (IHC) and real time reverse transcription polymerase chain reaction (Real Time RT-PCR). Intracellular bacterial killing was assessed by gentamicin protection assay.

**Results:** GM-CSF and Flt3L induce similar DC growth *in vivo*, but unlike GM-CSF, Flt3L exacerbates clinical and biological severity of experimental colitis. GM-CSF, but not Flt3L, potentiates TLR-mediated IFN-I production in the intestine. IFN-I enhances intracellular bacterial killing and induces gene expression of antimicrobial peptides. GM-CSF, but not Flt3L, enhances IFN-I mediated antimicrobial effects.

**Conclusions:** The protective role of DCs in intestinal immune response depends on local IFN-I production. IFN-I exerts antimicrobial functions in the intestinal mucosa, including intracellular bacterial killing and antimicrobial peptide production. GM-CSF, but not Flt3L, augments IFN-I dependent antimicrobial effects. These findings shed a new light on the role of DC mediated IFN-I production in the context of intestinal inflammation.

## VI. Literature

1. Crohn BB, G.L., Oppenheimer GD., *Landmark article Oct 15, 1932. Regional ileitis. A pathological and clinical entity. By Burril B. Crohn, Leon Ginzburg, and Gordon D. Oppenheimer.* JAMA, 1984. **251**: p. 73-79.
2. Wilks, S., *Morbid appearances in the intestine of Miss Bankes.* London Medical Times & Gazette, 1859. **2**: p. 264.
3. Baumgart, D.C. and S.R. Carding, *Inflammatory bowel disease: cause and immunobiology.* The Lancet, 2007. **369**(9573): p. 1627-1640.
4. Schreiber S, R.P., Albrecht M, Hampe J, Krawczak M., *Genetics of Crohn disease, an archetypal inflammatory barrier disease.* Nat Rev Genet, 2005. **6**: p. 376-388.
5. Underwood, J.C.E., *General and systematic Pathology.* 2004, Edinburgh: Churchill & Livingstone.
6. H. Renz-Polster, S.K., J. Braun., *Basislehrbuch Innere Medizin.* 2004, München: Urban&Elsevier.
7. EV., L., *Clinical epidemiology of inflammatory bowel disease: incidence, prevalence and environmental influences.* Gastroenterology, 2004. **126**: p. 1504-17.
8. Kurata JH, K.-F.S., Frankl H, Godby P, Vadheim CM., *Crohn's disease among ethnic groups in a large health maintenance organization.* Gastroenterology, 1992. **102**: p. 9.
9. Nguyen GC, T.E., Regueiro M, Bromfield G, Bitton A, Stempak J, Dassopoulos T, Schumm P, Gregory FJ, Griffiths AM, Hanauer SB, Hanson J, Harris ML, Kane SV, Orkwis HK, Lahaie R, Oliva-Hemker M, Pare P, Wild GE, Rioux JD, Yang H, Duerr RH, Cho JH, Steinhart AH, Brant SR., *Inflammatory Bowel Disease Characteristics Among African Americans, Hispanics, and Non-Hispanic Whites: Characterization of a Large North American Cohort.* Am J Gastroenterol, 2006. **101**(5): p. 1012-1023.
10. Monk M, M.A., Siegel CL., *An epidemiological study of ulcerative colitis and regional enteritis among adults in Baltimore. II. Social and demographic factors.* Gastroenterology, 1969. **56**: p. 847-858.
11. Niv, Y., G. Abuksis, and G.M. Fraser, *Epidemiology of ulcerative colitis in Israel: a survey of Israeli Kibbutz settlements.* Am J Gastroenterol, 2000. **95**(3): p. 693-698.
12. Leong, R., J. Lau, and J. Sung, *The epidemiology and phenotype of Crohn's disease in the Chinese population.* Inflamm Bowel Dis, 2004. **10**: p. 646-51.
13. Zheng JJ, Z.X., Huangfu Z, Gao ZX, Guo ZR, Wang Z., *Crohn's disease in mainland China: a systematic analysis of 50 years of research.* Chin J Dig Dis, 2005. **6**: p. 175-81.
14. Klement E, C.R., Boxman J, Joseph A, Reis S., *Breastfeeding and risk of inflammatory bowel disease: a systematic review with meta-analysis.* Am J Clin Nutr, 2004. **80**: p. 1342-52.
15. Hugot JP, A.C., Berrebi D, Bingen E, Cezard JP., *Crohn's disease: the cold chain hypothesis.* Lancet, 2003. **362**: p. 2012-5.
16. Forbes A, K.T., *Crohn's disease: the cold chain hypothesis.* Int J Colorectal Dis, 2006. **21**(5): p. 399-401.
17. Russel, R. and J. Satsangi, *IBD: a family affair.* Best Pract Res Clin Gastroenterol, 2004. **18**: p. 525-39.
18. Satsangi J, G., C. Holt H, Jewell DP., *Clinical patterns of familial inflammatory bowel disease.* Gut, 1996. **38**(5): p. 738-741.
19. Hampe J, H.K., Kruis W, Raedler A, Fölsch UR, Schreiber S., *Anticipation in inflammatory bowel disease: a phenomennon caused by an accumulation of confounders.* Am Med Gent, 2000. **92**: p. 178-83.
20. Heresbach D, G.-A.B., Lesser M, Akolkar PN, Lin XY, Heresbach-Le Berre N, Bretagne JF, Katz S, Silver J., *Anticipation in Crohn's disease may be influenced by*

- gender and ethnicity of the transmitting parent.* Am J Gastroenterol, 1998. **93**: p. 2368-72.
21. Tysk C, L.E., Jarnerot G, Floderus-Myrhed B., *Ulcerative colitis and Crohn's disease in an unselected population of monozygotic and dizygotic twins. A study of heritability and the influence of smoking.* Gut, 1988. **29**(7): p. 990-996.
  22. Thompson NP, D.R., Pounder RE, Wakefield AJ., *Genetics versus environment in inflammatory bowel disease: results of a British twin study.* BMJ, 1996. **312**(7023): p. 95-96.
  23. Spehlmann ME, B.A., Burghardt P, Lepage P, Raedler A, Schreiber S., *Epidemiology of inflammatory bowel disease in a German twin cohort: Results of a nationwide study.* Inflammatory Bowel Disease, 2008. **14**(7): p. 968-976.
  24. Hugot JP, L.-P.P., Gower-Rousseau C, Olson JM, Lee JC, Beaugier L, Naom I, Dupas JL, Van Gossum A, Orholm M, Bonaiti-Pellie C, Weissenbach J, Mathew CG, Lennard-Jones JE, Cortot A, Colombel JF, Thomas G., *Mapping of a susceptibility locus for Crohn's disease on chromosome 16.* Nature, 1996. **379**(6568): p. 821-3.
  25. Hampe J, C.A., Croucher PJ, Mirza MM, et al, *Association between insertion mutation in NOD2 gene and Crohn's disease in German and British populations.* Lancet, 2001. **357**(9272): p. 1952-8.
  26. Hugot JP, C.M., Zouali H, Lesage S, Cezard JP, Belaiche J, Almer S, Tysk C, O'Morain CA, Gassull M, Binder V, Finkel Y, Cortot A, Modigliani R, Laurent-Puig P, Gower-Rousseau C, Macry J, Colombel JF, Sahbatou M, Thomas G., *Association of NOD2 leucine-rich repeat variants with susceptibility to Crohn's disease.* Nature, 2001. **411**(6837): p. 599-603.
  27. Ogura Y, B.D., Inohara N, Nicolae DL, Chen FF, Ramos R, Britton H, Moran T, Karaliuskas R, Duerr RH, Achkar JP, Brant SR, Bayless TM, Kirschner BS, Hanauer SB, Nunez G, Cho JH., *A frameshift mutation in NOD2 associated with susceptibility to Crohn's disease.* Nature, 2001. **411**(6837): p. 603-606.
  28. Inohara N, O.Y., Fontalba A, Gutierrez O, Pons F, Crespo J, Fukase K, Inamura S, Kusumoto S, Hashimoto M, Foster SJ, Moran AP, Fernandez-Luna JL, Nuñez G., *Host recognition of bacterial muramyl dipeptide mediated through NOD2. Implications for Crohn's disease.* J Biol Chem, 2003. **278**(5509-12).
  29. Jing Li, T.M., Eric Swanson, Christina Julian, Jeremy Harris, Denise K. Bonen, and D.L.N. Matija Hedl, Clara Abraham and Judy H. Cho, *Regulation of IL-8 and IL-1b expression in Crohn's disease associated NOD2/CARD15 mutations.* Human Molecular Genetics, 2004. **13**(16): p. 1715-1725.
  30. Fellerman K, S.D., Schaeffeler E, Schmalzl H, Wehkamp J, Bevins CL, Reinisch W, Teml A, Schwab M, Lichter P, Radlwimmer B, Stange EF, *A chromosome 8 gene-cluster polymorphism with low human beta-defensin 2 gene copy number predisposes to Crohn disease of the colon.* Am J Hum Genet., 2006. **79**(3): p. 439-48.
  31. Voss E, W.J., Wehkamp K, Stange EF, Schröder JM, Harder J, *NOD2/CARD15 mediates induction of the antimicrobial peptide human beta-defensin-2.* J. Biol. Chem., 2006. **281**(4): p. 2005-11.
  32. Maeda S, H.L., Liu H, Bankston LA, Iimura M, Kagnoff MF, Eckmann L, Karin M., *Nod2 Mutation in Crohn's Disease Potentiates NF- $\kappa$ B Activity and IL-1 $\beta$  Processing.* Science, 2005. **307**(5710): p. 734-738.
  33. Katz KD, H.D., Vadheim CM, McElree C, Delahunty T, Dadufalza VD, Krugliak P, Rotter JL., *Intestinal permeability in patients with Crohn's disease and their healthy relatives.* Gastroenterology, 1989. **4**: p. 927-31.
  34. Wyatt J, V.H., Hübl W, Waldhöer T, Lochs H., *Intestinal permeability and the prediction of relapse in Crohn's disease.* Lancet, 1993. **341**: p. 1437-9.

35. Munkholm P, L.E., Hollander D, Thornberg K, Orholm M, Katz KD, Binder V., *Intestinal permeability in patients with Crohn's disease and ulcerative colitis and their first degree relatives*. Gut, 1994. **35**(1): p. 68-72.
36. Panwala, C., J. Jones, and A. Viney, *A novel model of inflammatory bowel disease: mice deficient for the multiple drug resistance gene, mdr 1 a, spontaneously develop colitis*. J Immunol, 1998. **161**: p. 5733-5744.
37. Heazlewood CK, C.M., Eri R, Price GR, Tauro SB, Taupin D, Thornton DJ, Png CW, Crockford TL, Cornall RJ, Adams R, Kato M, Nelms KA, Hong NA, Florin TH, Goodnow CC, McGuckin MA., *Aberrant mucin assembly in mice causes endoplasmic reticulum stress and spontaneous inflammation resembling ulcerative colitis*. PLoS Med, 2008. **5**(3): p. e54.
38. Sartor, B., *Mechanisms of Disease: pathogenesis of Crohn's disease and ulcerative colitis*. Nature, 2006. **3**: p. 390-407.
39. Hampe J, F.A., Rosenstiel P, Till A, Teuber M, Huse K, Albrecht M, Mayr G, De La Vega FM, Briggs J, Günther S, Prescott NJ, Onnie CM, Häsler R, Sipos B, Fölsch UR, Lengauer T, Platzer M, Mathew CG, Krawczak M, Schreiber S., *A genome-wide association scan of nonsynonymous SNPs identifies a susceptibility variant for Crohn disease in ATG16L1*. Nat Genet, 2007. **39**(2): p. 207-211.
40. Hampe J, C.A., Croucher PJ, Mirza MM, Mascheretti S, Fisher S, Frenzel H, King K, Hasselmeyer A, MacPherson AJ, Bridger S, van Deventer S, Forbes A, Nikolaus S, Lennard-Jones JE, Foelsch UR, Krawczak M, Lewis C, Schreiber S, Mathew CG., *Association between insertion mutation in NOD2 gene and Crohn's disease in German and British populations*. The Lancet, 2001. **357**(9272): p. 1925-1928.
41. Stoll M, C.B., Costello CM, Waetzig GH, Mellgard B, Koch WA, Rosenstiel P, Albrecht M, Croucher PJ, Seegert D, Nikolaus S, Hampe J, Lengauer T, Pierrou S, Foelsch UR, Mathew CG, Lagerstrom-Fermer M, Schreiber S., *Genetic variation in DLG5 is associated with inflammatory bowel disease*. Nat. Genet., 2004. **36**: p. 476-480.
42. Peltekova VD, W.R., Rubin LA, Amos CI, Huang Q, Gu X, Newman B, Van Oene M, Cescon D, Greenberg G, Griffiths AM, St George-Hyslop PH, Siminovitch KA., *Functional variants of OCTN cation transporter genes are associated with Crohn disease*. Nat. Genet., 2004. **36**: p. 471-475.
43. Koslowski MJ, M.J., Kübler I, Chamaillard M, Schaeffeler E, Reinisch W, Wang G, Beisner J, Teml A, Peyrin-Biroulet L, Winter S, Herrlinger KR, Rutgeerts P, Vermeire S, Cooney R, Fellermann K, Jewell D, Bevins CL, Schwab M, Stange EF, Wehkamp J., *Genetic Variants of Wnt Transcription Factor TCF-4 (TCF7L2) Putative Promoter Region Are Associated with Small Intestinal Crohn's Disease*. PLoS ONE, 2009. **4**(2): p. e4496.
44. Brosbøl-Ravnborg A, H.C., Agnholt J, Dahlerup JF, Vind I, Till A, Rosenstiel P, Höllsberg P., *Toll-like receptor-induced granulocyte-macrophage colony-stimulating factor secretion is impaired in Crohn's disease by nucleotide oligomerization domain 2-dependent and -independent pathways*. Clinical & Experimental Immunology, 2009. **155**(3): p. 487-495.
45. van Heel DA, G.S., Hunt KA, Mathew CG, Forbes A, Jewell DP, Playford RJ., *Synergy between TLR9 and NOD2 innate immune responses is lost in genetic Crohn's disease*. Gut, 2005. **54**(11): p. 1553-1557.
46. Franchimont D, V.S., El Housni H, Pierik M, Van Steen K, Gustot T, Quertinmont E, Abramowicz M, Van Gossum A, Devière J, Rutgeerts P., *Deficient host-bacteria interactions in inflammatory bowel disease? The toll-like receptor (TLR)-4 Asp299gly polymorphism is associated with Crohn's disease and ulcerative colitis*. Gut, 2004. **53**: p. 987-92.

47. Steinbrecher KA, H.-L.E., Sitcheran R, Baldwin AS., *Loss of Epithelial RelA Results in Deregulated Intestinal Proliferative/Apoptotic Homeostasis and Susceptibility to Inflammation*. J Immunol, 2008. **180**(4): p. 2588-2599.
48. Dieckgraefe BK, K.J., Husain A, Dieruf L., *Association of glycogen storage disease Ib and Crohn disease: results of a North American survey*. Eur J Pediatr., 2002. **161**: p. 88-92.
49. Caradonna L, A.L., Lella P, Jirillo E, Caccavo D., *Phagocytosis, killing, lymphocyte-mediated antibacterial activity, serum autoantibodies, and plasma endotoxins in inflammatory bowel disease*. Am J Gastroenterol, 2000. **95**(6): p. 1495-1502.
50. Sina C, G.O., Förster M, Till A, Derer S, Hildebrand F, Raabe B, Chalaris A, Scheller J, Rehmann A, Franke A, Ott S, Häslér R, Nikolaus S, Fölsch UR, Rose-John S, Jiang HP, Li J, Schreiber S, Rosenstiel P., *G protein-coupled receptor 43 is essential for neutrophil recruitment during intestinal inflammation*. J Immunol, 2009. **183**: p. 7514-22.
51. Cebon J, L.J., Maher D, Morstyn G., *Endogenous haemopoietic growth factors in neutropenia and infection*. Br. J. Haematol, 1994. **86**(2): p. 265-74.
52. Seymour JF, L.G., Grail D, Quilici C, Hodgson G, Dunn AR., *Mice Lacking Both Granulocyte Colony-Stimulating Factor (CSF) and Granulocyte-Macrophage CSF Have Impaired Reproductive Capacity, Perturbed Neonatal Granulopoiesis, Lung Disease, Amyloidosis, and Reduced Long-Term Survival*. Blood, 1997. **90**(8): p. 3037-3049.
53. Hamilton, J.A., *Coordinate and noncoordinate colony stimulating factor formation by human monocytes*. J Leukoc Biol, 1994. **55**(3): p. 355-361.
54. Brissette WH, B.D., Stam EJ, Umland JP, Griffiths RJ., *GM-CSF rapidly primes mice for enhanced cytokine production in response to LPS and TNF*. Cytokine, 1995. **7**(3): p. 291-295.
55. Fleischmann J, G.D., Weisbart RH, Gasson JC., *Granulocyte-macrophage colony-stimulating factor enhances phagocytosis of bacteria by human neutrophils*. Blood, 1986. **68**(3): p. 708-711.
56. Zhan Y, L.G., Grail D, Dunn AR, Cheers C., *Essential Roles for Granulocyte-Macrophage Colony-Stimulating Factor (GM-CSF) and G-CSF in the Sustained Hematopoietic Response of Listeria monocytogenes-Infected Mice*. Blood, 1998. **91**(3): p. 863-869.
57. Gonzalez-Juarrero M, H.J., Izzo A, Junqueira-Kipnis AP, Shim TS, Trapnell BC, Cooper AM, Orme IM., *Disruption of granulocyte macrophage-colony stimulating factor production in the lungs severely affects the ability of mice to control Mycobacterium tuberculosis infection*. J Leukoc Biol, 2005. **77**(6): p. 914-922.
58. XU Y, H.N., Bao S., *The role of granulocyte macrophage colony stimulating factor in acute intestinal inflammation*. Cell Research, 2008. **12**: p. 1220-9.
59. Han X, U.K., Jurickova I, Koch D, Willson T, Samson C, Bonkowski E, Trauernicht A, Kim MO, Tomer G, Dubinsky M, Plevy S, Kugathsan S, Trapnell BC, Denson LA., *Granulocyte-Macrophage Colony-Stimulating Factor Autoantibodies in Murine Ileitis and Progressive Ileal Crohn's Disease*. Gastroenterology, 2009. **136**(4): p. 1261-1271.e3.
60. Korzenik JR, D.B., Valentine JF, Hausman DF, Gilbert MJ; Sargramostim in Crohn's Disease Study Group., *Sargramostim for Active Crohn's Disease*. N Engl J Med., 2005. **352**(21): p. 2193-2201.
61. Daro E, P.B., Brasel K, Teepe M, Pettit D, Lynch DH, Vremec D, Robb L, Shortman K, McKenna HJ, Maliszewski CR, Maraskovsky E., *Polyethylene Glycol-Modified GM-CSF Expands CD11bhighCD11chigh But Not CD11blowCD11chigh Murine*



- Dendritic Cells In Vivo: A Comparative Analysis with Flt3 Ligand*. J Immunol, 2000. **165**(1): p. 49-58.
62. Steinman, R. and M. Nussenzweig, *Inaugural Article: Avoiding horror autotoxicus: The importance of dendritic cells in peripheral T cell tolerance*. PNAS, 2002. **99**(1): p. 351-358.
  63. Sainathan SK, H.E., Gong Q, Bishnupuri KS, Luo Q, Colonna M, White FV, Croze E, Houchen C, Anant S, Dieckgraefe BK., *Granulocyte macrophage colony-stimulating factor ameliorates DSS-induced experimental colitis*. Inflammatory Bowel Diseases, 2008. **14**(1): p. 88-99.
  64. Abe K, N.K., Fine SD, Mo JH, Shen C, Shenouda S, Corr M, Jung S, Lee J, Eckmann L, Raz E., *Conventional dendritic cells regulate the outcome of colonic inflammation independently of T cells*. PNAS, 2007. **104**(43): p. 17022-17027.
  65. Ralph†, M.S., *Dendritic cells: Understanding immunogenicity*. European Journal of Immunology, 2007. **37**(S1): p. S53-S60.
  66. Steinman RM, A.J., Cohn ZA., *Identification of a novel cell type in peripheral lymphoid organs of mice. IV. Identification and distribution in mouse spleen*. J Exp Med. , 1975. **141**(4): p. 804-20.
  67. Steinman RM, C.Z., *Identification of a novel cell type in peripheral lymphoid organs of mice. I. Morphology, quantitation, tissue distribution*. J Exp Med., 1973. **137**(5): p. 1142-62.
  68. Fitzgerald-Bocarsly P, F.M., Mendelsohn M, Curl S, Lopez C., *Human mononuclear cells which produce interferon-alpha during NK(HSV-FS) assays are HLA-DR positive cells distinct from cytolytic natural killer effectors*. J Leukoc Biol, 1988. **43**(4): p. 323-34.
  69. Dudziak D, K.A., Heidkamp GF, Buchholz VR, Trumfheller C, Yamazaki S, Cheong C, Liu K, Lee HW, Park CG, Steinman RM, Nussenzweig MC., *Differential Antigen Processing by Dendritic Cell Subsets in Vivo*. Science, 2007. **315**(5808): p. 107-111.
  70. Rönnblom L, R.U., Alm GV., *Properties of human natural interferon-producing cells stimulated by tumor cell lines*. Eur J Immunol, 1983. **13**(6): p. 471-6.
  71. Lyman SD, J.S., *c-kit Ligand and Flt3 Ligand: Stem/Progenitor Cell Factors With Overlapping Yet Distinct Activities*. Blood, 1998. **91**(4): p. 1101-1134.
  72. Adolfsson J, B.O., Bryder D, Theilgaard-Mönch K, Astrand-Grundström I, Sitnicka E, Sasaki Y, Jacobsen SE., *Upregulation of Flt3 Expression within the Bone Marrow Lin Sca1+c-kit+ Stem Cell Compartment Is Accompanied by Loss of Self-Renewal Capacity*. Immunity, 2001. **15**(4): p. 659-669.
  73. Christensen JL, W.I., *Flk-2 is a marker in hematopoietic stem cell differentiation: a simple method to isolate long-term stem cells*. Proc. Natl. Acad. Sci., 2001. **98**: p. 14541-14546.
  74. Laouar Y, W.T., Fu XY, Flavell RA., *STAT3 Is Required for Flt3L-Dependent Dendritic Cell Differentiation*. Immunity, 2003. **19**(6): p. 903-912.
  75. McKenna HJ, S.K., Miller RE, Brasel K, De Smedt T, Maraskovsky E, Maliszewski CR, Lynch DH, Smith J, Pulendran B, Roux ER, Teepe M, Lyman SD, Peschon JJ., *Mice lacking flt3 ligand have deficient hematopoiesis affecting hematopoietic progenitor cells, dendritic cells, and natural killer cells*. Blood, 2000. **95**(11): p. 3489-3497.
  76. Maraskovsky E, B.K., Teepe M, Roux ER, Lyman SD, Shortman K, McKenna HJ., *Dramatic increase in the numbers of functionally mature dendritic cells in Flt3 ligand-treated mice: multiple dendritic cell subpopulations identified*. J Exp Med. , 1996. **184**(5): p. 1953-62.

77. Karsunky H, M.M., Cozzio A, Weissman IL, Manz MG., *Flt3 Ligand Regulates Dendritic Cell Development from Flt3+ Lymphoid and Myeloid-committed Progenitors to Flt3+ Dendritic Cells In Vivo*. J Exp. Med., 2003. **198**(2): p. 305-313.
78. Chirido FG, M.O., Beacock-Sharp H, Mowat AM., *Immunomodulatory dendritic cells in intestinal lamina propria*. European Journal of Immunology, 2005. **35**(6): p. 1831-1840.
79. Kingham TP, C.U., Plitas G, Katz S, Raab J., DeMatteo P.. *Murine liver plasmacytoid dendritic cells become potent immunostimulatory cells after Flt-3 ligand expansion*. Hepatology, 2007. **45**(2): p. 445-454.
80. Kim HS, B.A., *Experimental colitis in animal models*. Scand J Gastroenterol., 1992. **27**: p. 529-537.
81. Miltenyi S, M.W., Weichel W, Radbruch A., *High gradient magnetic cell separation with MACS*. Cytometry, 1990. **11**(2): p. 231-8.
82. Chomczynski P, S.N., *Single-step method of RNA isolation by acid guanidinium thiocyanate-phenol-chloroform extraction*. Anal Biochem, 1987. **162**(1): p. 156-9.
83. Mullis K, F.F., Scharf S, Saiki R, Horn G, Ehrlich H., *Specific enzymatic amplification of DNA in vitro: the polymerase chain reaction*. 1986. Biotechnology, 1992. **24**: p. 17-27.
84. Katakura K, L.J., Rachmilewitz D, Li G, Eckmann L, Raz E., *Toll-like receptor 9-induced type I IFN protects mice from experimental colitis*. Journal of Clinical Investigation, 2005. **115**(3): p. 7.
85. Bleich A, J.L., Smoczek A, Westendorf AM, Strauch U, Mähler M, Hedrich HJ, Fichtner-Feigl S, Schölmerich J, Falk W, Hofmann C, Obermeier F., *CpG Motifs of Bacterial DNA Exert Protective Effects in Mouse Models of IBD by Antigen-Independent Tolerance Induction*. Gastroenterology, 2009. **136**(1): p. 278-287.
86. Honda K, Y.H., Takaoka A, Taniguchi T., *Regulation of the type I IFN induction: a current view*. Int Immunol, 2005. **17**(11): p. 1367-78.
87. Taniguchi T, T.A., *A weak signal for strong responses: interferon-alpha/beta revisited*. Nat Rev Mol Cell Biol, 2001. **2**(5): p. 378-386.
88. Sidky YA, B.E., Weeks CE, Reiter MJ, Hatcher JF, Bryan GT, *Inhibition of murine tumor growth by an interferon-inducing imidazoquinolinamine*. Cancer Res, 1992. **52**(13): p. 3528-33.
89. Blasius A, V.W., Krug A, Facchetti F, Cella M, Colonna M., *A cell-surface molecule selectively expressed on murine natural interferon-producing cells that blocks secretion of interferon-alpha*. Blood, 2004. **103**(11): p. 4201-4206.
90. Blasius AL, C.M., *Sampling and signaling in plasmacytoid dendritic cells: the potential roles of Siglec-H*. Trends in Immunology, 2006. **27**(6): p. 255-260.
91. Xu Y, Z.Y., Lew AM, Naik SH, Kershaw MH., *Differential Development of Murine Dendritic Cells by GM-CSF versus Flt3 Ligand Has Implications for Inflammation and Trafficking*. J Immunol, 2007. **179**(11): p. 7577-7584.
92. Saxena V, O.J., Magnusen AF, Munn DH, Katz JD., *The Countervailing Actions of Myeloid and Plasmacytoid Dendritic Cells Control Autoimmune Diabetes in the Nonobese Diabetic Mouse*. J Immunol, 2007. **179**(8): p. 5041-5053.
93. Dieleman LA, R.B., Tennyson GS, Beagley KW, Bucy RP, Elson CO., *Dextran sulfate sodium-induced colitis occurs in sever combined immunodeficient mice*. Gastroenterology, 1994. **107**: p. 1643-1652.
94. Pauleau AL, M.P., *Role of Nod2 in the Response of Macrophages to Toll-Like Receptor Agonists*. Mol. Cell. Biol., 2003. **23**(21): p. 7531-7539.
95. Fitzgerald-Bocarsly P, D.J., Singh S., *Plasmacytoid dendritic cells and type I IFN: 50 years of convergent history*. Cytokine & Growth Factor Reviews, 2008. **19**(1): p. 3-19.

96. Daro E, B.E., Smith J, Teepe M, Maliszewski CR, McKenna HJ., *Comparison of the functional properties of murine dendritic cells generated in vivo with Flt3L ligand, GM-CSF and Flt3 ligand plus GM-CSF*. Cytokine, 2002. **17**(3): p. 119-130.
97. Gilliet M, B.A., Patrel C, Antonenko S, Xu XL, Trinchieri G, O'Garra A, Liu YJ., *The Development of Murine Plasmacytoid Dendritic Cell Precursors Is Differentially Regulated by FLT3-ligand and Granulocyte/Macrophage Colony-Stimulating Factor*. J Exp. Med. , 2002. **195**(7): p. 953-958.
98. von Wulffen W, S.M., Herold S, Marsh LM, Bulau P, Seeger W, Welte T, Lohmeyer J, Maus UA., *Lung Dendritic Cells Elicited by Fms-like Tyrosin 3-Kinase Ligand Amplify the Lung Inflammatory Response to Lipopolysaccharide*. Am. J. Respir. Crit. Care Med., 2007. **176**(9): p. 892-901.
99. Winter C, T.K., Langer F, Mack M, Briles DE, Paton JC, Maus R, Srivastava M, Welte T, Maus UA., *FMS-Like Tyrosine Kinase 3 Ligand Aggravates the Lung Inflammatory Response to Streptococcus pneumoniae Infection in Mice: Role of Dendritic Cells*. J Immunol, 2007. **179**(5): p. 3099-3108.
100. Newman KC, R.E., *Whatever turns you on: accessory-cell-dependent activation of NK cells by pathogens*. Nat Rev Immunol, 2007. **7**(4).
101. Yang H, W.J., Zhang H, Lin L, Zhang W, He S., *Upregulation of Toll-like receptor (TLR) expression and release of cytokines from P815 mast cells by GM-CSF*. BMC Cell Biology, 2009. **10**(1): p. 37.
102. Waskow C, L.K., Darrasse-Jeze G, Guermontprez P, Ginhoux F, Merad M, Shengelia T, Yao K, Nussenzweig M., *The receptor tyrosine kinase Flt3 is required for dendritic cell development in peripheral lymphoid tissues*. Nat Immunol, 2008. **9**(6): p. 676.
103. Shortman K, N.S., *Steady-state and inflammatory dendritic-cell development*. Nat Rev Immunol, 2007. **7**.
104. Krieg AM, *Now I know my CpGs*. Trends Microbiol, 2001. **9**: p. 249-252.
105. Krieg AM, Y.A., Matson S, Waldschmidt TJ, Bishop GA, Teasdale R, Koretzky GA, Klinman DM, *CpG motifs in bacterial DNA trigger direct B-cell activation*. Nature, 1995. **6**(374): p. 546-9.
106. C Burge, A.M.C., and S Karlin, *Over- and under-representation of short oligonucleotides in DNA sequences*. PNAS, 1992. **89**(4): p. 1358–1362.
107. Stacey KJ, Y.G., Clark F, Sester DP, Roberts TL, Naik S, Sweet MJ, Hume DA., *The molecular basis for the lack of immunostimulatory activity of vertebrate DNA*. J Immunol, 2003. **1**(170): p. 3614-20.
108. Krieg, A.M., *CpG motifs in bacterial DNA and their immune effects*. Annual Review of Immunology, 2002. **20**(1): p. 709-760.
109. Wagner, H., *Bacterial CpG DNA activates immune cells to signal infectious danger*. Adv. Immunol, 1999. **73**: p. 329.
110. Hemmi H, K.T., Takeda K, Akira S., *The Roles of Toll-Like Receptor 9, MyD88, and DNA-Dependent Protein Kinase Catalytic Subunit in the Effects of Two Distinct CpG DNAs on Dendritic Cell Subsets*. J Immunol, 2003. **170**(6): p. 3059-3064.
111. Honda K, O.Y., Yanai H, Negishi H, Mizutani T, Takaoka A, Taya C, Taniguchi T., *Spatiotemporal regulation of MyD88-IRF-7 signalling for robust type-I interferon induction*. Nature, 2005. **434**(7036): p. 1035-1040.
112. G. Pedersen, L.A.M.W.M.J.R.-M.J.B., *Expression of Toll-like receptor 9 and response to bacterial CpG oligodeoxynucleotides in human intestinal epithelium\**. Clinical & Experimental Immunology, 2005. **141**(2): p. 298-306.
113. Lee J, M.J., Katakura K, Alkalay I, Rucker AN, Liu YT, Lee HK, Shen C, Cojocaru G, Shenouda S, Kagnoff M, Eckmann L, Ben-Neriah Y, Raz E., *Maintenance of colonic homeostasis by distinctive apical TLR9 signalling in intestinal epithelial cells*. Nat Cell Biol, 2006. **8**(12): p. 1327-36.

114. Rachmilewitz D, K.F., Takabayashi K, Hayashi T, Leider-Trejo L, Lee J, Leoni LM, Raz E., *Immunostimulatory DNA ameliorates experimental and spontaneous murine colitis*. Gastroenterology, 2002. **122**(5): p. 1428-41.
115. Obermeier F, D.N., Strauch UG, Hofmann C, Bleich A, Grunwald N, Hedrich HJ, Aschenbrenner E, Schlegelberger B, Rogler G, Schölmerich J, Falk W., *CpG Motifs of Bacterial DNA Essentially Contribute to the Perpetuation of Chronic Intestinal Inflammation*. Gastroenterology, 2005. **129**(3): p. 913-927.
116. Obermeier F, S.U., Dunger N, Grunwald N, Rath HC, Herfarth H, Schölmerich J, Falk W., *In vivo CpG DNA/toll-like receptor 9 interaction induces regulatory properties in CD4+CD62L+ T cells which prevent intestinal inflammation in the SCID transfer model of colitis*. Gut, 2005. **54**(10): p. 1428-1436.
117. Hisamatsu T, S.M., Reinecker HC, Nadeau WJ, McCormick BA, Podolsky DK., *CARD15/NOD2 functions as an antibacterial factor in human intestinal epithelial cells*. Gastroenterology, 2003. **124**(4): p. 993-1000.
118. Hornef MW, P.K., Karlsson J, Refai E, Andersson M., *Increased diversity of intestinal antimicrobial peptides by covalent dimer formation*. Nat Immunol, 2004. **5**(8): p. 836-43.
119. Sellon RK, T.S., Schultz M, Dieleman LA, Grenther W, Balish E, Rennick DM, Sartor RB., *Resident enteric bacteria are necessary for development of spontaneous colitis and immune system activation in interleukin-10-deficient mice*. Infect Immun, 1998. **66**: p. 5224-31.
120. Kim SC, T.S., Albright CA, Tsang J, Balish EJ, Braun J, Huycke MM, Sartor RB., *Variable phenotypes of enterocolitis in interleukin 10-deficient mice monoassociated with two different commensal bacteria*. Gastroenterology, 2005. **128**(4): p. 891-906.
121. Ott SJ, M.M., Wenderoth DF, Hampe J, Brandt O, Fölsch UR, Timmis KN, Schreiber S., *Reduction in diversity of the colonic mucosa associated bacterial microflora in patients with active inflammatory bowel disease*. Gut, 2004. **53**(5): p. 685-693.
122. Frank DN, A.L., Amand St, Feldman RA, Boedeker EC, Harpaz N, Pace NR., *Molecular-phylogenetic characterization of microbial community imbalances in human inflammatory bowel disease*. PNAS, 2007. **104**(34): p. 13780-13785.

## Additional information - Materials

### Antibodies

Name	Species, Dilution	Conjugates Dye	Company
<b>Primary</b>			
CD8a	Rat, 1:50	FITC	eBioscience
CD11b	Rat, 1:50	Biotin/FITC	eBioscience
CD11c	AH, 1:50	Biotin/FITC	eBioscience
CD45R/B220	Rat, 1:50	Biotin/FITC/PE	BD Bioscience
Ly6c	Rat, 1:50	FITC	BD Bioscience
IgG1, lambda 1	AH, 1:50	PE	BD Bioscience
IgG2a, kappa	Rat, 1:50	FITC	BD Bioscience
IgG2a, kappa	Rat, 1:50	Biotin	BD Bioscience
mPDCA-1	Rat, 1:50	APC	Miltenyi Biotec
MHC-II	Rat, 1:50	FITC	Southern Biotech
CD16/CD32	Rat, 1:50	None	Gift of Marco Colonna
440c	Rat, 1:50	none	Gift of Marco Colonna
<b>Secondary</b>			
Streptavidin PerCP	Rat, 1:50	PerCP	eBioscience
<b>AB conjugated to magnetic beads</b>			
CD11c	Hamster		Miltenyi Biotec
mPDCA-1	Rat		Miltenyi Biotec

**Table 16 List of Antibodies.**

AH = Armenina Hamster. PE, FITC, APC describes the dye, conjugated to antibodies, PE= Phycoerithrin, FITC= Fluorescein Isothiocyanate, APC= Allophycocyanin, PerCP= Peridin chlorophyll

### Oligonucleotides

Primername	Sequence (5'→3')	T <sub>anneal</sub>
β-actin-F	atcattgctctcctgagcg	60
β-actin-R	gctgatccacatctggaa	60
TNFα-F	gacctcactcagatcatccttct	60
TNFα-R	acgctggctcagccactc	60
IL-1β-F	tcgctcagggtcacaagaaa	60
IL-1β-R	catcagaggcaaggaggaaaac	60
IFNα2-F	gaacctcctctgaccaggaa	60
IFNα2-R	ggtacacagtgatcctgtggaaata	60
IFNα9-F	tggaatgcaaccctctagact	60

IFN $\alpha$ 9-R	acagccttgaggcattgag	60
IRF7-F	gaagaccctgatcctgggtga	60
IRF7-R	ccaggtccatgaggaagtgt	60
Ifit3-F	gaggacaaccggaagtgtgt	60
Ifit3-R	ggatgagcagaggagtccagg	60
Defensin $\alpha$ 1-F	gcatgaatggaacctgcagaaa	60
Defensin $\alpha$ 1-R	accagcatcagtggcctcagta	60
Defensin related cryptdin 4-F	ttcatgaaaaatctttgagaggtttgt	60
Defensin related cryptdin 4-R	gcagtacaaaaatcgtattccacaagt	60
Defensin related cryptdin 6-F	tgaagacactaatcctcctctctgc	60
Defensin related cryptdin 6-R	gctcctcagtttagtctctcatctgta	60
CARD15-F	actgggctttggcgttctg	60
CARD15-R	tgctctttcctcctcatcgtg	60
hBD-3-F	gctgccttccaaaggagga	60
hBD-3-R	tcttcggcagcatttttcg	60
<b>Others than primer</b>		
CpG-ODN 1018	tgactgtgaacgttcgagatga	

### Cell reagents

Name	Species	Company
Mouse Interferon Alpha A	mouse	PBL/NJ
CpG-ODN 1018		Integrated DNA Technologies
Imiquimod R837		InvivoGen/ CA
pegGM-CSF	mouse	Hybridoma Cell (Dieckgraefe Lab)
Flt3L	mouse	Hybridoma Cell (Dieckgraefe Lab)
Interferon beta	human	R&D Systems

### Kits and ready to use solutions

Name	Company
Starting Block T20 Blocking Solution	Pierce
Vybrant CFDA SE Cell Tracer Kit	Invitrogen
Oligotex mRNA Isolation Kit	Qiagen/CA
TBE Buffer 10x	Bio Rad / CA
OCT Freeze Medium	Tissue Tek / CA
Auto Macs Running Buffer	Miltenyi / CA
DNA-Ladder 100bp	Promega
Gel Loading Buffer (6x)	Promega
Superscript II Reverse Transcriptase	Invitrogen
RNAse Out (RNAse Inhibitor)	Invitrogen
Random Hexamer Primer	Invitrogen
DTT Buffer	Invitrogen

**Buffer, Solutions, Mediums**

<b>Name</b>	<b>Company</b>
CO2-independent Medium	Cellgro
Gentamicin	Cellgro
RPMI-1640	Biowithaker
DMEM	Biowithaker
MEM	Biowithaker
PBS	Cellgro
HBSS	Cellgro
Trypsin-EDTA	Cellgro
Anitbiotic/Antimycotic Solution	Cellgro
L-Glutamine	Cellgro
Non-essential Amino acid Mix	Cellgro
Sodium Pyruvate	Cellgro
Fetal Calf serum (FCS)	Cellgro
Bovine Serum Albumin (BSA), Fraction V	Sigma / MO
Tris-CL Buffer	Cellgro
DEPC-treated Water	Cellgro
Flow Cytometry Washing Buffer (PBS + 0.05% BSA, Fraction V)	Dieckgraefe Lab
Flow Cytometry Blocking Buffer (PBS + 10% BSA)	Dieckgraefe Lab
Flow Cytometry Fixing Buffer (PBS + 10% PFA)	Dieckgraefe Lab
ACK Lysis Buffer	Cellgro

## Publications and activities

Bishnupuri KS, Luo Q, Sainathan SK, Kikuchi K, Sureban SM, Sabarinathan M, Gross JH, **Aden K**, May R, Houchen CW, Anant S, Dieckgraefe BK. *Reg IV regulates normal intestinal and colorectal cancer cell susceptibility to radiation-induced apoptosis. Gastroenterology 2010, 138 (2), 616-26*

**Aden K**, Sainathan SK, Bishnupuri KS, Luo Q, Gong Q, Newberry R, Konfucja V, Schreiber S, Rosenstiel P and Dieckgraefe BK. *Fundamental differences of the hematopoietic growth factors Fms-like tyrosine 3-kinase ligand and GM-CSF on experimental colitis is linked with type I-IFN mediated antimicrobial effects on intestinal immune response.* (in submission)

### Poster Presentations:

**Aden K**, Sainathan SK, Bishnupuri KS, Luo Q, Schreiber S, Dieckgraefe BK.  
*Fundamental difference in hemopoietic growth factors (Flt3L, GM-CSF) on experimental mouse colitis.*  
Digestive Disease Week (DDW) 2008, San Diego/CA

Sainathan SK, **Aden K**, Bishnupuri KS, Luo Q, Houchen CW, Anant S and Dieckgraefe BK.  
*Activation of innate immunity with a TLR 7 agonist, imiquimod, ameliorates acute DSS colitis.*  
DDW 2008, San Diego/CA

Sainathan SK, Bishnupuri KS, **Aden K**, Luo Q, Houchen CW, Anant S and Dieckgraefe BK.  
*TLR7 agonist; Its role in acute intestinal inflammation and protection against pathogen in human epithelial cells.*  
DDW 2009, Chicago/IL

**Aden K**, Sainathan SK, Bishnupuri KS, Luo Q, Gong Q, Newberry R, Konfucja V, Schreiber S, Philip Rosenstiel P and Dieckgraefe BK  
*Fundamental differences of the hematopoietic growth factors Flt3L and GM-CSF on experimental colitis depend on IFN-I mediated antimicrobial effects on intestinal immunity.*  
DDW 2010, New Orleans/LO

### Additional Training:

Lebenswissenschaftliches Kolleg der Studienstiftung des deutschen Volkes, Oktober 2006: Cancer Biology



## Acknowledgements

I want to thank Prof. Dr. med. Stefan Schreiber (Director Institute of clinical molecular biology, Head of internal medicine, UKSH-Kiel) and Brian K. Dieckgraefe ( M.D., Ph.D.; Associate Professor of Medicine, Washington University School of Medicine) for giving me the opportunity to pursue my doctoral thesis in their institutes.

I'm deeply indebted to my mentor Prof. Dr. med. Philip Rosenstiel. His enthusiasm in the scientific topic, his optimism in the progress of the experimental work and his effort to foster my exchange year in St.Louis/MO paved the way for the success of this project.

I'm thankful to Dr. Andreas Till and all colleagues in the Institute of clinical molecular biology for introducing me into the experimental work in molecular biology and helping me to avoid the pitfalls of laboratory work.

I'm thankful to Satheesh Sainathan, Kumar S. Bishnupuri and Quizhi Luo from the Dieckgraefe Lab for mental and physical assistance in and above lab work in St. Louis.

I thankfully acknowledge the help of Prof. Rodney Newberry from the Division of Gastroenterology (Washington University School of Medicine) in cell staining and flow cytometry as well as the help of Dr. Vjollca Konjufca and Dr. Bernd Zinselmeyer (Division of Pathology and Immunology, Washington University School of Medicine) for introducing me into immunohistochemical staining and fluorescence microscopy.

For critical comments, inspiring conversations and mental support I want to thank my friends in Kiel, Tübingen and Essen.

Most of all, I'm deeply thankful for the constant support of my entire family.

*...und vergiss nicht, was er Dir Gutes getan hat: ... (Psalm 103, 2)*

# Curriculum vitae

## PERSONAL INFORMATION

Name	<b>ADEN, KONRAD ARNOLD ALTRID</b>
Date of birth	27.08.1982
Place of birth	Essen/Germany
Nationality	GERMAN
Parents	PROF. DR. IUR MENNO ADEN DR. MED. PATRICIA ADEN ( FAMILY NAME: SCHLEGELBERGER)
Siblings	<ul style="list-style-type: none"> <li>• FRANZISKA STÖCKMANN (FAMILY NAME: ADEN) * 1977</li> <li>• DR. JUR GESINE ADEN * 1979</li> <li>• FELIX ADEN * 1985</li> <li>• DIETRICH ADEN * 1988</li> </ul>
Contact	TAUBENSTRASSE 33, 45389 ESSEN
Marital status	SINGLE

## EDUCATION AND TRAINING

- 1988-1992 Elementary School Essen-Burgaltendorf
- 1992-2002 Gymnasium Essen-Überruhr, Abitur, grade: very good(1,9)
- 2002-2003 Military Service: Zentrum für operative Information Mayen/ Rheinland Pfalz  
Radio Andernach
- 2003-2003 Eberhard-Karls-University Tübingen/Germany, Law
- 2003-2005 Christian-Albrechts-University Kiel / Germany, Pre-clinical studies (Physikum) Final result: 2.0
- 2003-2005 Christian-Albrechts-University Kiel/ Germany Clinical studies
- 2007-2008 Washington University School of Medicine, St. Louis/MO
- 2008-2009 Christian-Albrechts-University Kiel/ Germany
- 2009-2010 Clinical Rotation
  - Internal Medicine: University Hospital Bern/Switzerland
  - Surgery: Friedrich-Ebert-Krankenhaus Neumünster/ SH
  - Neurology: University Hospital Kiel (UKSH)/ SH

## ADDITIONAL INFORMATION

Private Interests	Music (Piano, Drums), Literature, Writing (Poems, Drama), Soccer, Running
SCHOLARSHIPS	<ul style="list-style-type: none"> <li>• Studienstiftung des deutschen Volkes, since 2005</li> <li>• 2006 MD Thesis-Scholarship of „Mucosa-Immunologie, University Kiel“</li> </ul>
ORGANISATIONS	<ul style="list-style-type: none"> <li>• Marburger Bund, Member of the „Sprecherrat der Medizinstudenten“</li> <li>• Corps Franconia Tübingen</li> </ul>